



VCU

Virginia Commonwealth University
VCU Scholars Compass

Theses and Dissertations

Graduate School

2016

INVESTIGATING THE MECHANISM OF THE COMPARTMENTALIZED CBP (CREB-BINDING PROTEIN) UBIQUITIN LIGASE ACTIVITIES

Oluwatoyin E. Akande
Virginia Commonwealth University

Follow this and additional works at: <https://scholarscompass.vcu.edu/etd>



Part of the [Molecular Biology Commons](#)

© The Author

Downloaded from

<https://scholarscompass.vcu.edu/etd/4438>

This Dissertation is brought to you for free and open access by the Graduate School at VCU Scholars Compass. It has been accepted for inclusion in Theses and Dissertations by an authorized administrator of VCU Scholars Compass. For more information, please contact libcompass@vcu.edu.

© Oluwatoyin E. Akande 2016
All Rights Reserved

**INVESTIGATING THE MECHANISM OF THE COMPARTMENTALIZED CBP
(CREB-BINDING PROTEIN) UBIQUITIN LIGASE ACTIVITIES**

A dissertation submitted in partial fulfillment of the requirements for the degree of
Doctor of Philosophy at Virginia Commonwealth University

by

Oluwatoyin E. Akande

Bachelor of Science, University of Ibadan, Nigeria
Master of Science, University of Ibadan, Nigeria

Advisor: Steven R. Grossman, M.D/Ph.D.
Dianne Nunnally Hoppes Chair in Cancer Research
Professor and Chair of Hematology, Oncology, and Palliative Care
Deputy Director of VCU Massey Cancer Center
Virginia Commonwealth University

Virginia Commonwealth University
Richmond, Virginia
August, 2016

Acknowledgements

I would like to take this opportunity to express my gratitude to all the people who have contributed to the success of this work. First of all, I would like to thank my Ph. D advisor, Dr. Steven Grossman for all the support and opportunities he has given me. I am grateful for all the intellectual input, patience and encouragement rendered throughout my studies. I would like to thank all my research committee members. Dr. Larisa Litovchick, thank you so much for all your assistance especially with the proteomics analysis and thank you for readily sharing ideas and resources, and for always being there to answer my questions. Dr. Kristoffer Valerie, thank you for all your support and kindness in sharing resources. Dr. Sumitra Deb, thank you for your words of encouragement. Dr. Joseph Landry, I appreciate all your thoughtful suggestions and intellectual discussions. Also, I would like to thank Dr. Gail Christie, the Molecular Biology and Genetics director, for always believing in my abilities and for rendering guidance throughout my studies.

A big thank you to all the members of Grossman lab. Special thanks to the lab manager, Barbara Szomju, who was always there to render whatever help I needed. I would also like to thank Dr. Priyadarshan Damle for all his assistance and also Dr. Michael Dcona for all his help. Also, a big thank you to members of Litovchick lab, especially Dr. Vijay Menon and Dr. Siddharth Saini for their willingness and readiness in rendering assistance.

I would like to thank Dr. Nicholas E. Sherman, of the Biomedical Mass Spectrometry Laboratory at University of Virginia (UVA), and Dr. Charles Lyons, of the Mass Spectrometry Resources at VCU (Dr. Moran's Lab), for their assistance with proteomics analyses.

To my siblings, friends, nephews and nieces who have constantly showered me with love and support, I thank you all. Finally, my deepest appreciation goes to my dearest husband, Omololu and our wonderful children, Feranmi and Mofe for their endless love and support for me. You are the best and this journey would not have been completed without you. God has indeed been faithful to me.

Table of Contents

Acknowledgements	iii
List of Tables	v
List of Figures	vi
List of Abbreviation and Symbols	ix
Abstract	xi
1.1 Initial Identification of CBP and its paralogue, p300	1
1.2 CBP and p300 are Histone Acetyltransferases.....	4
1.3 The Role of CBP/p300 in Transcription and other Cellular Processes	5
1.4 CBP and Human Diseases	10
1.5 CBP as a Therapeutic Agent	16
1.6 The Regulation of CBP Co-activator Role in Transcription.....	17
1.7 E3 and E4 Ubiquitin Ligases	24
1.8 The Dual Roles of CBP in p53 Regulation.....	29
1.9 Summary	34
Chapter 2: Activation of Nuclear CBP E3 Autoubiquitination Activity and Differential CBP Post-Translational Modifications in Response to DNA Damage.	36
2.1 Introduction.....	36
2.2 Materials and Methods	39
2.3 Results	46
2.4 Summary	65
Chapter 3: Novel Interaction between CBP and DBC1 and Regulation of CBP Ubiquitin Ligase Activities	66
3.1 Introduction.....	66
3.2 Materials and Methods	68
3.3 Results	77
3.4 Summary	118
Chapter 4: Discussion and Future Perspective	119
Appendix	132
List of References	139

List of Tables

Table 1: Post-translational Modification (PTM) of cytoplasmic and nuclear CBP identified by mass spectrometry	61
Table 2: List of cytoplasmic CBP-interacting proteins ranked from highest to lowest total spectrum count. (1-18).....	82
Table 2: List of cytoplasmic CBP-interacting proteins ranked from highest to lowest total spectrum count. (19-36).....	83
Table 2: List of cytoplasmic CBP-interacting proteins ranked from highest to lowest total spectrum count. (37-55).....	84
Table 2: List of cytoplasmic CBP-interacting proteins ranked from highest to lowest total spectrum count. (56-70).....	85
Table 3: List of nuclear CBP-interacting proteins ranked from highest to lowest total spectrum count. (1-18).....	86
Table 3: List of nuclear CBP-interacting proteins ranked from highest to lowest total spectrum count. (19-33).....	87
Table 3: List of nuclear CBP-interacting proteins ranked from highest to lowest total spectrum count. (34-48).....	88
Table 4: Gene alterations of TP53 and DBC1 obtained from the Cancer Genome Atlas (TCGA) database across cancer types	116
Table 5: List of cytoplasmic-interacting CBP proteins after DNA damage ranked from highest to lowest total spectrum count. (1-20).....	134
Table 5: List of cytoplasmic-interacting CBP proteins after DNA damage ranked from highest to lowest total spectrum count. (21-40).....	135
Table 5: List of cytoplasmic-interacting CBP proteins after DNA damage ranked from highest to lowest total spectrum count. (41-60).....	136
Table 6: List of nuclear CBP-interacting proteins after DNA damage ranked from highest to lowest total spectrum count. (1-19).....	137
Table 6: List of nuclear CBP-interacting proteins after DNA damage ranked from highest to lowest total spectrum count. (20-37).....	138

List of Figures

Chapter 1

Figure 1.1 Schematic representation of CBP and p300.	3
Figure 1.2 Mechanism of CBP/p300 transcriptional co-activation	7
Figure 1.3 Schematic representation of protein ubiquitination and proteasome degradation pathway	27
Figure 1.4 Schematic representation of different types of ubiquitin modifications on protein substrate and their functional outcomes	28
Figure 1.5 Schematic representation of the dual roles of CBP in p53 regulation	33

Chapter 2

Figure 2.1 Activation of nuclear CBP autoubiquitination in response to doxorubicin	47
Figure 2.2 Activation of nuclear CBP autoubiquitination in response to etoposide.....	48
Figure 2.3 Activation of nuclear CBP autoubiquitination in response to gamma irradiation (IR)	49
Figure 2.4 Activation of nuclear CBP autoubiquitination in response to	50
Figure 2.5 ATM kinase activity is not necessary for DNA damage-induced nuclear CBP autoubiquitination.....	53
Figure 2.6 Inhibition of ATR kinase activity reduces the DNA damage-induced nuclear CBP autoubiquitination	54
Figure 2.7 ATR depletion reduces the DNA damage-induced nuclear CBP autoubiquitination.....	55
Figure 2.8 Immunofluorescence microscopy of CBP nuclear distribution in the presence and absence of DNA damage.....	57
Figure 2.9 Immunofluorescence microscopy of CBP and PML in nuclear bodies in response to doxorubicin.....	58
Figure 2.10 Acetylation of CBP in response to Doxorubicin	62
Figure 2.11 Doxorubicin-induced p53 ubiquitination	64

Chapter 3

Figure 3.1 Identification of activators and/or inhibitors of CBP E3 autoubiquitination....	78
Figure 3.2 Silver staining of CBP immunoprecipitations from cytoplasmic and nuclear fractions of U2OS cells	80
Figure 3.3 Identification of CBP by MudPIT analysis from cytoplasmic and nuclear CBP IPs of U2OS cells	81
Figure 3.4 Venn diagram representation of cytoplasmic CBP interacting proteins from two independent experiments.....	89
Figure 3.5 Venn diagram representation of nuclear CBP interacting proteins from two independent experiments.....	90
Figure 3.6 Venn diagram representation of CBP-interacting proteins.	91
Figure 3.7 Identification of DBC1 by MudPIT analysis from cytoplasmic and nuclear CBP IPs of U2OS cells	93
Figure 3.8 DBC1 stably interacts with CBP in cells	94
Figure 3.9 Immunofluorescence microscopy of CBP and DBC1 in U2OS and H1299 cells.....	95
Figure 3.10 Schematic diagram of full-length (FL) DBC1, full-length CBP and deletion mutants of DBC1 and CBP.....	97
Figure 3.11 N-terminus of DBC1 is required for the CBP-DBC1 interaction.....	98
Figure 3.12 Both N- and C- terminal regions of CBP are necessary for the CBP-DBC1 interaction	99
Figure 3.13 DBC1 inhibits nuclear CBP E3 autoubiquitination activity	101
Figure 3.14 DBC1 depletion decreases p53 half life	104
Figure 3.15 DBC1 depletion increases p53 polyubiquitination	105
Figure 3.16. U2OS cells expressing DBC1 shRNA	106
Figure 3.17 Re-expression of DBC1 stabilizes p53 in the Cytoplasmic compartment of DBC1 depleted cells.....	107
Figure 3.18 Re-expression of DBC1 stabilizes p53 in the Nuclear compartment of DBC1 depleted cells	108
Figure 3.18 Re-expression of DBC1 reduces p53 polyubiquitination in DBC1 depleted cells.....	109

Figure 3.19 Interaction of CBP and DBC1 in response to doxorubicin-induced DNA damage	111
Figure 3.20 Analysis of p53-dependent targets following Dox treatment in CBP and DBC1 stably deficient cells	114
Figure 3.21 Analysis of p53-induced apoptosis in CBP and DBC1 stably deficient cells.....	115
Figure 3.22 TCGA database of tumors with DBC1 alterations retaining wild-type p53 status.	117
Figure 4.1 Graphic summary of CBP-DBC1 interaction and p53 degradation in the absence of cellular stress.	131

List of Abbreviation and Symbols

α	Alpha
a.a.....	Amino acid
ATM.....	Ataxia telangiectasia mutated
ATR.....	ATM and RAD-3 related
ATP.....	Adenosine triphosphate
AD.....	Alzheimer disease
ADI.....	Androgen depletion independent
β	Beta
BRCA1.....	Breast cancer 1
CARM1.....	Co-activator associated arginine methyltransferase
CBP.....	CREB binding protein
CREB.....	Cyclic adenosine monophosphate response element-binding protein
CH.....	Cysteine histidine
Δ	Deletion
DBC1.....	Deleted in breast cancer 1
DNA.....	Deoxyribonucleic acid
DOX.....	Doxorubicin
DSB.....	Double strand breaks
E1.....	Ubiquitin activating enzyme
E1A.....	Early region 1 A
E2.....	Ubiquitin Conjugating enzyme

E3.....Ubiquitin ligase enzyme
E4.....Ubiquitin chain conjugating factor
E6AP.....Human papillomavirus E6-associated protein
ETP.....Etoposide
HAT.....Histone acetyltransferase
HDAC.....Histone deacetylase
HECT.....Homologous to the E6AP carboxyl terminus
IgG.....Immunoglobulin G
IP.....Immunoprecipitation
IR.....Irradiation
KAT.....Lysine acetyltransferase
MudPIT.....Multi dimensional protein identification technology
NF κ B.....Nuclear factor kappa-light-chain-enhancer of activated B cells
PBS.....Phosphate buffered saline
PML.....Promyelocytic leukemia
PTM.....Post translational modification
RING.....Really interesting gene
shRNA.....Short interfering ribonucleic acid
siRNA.....Small interfering ribonucleic acid
 μMicro
 μ M.....Micromolar
Ub.....Ubiquitin
WB.....Western blot

Abstract

INVESTIGATING THE MECHANISM OF THE COMPARTMENTALIZED CBP (CREB-BINDING PROTEIN) UBIQUITIN LIGASE ACTIVITIES

By Oluwatoyin E. Akande, PhD

A dissertation submitted in partial fulfillment of the requirements for the degree of Doctor of Philosophy at Virginia Commonwealth University

Virginia Commonwealth University, 2016

Advisor: Steven R. Grossman, M.D/Ph.D.
Dianne Nunnally Hoppes Chair in Cancer Research
Professor and Chair of Hematology, Oncology, and Palliative Care
Deputy Director of VCU Massey Cancer Center
Virginia Commonwealth University

CBP (CREB Binding Protein) is global transcriptional co-activator and histone acetyltransferase. CBP is involved in the modulation of the transcription of many genes via histone acetylation at the promoter regions of the target genes. Also, non-histone proteins and transcription factors can be acetylated by CBP to promote their transcriptional activation. In addition to its transcription co-activator role, CBP is involved in many other pathological and physiological cellular processes such as cell growth and differentiation, cell transformation and development, response to stress, cell cycle regulation and apoptosis.

CBP and its paralogue p300, play double-edged roles in the regulation of p53, a well characterized tumor suppressor protein, via ubiquitination and acetylation activities. Prior work has shown that CBP and p300 contribute to the maintenance of physiologic p53 levels in unstressed cells via a cytoplasmic but not nuclear, p53-directed E4 polyubiquitin ligase activity, subsequently leading to p53 proteasomal degradation. Our

previous work also revealed that CBP and p300 possess intrinsic cytoplasmic but not nuclear E3 autoubiquitination activity in the absence of cellular stress. The mechanism of the compartmentalized CBP/p300 ubiquitin ligase activities was not studied. In this thesis, I present insights gained from efforts to determine the regulation of CBP ubiquitin ligase activities in the cytoplasm versus nucleus, in the absence and presence of DNA damage stress. Chapter two discusses the effect of DNA damage on CBP E3 autoubiquitination activity and also addresses the differential post translational modifications between cytoplasmic and nuclear CBP, in the absence and presence of DNA damage. Aspects of the regulation of the compartmentalized CBP ubiquitin ligase activities in the absence of cellular stress were covered in chapter three. We employed Multidimensional Protein Identification Technology (MudPIT) and mass spectrometry analysis of purified cytoplasmic and nuclear CBP to identify nuclear and cytoplasmic CBP interacting proteins. MudPIT analysis revealed that Cell Cycle and Apoptosis Regulator protein (CCAR2), also known as Deleted in Breast Cancer 1 protein (DBC1), is a novel CBP-interacting protein, in the cytoplasmic and nuclear compartments. Functional analysis suggested that DBC1 directly regulates cellular compartmentalization of CBP E3 and p53-directed E4 ubiquitination activities. This work identifies the different regulatory mechanisms of differential CBP ubiquitin ligase activities in the absence and presence of DNA damage. Remarkably, DBC1 was identified as a novel binding partner of CBP and a critical regulator of CBP ubiquitination activities towards p53. This work may provide novel strategies for the development of cancer therapeutics against tumors maintaining wild type p53, which have deleted DBC1.

Chapter 1: Introduction

1.1 Initial Identification of CBP and its paralogue, p300

CBP (cyclic adenosine monophosphate (cAMP) response element binding protein (CREB)-binding-protein) was originally identified in 1993 by John Chrivia in Goodman's group, as a binding partner of phosphorylated CREB [1]. A human thyroid λ gt11 library was screened with recombinant CREB labeled with (γ - 32 P) ATP and the complementary DNA obtained from the positive clone was in turn used to screen a mouse brain cDNA library, resulting in the discovery of 265kDa mouse CBP [1]. This group demonstrated that the activation domain of phosphorylated CREB is required for binding CBP and that non phosphorylated CREB could not interact with CBP. Using indirect immunofluorescence technique, they showed that CBP mostly localizes to the nucleus with some found in the cytoplasm [1].

p300, a nuclear phosphoprotein, is a functional homologue of CBP [2]. p300, like CBP, binds phosphorylated CREB and participates in the transcription of CREB-modulated genes through evolutionary conserved domains [2]. p300 was initially identified as a binding partner of the human adenovirus early-region 1A (E1A) protein in the early 1980's. The identification of this 300kDa protein resulted from an attempt to elucidate the domains required for the transformation and oncogenic properties of human adenovirus E1A, the first viral proteins that are produced following adenovirus

infection [3]. Later in 1988, Cay Egan and his group revealed that the binding site of p300 lies in the extreme amino-terminus region of E1A, a region required for its oncogenic transformation property [4]. In a separate study carried out in 1992, the oncogenic transformation and transcription repression abilities of E1A were examined in response to abolishing the interaction between E1A and p300 [5]. The mutant forms of E1A incapable of interacting with p300 were observed to have reduced oncogenic transformation ability and also failed to repress transcription from different promoters tested [5]. CBP was also found to interact with the human adenovirus E1A protein [2].

Even though different genes encode CBP and p300, they are both very similar structurally and functionally (Fig. 1.1). As a result, these two proteins are oftentimes referred to in many literatures as CBP/p300. It is noteworthy however, that there are notable functional differences between CBP and p300 and as such, are not all the time interchangeable. Both proteins contain more than 2400 residues with the following interaction domains: the nuclear receptor interaction domain (RID), the CREB and MYB interaction domain (KIX), three cysteine/histidine regions (TAZ1/CH1, CH2, and TAZ2/CH3), the bromo domain, the histone acetyltransferase domain and the C-terminus glutamine-proline rich region (Fig. 1.1).

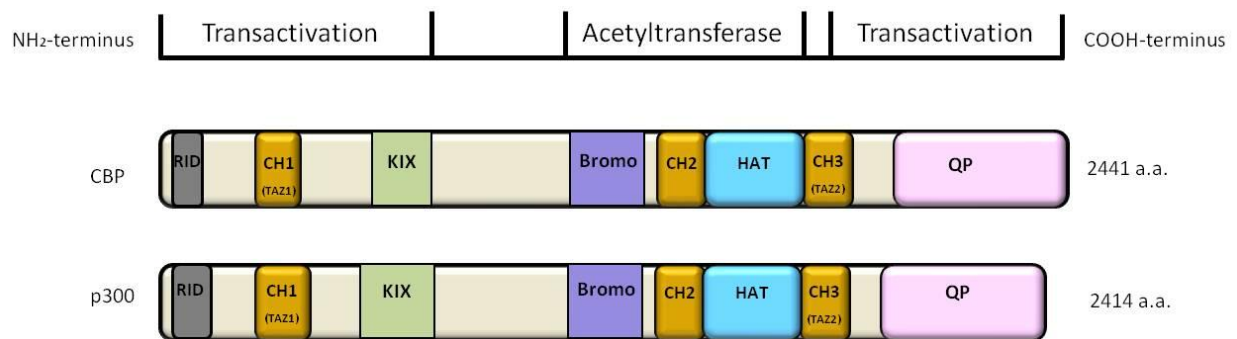


Figure 1.1 Schematic representation of CBP and p300. RID, receptor-interacting domain; CH1-3, cysteine and histidine-rich regions 1-3; KIX, binding site of CREB; BD, bromodomain; HAT, histone acetyltransferase domain; QP, glutamine- and proline-rich domain

1.2 CBP and p300 are Histone Acetyltransferases

Histone acetyltransferases (HATs) are enzymes that participate in the acetylation of specific lysine residues on histone proteins thereby promoting gene activation and transcription. Histone acetylation is a type of post-translational modification that correlates with chromatin remodeling. HATs function by transferring acetyl group from acetyl-coenzyme A to the epsilon amino group of lysine side chains on the N-terminal region of histone tails. Mammalian HATs are grouped into four families based on sequence similarity and based on related substrate specificity within families [6]. The families are: the MYST family, GCN5 and PCAF family, KATs (lysine or K-acetyltransferases) family and the nuclear receptor co activator family [6, 7]. Despite the high degree of sequence similarity between HAT family members, there are differences in the HAT domain sequences between families [6].

CBP and p300 are homologous proteins that comprise the KAT3 family of HATs [6, 8]. Both proteins consist of over 2400 amino acids. It has been shown that both CBP and p300 possess the ability to acetylate all four histone proteins in nucleosomes even though they do not contain the conserved motif present in other acetyltransferases [7, 8]. The histone acetyltransferase domain of p300 was shown to be located between the bromodomain and the E1A-binding domain and in CBP, between the residues 1174-1850, which is the corresponding region [8]. Most of the well-studied conserved domains of CBP and p300 have diverse arrays of interacting protein partners. Despite the high levels of homology between CBP and p300, both proteins exhibit unique

differential functions and they also have differential substrate specificity profiles and therefore not interchangeable.

The HAT activity of CBP/p300 has become an important therapeutic target and has been shown to be inhibited by the adenoviral protein E1A, interaction with various transcription factors and by synthetic and non-synthetic specific inhibitors [9-13]. The design and application of peptide CoA conjugates as selective synthetic HAT inhibitors was first described in 2000 where Lys-CoA was found to specifically inhibit p300 acetyltransferase activity in in vitro transcriptional studies [11]. Curcumin (diferuloylmethane), an anti-tumor and anti-inflammatory agent was reported to repress acetylation of histones by CBP/p300 thereby inhibiting transcription and in addition, inhibited p300-mediated acetylation of p53 [12].

On the basis of the structure of the p300 HAT domain, a selective, potent and cell permeable small molecule inhibitor known as C646 was developed and has been used to determine the role and importance of p300 HAT in prostate cancer [13]. It has been shown that inhibition of p300 HAT using C646 has effect on tumor cell progression, cellular senescence and DNA damage response in melanoma cell lines [14]. Aberrant HAT activity has been implicated in several human diseases such as cancer, metabolic processes and inadequate long-term memory formation [6, 15].

1.3 The Role of CBP/p300 in Transcription and other Cellular Processes

A. Role in Transcription

Eukaryotic gene transcription is a process regulated by DNA binding transcription factors that recognize promoters of target genes. CBP and p300 are highly conserved

co-activators that can interact with the basal transcription machinery and also with different DNA binding transcription factors. As a result, they are being referred to as global regulators of transcription [16]. CBP/p300 also functions as co-activators for nuclear receptors [17, 18]. Recruitment of CBP/p300 to the basal transcription machinery by DNA binding factors can occur via direct and indirect interactions, and the transactivation domains (TADs) of CBP/p300 mediate protein-protein interactions with TADs of DNA-binding transcription factors and basal transcription machinery as well as with TADs of different transcription activators [19, 20]. Even though histone acetylation through the intrinsic HAT domain of CBP/p300 has been considered as the major universal mechanism by which CBP/p300 modulate transcription of target genes, [21] other mechanisms have also been described. These mechanisms are: acetylation of non-histone transcription factors such as p53, E2F1, MEF2 [22-24], physical bridges or scaffold for DNA-binding and general transcription factors [25, 26], and recruitment of components of RNA polymerase II machinery [27] (Fig. 1.2).

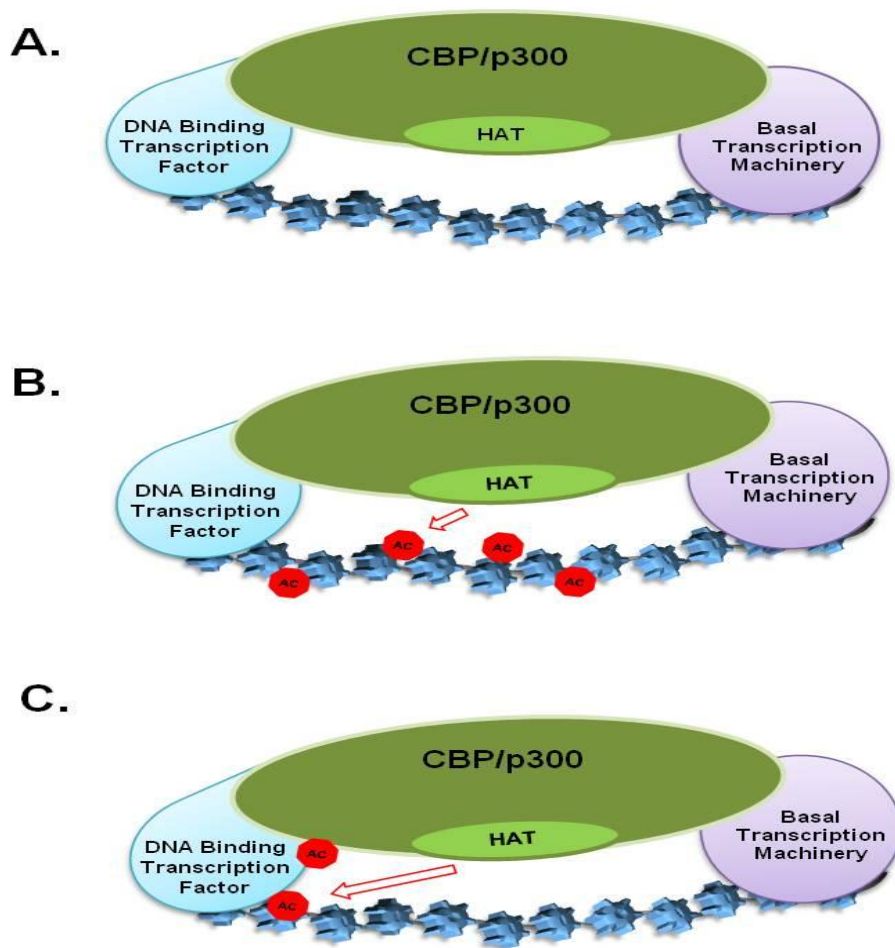


Figure 1.2 Mechanism of CBP/p300 transcriptional co-activation. A. CBP/p300 as bridges between DNA binding transcription factors and the basal transcription machinery. B. CBP/p300 as histone acetyltransferase causing chromatin relaxation thereby promoting transcription of target genes. C. CBP/p300 as non-histone acetyltransferase. Acetylation of certain DNA binding transcription factors.

B. Acetylation of non-histone proteins by CBP/p300

The global transcriptional coactivators CBP and p300, in addition to possessing intrinsic histone acetyltransferase property also have the ability to acetylate other non-histone proteins and transcription factors thereby stimulating transcription [21]. The first discovered and well-studied non-histone protein acetylated by both CBP and p300 is p53 [22, 28]. p53 is a DNA sequence specific transcription factor and a tumor suppressor protein that in response to DNA damage initiates cell cycle arrest or apoptosis. Its transcriptional activity is tightly regulated in particular by posttranslational modifications of the C-terminal regulatory regions [28-30]. In response to DNA damage, carboxyl-terminal lysine residues of p53 become acetylated via its direct interaction with CBP/p300. This acetylation process was observed in both in-vivo and in-vitro studies and was shown to greatly increase the transcriptional activity of p53 [27]. Another non-histone protein acetylated by CBP is the E2F transcription factor [23]. E2F is required for the transcription of S-phase genes during the cell cycle. It was shown that acetylation of E2F by CBP/p300 and CBP/p300-associated factor P/CAF stimulates the functions of E2F [23]. Other non-histone proteins whose transcriptional activation is enhanced as a result of acetylation by CBP and/or p300 include; c-Myb, an oncoprotein and regulator of proliferation and differentiation of certain cell types [31, 32], myocyte enhancer factor 2 (MEF2) protein [24], GATA-1 which is involved in the differentiation of certain blood cells [33], erythroid kruppel-like factor (EKLF), a vertebrate red blood cell specific transcription factor [34, 35].

C. Role in Other Cellular Processes

In addition to regulating transcription of target genes, CBP and p300 are involved in a variety of other complex pathological and physiological cellular processes. These processes include; cell growth and differentiation, cell transformation, response to stress, cell cycle regulation and apoptosis [36-44].

Aberrant expression of CBP/p300 results in developmental abnormalities such as Rubinstein and Taybi syndrome (RTS) in humans and in animal models [36]. RTS is a well-characterized human developmental disorder resulting from mutations in CBP and characteristic features of this disorder include mental retardation, abnormal facial structure, growth retardation, microcephaly and other digital anomalies [36]. Also, it was found that interaction of the adenovirus protein E1A with CBP/p300 was crucial for E1A to induce transformation of rodent cells [37] where E1 A mutants incapable of interacting with CBP/p300 lost the ability to induce transformation of rodent cells. CBP and p300 are also integral players in cellular responses to stress and in cell cycle regulation. During oxygen deprivation, CBP/p300 forms a complex with the heterodimeric transcription factor hypoxia- inducible factor (HIF)-1 α . This complex participates in signaling events that eventually lead to the activation of multiple hypoxia-activated genes [38].

Studies carried out in *Caenorhabditis elegans* and in mice by Rebel *et al.*, (2002) suggested that CBP/p300 play a crucial role in hematopoietic stem cell (HSC) fate self-renewal and differentiation [42]. It was observed from these studies that full dose of CBP but not p300 was necessary for HSC self-renewal. Monoallelic loss of CBP

resulted in a critical reduction in HSC self-renewal ability while a much less reduction was observed in a single loss of p300. Conversely, their data indicated that p300 but not CBP was significantly important for proper hematopoietic differentiation [42].

In 2000, Ait-Si-Ali demonstrated the importance of CBP/p300 during the G1/S transition of the cell cycle. By artificial modulation of CBP/p300 levels in cells using microinjection of specific antibodies and expression vectors, they showed the requirement of CBP/p300 in cell proliferation and in G1/S transition [43]. By measuring BrdU incorporation, synchronized serum-deprived NIH3T3 cells injected with anti CBP/p300 antibodies showed delayed entry into S phase when compared to control cells. In this same study, it was observed that CBP/p300 is necessary for the activity of E2F transcription factor during the transition from G1 to S phase of the cell cycle.

The role of p300 but not CBP in apoptosis induced by DNA damage caused by cell irradiation has been described. It was observed that p300 but not CBP regulates the sensitivity of human MCF-7 breast cancer cells to irradiation and also plays a role in apoptosis in response to DNA damage [44]. The results from this study showed that p300 deficient cells had less irradiation- induced sub G1 DNA content when compared to controls and CBP deficient cells [44].

1.4 CBP and Human Diseases

CBP plays important roles in a number of human diseases and cancer. This is not surprising as CBP is involved in numerous cellular physiological and pathological processes.

A. Role in Cancer

Whether CBP functions as a tumor suppressor or contributes to tumor development has been an issue of debate that majorly depends on the physiologic characteristic of the tumor and the overall cellular background or context. CBP participates in many tumor-suppressor pathways and is also required for the action of many oncogenes [36]. Interaction of CBP with p53 is an example of the tumor suppression function of CBP. Acetylation of p53 by CBP/p300 contributes to the ability of p53 to activate transcription of genes that are involved in the response to DNA damage thereby suppressing tumor growth [22, 28, 45].

CBP also interacts physically and functionally with BRCA1, a breast and ovarian cancer-specific tumor suppressor protein and a transcription factor involved in DNA damage repair [46]. This interaction was observed in both in vitro and in vivo experiments and p300 promoted BRCA1-mediated transactivation. In this study it was further indicated that the adenovirus E1A oncoprotein suppressed the interaction between CBP/p300 and BRCA1 and this led to inhibition of the tumor suppression function of BRCA1 [46]. CBP also interacts with other tumor suppressors and protooncoproteins such as c-Myb as previously mentioned [32, 36, 47], c-Jun and c-Fos [48-51]. The viral oncoprotein, human T-cell leukemia virus (HTLV-1), also requires interaction with the CREB binding domain of CBP/p300 for its transcriptional functions [36, 52-54].

Early studies have shown that some other viral oncoproteins such as adenovirus E1A, human papillomavirus E6 and simian virus (SV) 40 T antigen, have inhibitory

effects on CBP/p300 functions [36, 55-57]. These viral oncoproteins tend to bind the third zinc finger domain of CBP/p300. This association interferes with interactions with transcription factors and other positive effectors such as RNA helicase A, transcription factor IIB (TFIIB), and the histone acetylase P/CAF, and as a result, abrogates the coactivator property of CBP/p300 [36, 56, 58]. The E6 protein was shown to direct ubiquitination and degradation of the tumor suppressor p53 by recruiting p53 into a complex containing the ubiquitin protein ligase E6 associated protein (E6AP) [59]. In a separate study carried out by Zimmermann and colleagues (1999), it was reported that the down regulation of p53 transcriptional activity occurs through targeting the p53 coactivators CBP and p300 [60]. Their data suggested that by targeting CBP/p300, an E6 from a high risk type but not a low risk HPV type repressed p53 dependent transcription. Similar effect of inhibition of transcriptional activity of p53 by targeting coactivator function of CBP and p300 was also observed with the E6 oncoprotein of bovine papillomavirus type 1 (BPV-1) [61].

Germline mutations (point mutations, translocations or deletions) of CBP result in Rubinstein-Taybi syndrome (RTS), a genetic developmental disorder characterized by broad thumbs and toes, short stature, abnormal facial features and mental disabilities [36, 62, 63]. RTS patients have a much greater risk of developing certain types of cancer especially childhood neural and developmental tumors [36, 64]. RTS is a haploinsufficiency disorder and clinically, only about 3-25% of patients have deletions that can be detected by fluorescence in situ hybridization (FISH) [65, 66]. Work done by another team however, suggested that the presence of a detectable deletion by FISH corresponds with a more severe phenotype [67]. Skeletal abnormalities resulting from

aberrant BMP-7 signaling have been described in mouse models of RTS [68], but it remains uncertain whether these abnormalities compare with those found in human RTS patients [69].

Chromosomal translocations targeting CBP gene have been found in leukemias and lymphomas. Two different somatic translocations involving CBP are seen in acute myeloid leukemia (AML); t (8,16) (p11, p13) and t (11,16) (q23, p13.3) [70-72]. The t (8,16) translocation was first observed in the M4/M5 French-American-British (FAB) subtype of AML [73, 74]. This abnormality is mostly characterized by erythrophagocytosis as seen in about 76% of t (8;16) cases. The two genes rearranged at the breakpoints resulting from t (8,16) (p11, p13) translocation in AML are CBP and the monocytic leukemia zinc finger protein (MOZ) gene which encodes MOZ protein, a putative acetyltransferase. The somatically acquired MOZ-CBP fusion protein combines MOZ DNA-binding motifs and the CBP acetyltransferase domain. This oncogenic MOZ-CBP protein was thought to promote leukemogenesis through aberrant chromatin acetylation [75]. It was shown that although the translocation breakpoints within CBP preserves most of its functional domains, though the domain that binds the nuclear receptor RAR α is lost. The resulting MOZ-CBP fusion protein therefore causes deregulation of retinoid pathways which play an important role in leukemogenesis [75].

The oncogenic role of CBP and p300 has been described in prostate cancer. Both CBP and p300 act as coactivators for androgen receptor (AR) protein, a sequence-specific DNA binding nuclear receptor that regulates ligand-dependent gene transcription and also plays a role in prostate cancer cellular proliferation [76-78]. CBP and p300 are both upregulated in prostate cancer and they also induce the transcription

of AR responsive genes [79]. It was demonstrated that CBP plays a role in the acquisition of therapy resistance in prostate cancer progression by the regulation of the action of the anti-androgen hydroxyflutamide [79]. In a separate study, CBP depletion was shown to have antiproliferation effects on the PC3 cancer cell line [13]. However, in the C4-2B cell line, p300 appears to be dominant over CBP in the transition from androgen dependent to androgen depletion independent (ADI) prostate cancer, an advanced form of prostate cancer [80].

It has also been suggested that overexpression of CBP and p300 may be involved in the poor prognosis of small cell lung cancer (SCLC) patients through inhibition of apoptosis and increased ability for lymph vessel formation [81].

B. Role in other Human Diseases

Apart from its role in human cancer types, CBP loss of function has been observed in different contexts in human neurodegenerative disorders such as Huntington disease (HD) [82], Alzheimer disease (AD) [83], amyotrophic lateral sclerosis (ALS) [84], polyglutamine (polyQ) diseases [85], spinocerebellar ataxia type 7 (SCA7) [86] and spinal and bulbar muscular atrophy (SBMA) [87]. Several reports have demonstrated that the interaction between the CBP HAT domain and the mutated form of the huntington protein (htt) causes inhibition of HAT activity which is responsible for the expanded polyQ aggregates seen in HD conditions [82, 88-89]. In 2003, in a separate study carried out by Haibing Jiang *et al.*, they found that polyQ-expanded htt promotes ubiquitination and degradation of CBP [90]. Alternatively, CBP loss of function in neurological disorders can also be attributed to caspase 6 –induced CBP degradation

as observed during neuronal apoptosis events [91]. This degradation was shown to lead to a decrease in histone acetylation and also a decrease in CBP dependent transcription.

The role of CBP in hepatic gluconeogenesis, a biological process essential in the maintenance of normal blood glucose levels has been described [92]. The effect of insulin and the molecular therapeutic effect of metformin, a first line treatment for diabetes mellitus, lead to CBP phosphorylation at Ser436 [93]. This phosphorylation event triggers the disassembly of a CREB- TORC2- CBP transcriptional complex formed on a cAMP responsive element site, thereby inhibiting transcription of gluconeogenic enzyme genes and ultimately resulting in the suppression of hepatic gluconeogenesis [92-96]. As demonstrated by Zhou *et al.*, and also by He *et al.*, metformin treatment failed to suppress high blood glucose levels in a mouse model with germline mutation of the CBP phosphorylation site [92, 94]. Their results point to the importance of CBP phosphorylation by insulin and metformin in the activation and regulation of hepatic gluconeogenesis.

A role for CBP in long-term memory formation is suggested by the findings that the histone acetyltransferase property of CBP is necessary for memory consolidation [97]. Transgenic mice expressing CBP with defective HAT activity show impaired long-term memory formation that can be rescued by suppression of transgene expression or by inhibition of histone deacetylase activity, suggestive of the importance of CBP HAT activity in the activation of genes controlling memory consolidation [97]. Mouse models have revealed the critical importance of CBP in normal embryonic development as mice

lacking CBP die at an early embryonic stage as a result of defective blood vessels formation in the central nervous system [68, 98].

1.5 CBP as a Therapeutic Agent

CBP and its paralog p300 play important roles in the regulation of transcription of many genes via histone and non-histone protein acetylation [16-20, 22-24]. These proteins are also critically involved in other cellular physiological processes. Specifically, aberrant functioning of the HAT domain of CBP and p300 is often associated with some human diseases and cancer [36, 46, 63, 64]. In addition, loss of function of CBP has been reported in different neurological disorders [82-87]. As a result, different ameliorative strategies targeting CBP for the treatment of these anomalies are constantly being studied.

In an attempt to reverse CBP loss of function found in neurological disorders, CBP activation was demonstrated to reduce polyQ aggregates and neurodegeneration as well as improve histone acetylation and CBP-dependent transcription [91]. It has also been shown that CBP over-expression is sufficient in reversing cellular toxicity in Huntington's disease models, further linking inadequate amount of CBP to the development of this disease [99]. Also, it was found that viral delivery of CBP into the brain of mouse models of Alzheimer's disease improves both learning and memory implying that CBP over-expression might be an ideal therapeutic intervention for brain disorders with CBP loss of function [100].

CBP/ β -catenin signaling is important in maintaining drug resistance in acute lymphoblastic leukemia (ALL), and disruption of this interaction using a specific small

molecule inhibitor ICG-001, was demonstrated to be sufficient in abrogating the drug resistance [101]. The therapeutic ability of CBP/ β -catenin antagonist was further shown to be effective in targeting cancer stem cells (CSC) without damaging the somatic stem cells (SSC), as well as in ameliorating pulmonary and renal fibrosis, and myocardial infarction [101-105].

Several small molecule inhibitors of CREB-CBP transcription factor/coactivator complex have been identified including Naphthol AS-TR phosphate (NASTrp) which was recently found to be a potential therapeutic agent for human lung cancer in particular [106, 107]. NASTrp is a modified form of the naphthol analog KG-501, initially identified as an inhibitor of CREB-CBP transcription factor/co-activator interaction [106]. It was demonstrated that NASTrp has inhibitory effects on cell proliferation, colony formation and anchorage-independent growth in a number of human lung, breast, and pancreatic cancer cell lines tested. In addition, NASTrp causes induction of endoplasmic reticulum stress, cell cycle arrest and suppression of autophagy in human lung cancer cell lines [107].

1.6 The Regulation of CBP Co-activator Role in Transcription

A. Regulation of CBP transcriptional role by other interacting partners

CBP possesses several activation domains and interacts with diverse arrays of proteins, many of which are transcription factors. As such, many researchers have reported and speculated the regulation of CBP activities. HAT dependent and HAT-independent mechanisms enable CBP to co-activate the transcription of target genes

[21-27]. Because CBP is also involved in other cellular activities, it is not surprising that its functions are regulated at different levels.

The enzymatic activity of CBP can be regulated via cooperation with other proteins. The transforming viral protein E1A was first identified as a positive regulator of CBP HAT enzymatic function by S. Ait-Si-Ali *et al.* in 1998. These investigators reported that E1A binds to a region near the HAT domain of CBP causing a conformational change in this domain that promotes increased catalytic activity [108]. This observation however contradicts the reports of some other groups that suggest an inhibitory effect of E1A on CBP HAT function [8, 109].

Transcription factors that promote cellular differentiation such as the hepatocyte nuclear factor-1 α (HNF-1 α) and the nuclear factor, erythroid-derived 2 (NF-E2) have been shown to stimulate the acetyltransferase activity of CBP in both in vivo and in vitro assays [9, 110]. Some other transcription activators, for example, the Epstein-Barr virus-encoded basic region zipper (b-zip) protein, Zta and C/EBP α have also been shown to augment the acetylation of nucleosomal histones by CBP [110]. On the other hand, cellular proteins such as Twist and the E1 A-like inhibitor of differentiation (EID-1) demonstrate inhibitory effects on CBP HAT function [109, 111].

B. Regulation of CBP transcriptional role by post translational modifications

Post translational modification is an enzymatic covalent reaction that occurs after a protein is synthesized. Most proteins undergo some type of modification following translation and these modifications can influence a protein's cellular localization and activities. CBP undergoes post translational modifications such as phosphorylation,

acetylation, ubiquitination, sumoylation, methylation and several lines of evidence have pointed to these modifications as important players in the regulation of CBP functions [36, 108, 112-119].

Phosphorylation:

Studies show that phosphorylation regulates certain CBP functions in response to different cellular signaling pathways [108, 112]. Phosphorylation by cyclin E-cyclin dependent kinase 2 (Cdk2) complex (cyclin E-Cdk2) modulates CBP HAT enzymatic activity in a cell-cycle dependent manner [108]. The phosphorylation site was mapped to the carboxyl terminal of CBP and treatment of phosphorylated CBP with phosphatase suppressed its enzymatic activation.

Calcium/calmodulin-dependent protein kinase type IV (CaMKIV), a serine/threonine protein kinase phosphorylates CBP on Ser301. This CaMKIV-mediated phosphorylation as demonstrated by Impey and his group facilitates CREB/CBP-dependent transcription while CaM kinase inhibitors blocked both the phosphorylation and CBP-dependent transcription events [112].

It has also been shown that CBP can be phosphorylated by MAP kinases. In vitro studies indicate that phosphorylation by p44 MAP kinase/ERK1 induces a conformational change in CBP which ultimately stimulates its acetyltransferase activity [113]. The phosphorylation site is at the carboxyl terminal of CBP, a region similar to that which is involved in CBP HAT activation upon phosphorylation by cycE-cdk2 [108, 113].

Further, phosphorylation of CBP by nuclear IKK α switches the binding preference of CBP from p53 to NF- κ B [114]. This IKK α - mediated CBP phosphorylation not only increases CBP HAT function, but also enhances NF- κ B-mediated gene transcription, promotes cell proliferation and in addition, contributes to tumorigenesis in the human cancer cell lines tested [114].

Acetylation:

CBP autoacetylation stimulates its interaction with other acetylated protein substrates such as acetylated histone proteins and acetylated p53 [115-117]. The acetyl lysine –binding property of the CBP bromodomain promotes its anchorage to acetylated chromatin and non-chromatin bound templates or to other acetylated transcription activators [115-117]. A study showed that autoacetylation of CBP induces a conformational change that positions CBP HAT domain and the bromodomain for easy recognition by their binding partners [117]. It was demonstrated in the study that CBP autoacetylation is necessary for CBP bromodomain to bind to acetylated lysines. Incubation of insect purified recombinant full-length CBP with acetyl CoA not only activated the ability of CBP to bind to unacetylated histone peptides via its HAT domain, but also its ability to bind to acetylated peptides via its bromodomain [117]. This CBP autoacetylation activity facilitates CBP HAT function and bromodomain mediated interactions which in turn assist in regulating transcription processes of target genes.

Ubiquitination:

Ubiquitination is the reversible covalent attachment of the short protein modifier ubiquitin to lysine residues of target proteins. The stability and function of a protein can be modulated by its ubiquitination status. Ubiquitination disrupts CBP function in neuronal cell viability in Huntington disease [90, 99]. Studies indicate that co-localization of CBP with the expanded poly - Q htt protein in nuclear aggregates in HT22 hippocampal neuronal cells, facilitates CBP degradation and the increase in the cellular toxicity of poly - Q htt aggregates. This disruption of CBP function by ubiquitination leads to reduction in the transcription of target genes [90, 99].

CBP like its paralogue p300, encode an intrinsic E3 ubiquitin ligase activity [118, 121]. Although the relevance of CBP autoubiquitination remains unclear, it is known that the regions required for this autoubiquitination process is also required for the p53-directed E4 polyubiquitin activity [118]. The first 616 amino acids of CBP, a region containing the C/H1-TAZ1 domain is required for its autoubiquitination and also sufficient to polyubiquitinate p53-monoUb conjugates [118]. Polyubiquitination of p53 leads to its proteasome-mediated degradation thereby maintaining its physiologic levels under basal cell conditions. It can therefore be speculated that CBP autoubiquitination facilitates its E4 polyubiquitination activity towards p53.

The role of Promyelocytic leukemia (PML) nuclear bodies in regulating CBP steady state and function has been described [122]. PML nuclear bodies are nuclear punctuate sub-structures that recruit a variety of unrelated proteins. PML is reported to be involved in the degradation of CBP in an ubiquitin dependent manner with the use of

histone deacetylase inhibitor, valproic acid which increases the co-localization of CBP to PML bodies and to ubiquitin nuclear speckles. This was shown to promote the subsequent degradation of CBP by the ubiquitin-proteasome pathway [122].

Sumoylation:

Sumoylation is an important post-translational modification that regulates the function of many proteins involved in various cellular processes. This modification can either occur by the covalent attachment of a member of the SUMO (small ubiquitin-like modifier) family of proteins to lysine residues in specific target proteins, or by the non-covalent SUMO binding via SIMs (SUMO-interacting motifs) [123, 124]. Four SUMO paralogues designated SUMO1-4 exist in mammals [125] and also, sumoylation process can be readily reversed by the action of a family of sentrin/SUMO-specific protease (SENP) enzymes [125, 126].

SUMO modification has become an important mechanism in regulating the activities of many transcriptional activators, including CBP, which can be modified covalently by SUMO-1 at lysine residues 999, 1034, 1057, both in vitro and in vivo [119]. SUMO modification of CBP facilitates its interaction with Daxx protein, a transcriptional co-repressor found in the nucleus [127]. The SUMO-dependent association of CBP with Daxx mediates the recruitment of histone deacetylase 2 (HDAC2) leading to transcriptional repression of CBP targets [119]. In a separate study, it was demonstrated that SUMO modification of CBP was necessary for its association with nuclear proteins, its accumulation in nuclear bodies and its role as a transcriptional co-activator [128].

Methylation:

This type of post-translational modification involves the transfer or addition of methyl group to a substrate. Methylation is a well-studied post-translational modification and enzymes called methyltransferases catalyze the process. Protein methylation usually occurs on arginine or lysine amino acid residues and studies have shown the importance of this modification in epigenetic inheritance and also in human cancers [129].

Methylation plays a role in the regulation of the co-activation activity of CBP. In vitro and in vivo studies from two separate laboratories have shown that the KIX domain of CBP located on its amino terminal region and also specific arginine residues (which are conserved in p300) outside of the KIX domain are methylated by CARM1 (co-activator associated arginine methyltransferase) [120, 129]. Functional studies by Chevillard-Briet *et al.*, reveal that methylation of CBP by CARM1 regulates CBP co-activating functions in steroid hormone-induced gene activation [120].

Since diverse CBP activities can be modulated by CBP-associating proteins and different post-translational modifications, there is possibility of crosstalk between these different mechanisms, although no direct evidence presently exists to support this.

Given the fact that CBP can be readily modified under various cell conditions, a particular type of post-translational modification may change CBP conformation, which in turn may control its protein binding preference, subsequently leading to regulation of specific functions. Alternatively, one type of CBP modification may be a requirement for a second type of post-translational modification, as seen with some other proteins. For example, in response to DNA damage, the ataxia-telangiectasia mutated (ATM) and

ATM-related Rad3 (ATR) kinases phosphorylate p53. Phosphorylation of p53 is necessary for its interaction with and acetylation by CBP/p300, which ultimately promotes the transactivation of p53 [28-29, 130-132]. A separate study also showed that acetylation of Foxo1, a transcription factor involved in many biological processes, increases the level of its phosphorylation, which subsequently regulates Foxo1 function (133).

With all these mentioned evidences, cross talk between the post-translational modifications of CBP may possibly modulate its protein-protein interactions which in turn, may regulate CBP activities and stability.

1.7 E3 and E4 Ubiquitin Ligases

Protein ubiquitination is a regulatory post translational modification that requires the collaboration of the cascading events of the E1 activating enzyme, E2 conjugating enzyme and E3 ubiquitin ligase. This process was first identified as a targeting signal for protein degradation via the proteasomal pathway [134], (Fig. 1.3). Ubiquitination also mediates the non-degradative regulation of other cellular processes such as signal transduction, enzymatic activation, cellular localization and DNA repair [135-138]. In the human genome, two E1 enzymes, about 40 E2 enzymes and over 600 putative E3 enzymes have been identified [139].

The first mammalian ubiquitin E3 ligase, E6AP, was identified in 1990. E6AP is a 100kDa protein that catalyzes the E6-dependent transfer of ubiquitin to p53, targeting it for degradation by the 26S proteasome [140]. E6AP belongs to the HECT (Homologous to E6-AP Carboxyl Terminus) family of E3s which contains the active-site cysteine in its

C-terminal lobe that forms a thioester with ubiquitin [141]. Alternatively, the RING (Really Interesting Gene) finger family of E3s forms a scaffold to facilitate the transfer of ubiquitin from the E2, directly to the protein substrate [142], (Fig. 1.3). A well characterized RING-type E3 ubiquitin ligase is Mdm2 (murine double minute 2) protein. Mdm2 is an important regulator of p53, that in the absence of stress, maintains low cellular levels of p53 by ubiquitinating p53, sending it for proteasomal degradation [143]. p53 in turn regulates Mdm2 transcription, thus, these two proteins form an autoregulatory negative feedback loop [142-144].

The proteolysis of some proteins requires multiubiquitin chain assembly. The polyubiquitin conjugating factor named E4 was reported to be necessary in catalyzing the polyubiquitin chain assembly needed for proteasomal degradation [145]. E4s function in concert with the E1, E2 and E3 enzymes by targeting proteins already modified with a single ubiquitin on one lysine residue, (monoubiquitinated (mono-Ub)), or by targeting proteins already modified by ubiquitin on multiple lysine residues (oligoubiquitinated (oligo-Ub)) [146], (Fig. 1.3). In 1999, the UFD2 protein of yeast was identified as the first E4 enzyme. This protein contains a U-box (UFD2-homology domain) domain which shares structural similarity with the canonical E3 RING finger domain [145]. A growing number of E4 family members are being identified and some of the reported members include the regulatory protein NOSA, the U-box containing protein, CHIP (C-terminus of Hsc70-interacting protein), which promotes the ubiquitinating activity of Parkin, BUL1/BUL2 complex, and the co-activators p300 and CBP [118, 120, 144-146].

Polyubiquitin chain formation uses different types of ubiquitin-ubiquitin chain linkages that could result in proteolytic and non-proteolytic functions. The two major ubiquitin chain linkages occur via Lys48 and Lys63 (Fig. 1.4). Ubiquitin chains linked by Lys48 have been generally accepted to target substrates for proteasomal degradation. Lys63-linked chains, in addition to their proteolytic function, are also involved in other non-proteolytic cellular activities such as intracellular trafficking, signal transduction, DNA damage repair, ribosomal biogenesis [134-137, 147, 148], (Fig. 1.4). The importance of these ubiquitin ligases in diverse cellular activities and in maintaining homeostasis cannot be underestimated.

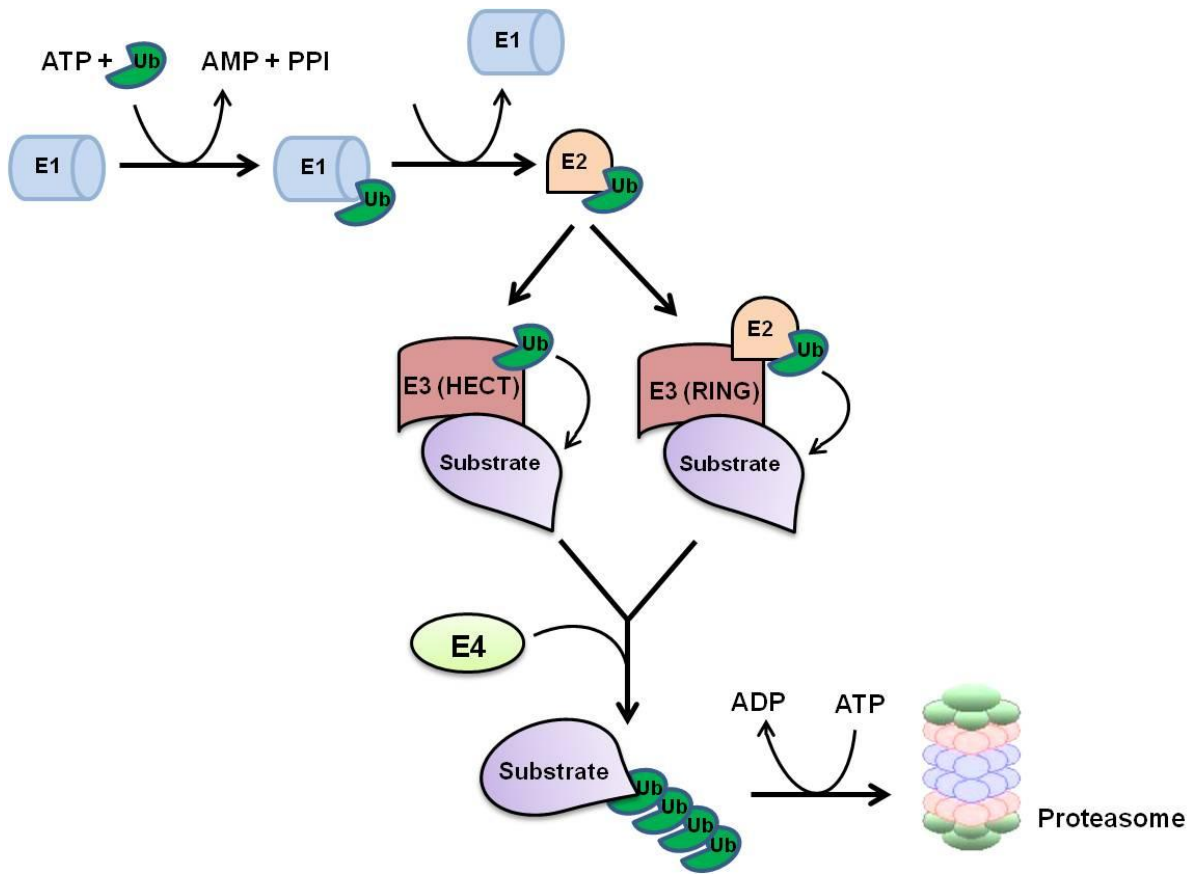


Figure 1.3 Schematic representation of protein ubiquitination and proteasome degradation pathway. In the first step, ubiquitin (Ub) gets activated by the Ub-activating enzyme (E1) in the presence of ATP. Next, activated Ub is transferred to one of several dozens of Ub-conjugating enzymes (E2) and then to one of the over 600 substrate-specific Ub-ligases E3 (HECT) or E3 (RING) which finally attaches Ub to the substrate. In some cases, additional elongation factors, termed E4 enzymes are required to catalyze the extension of short ubiquitin chains targeting the substrate for proteasomal degradation.

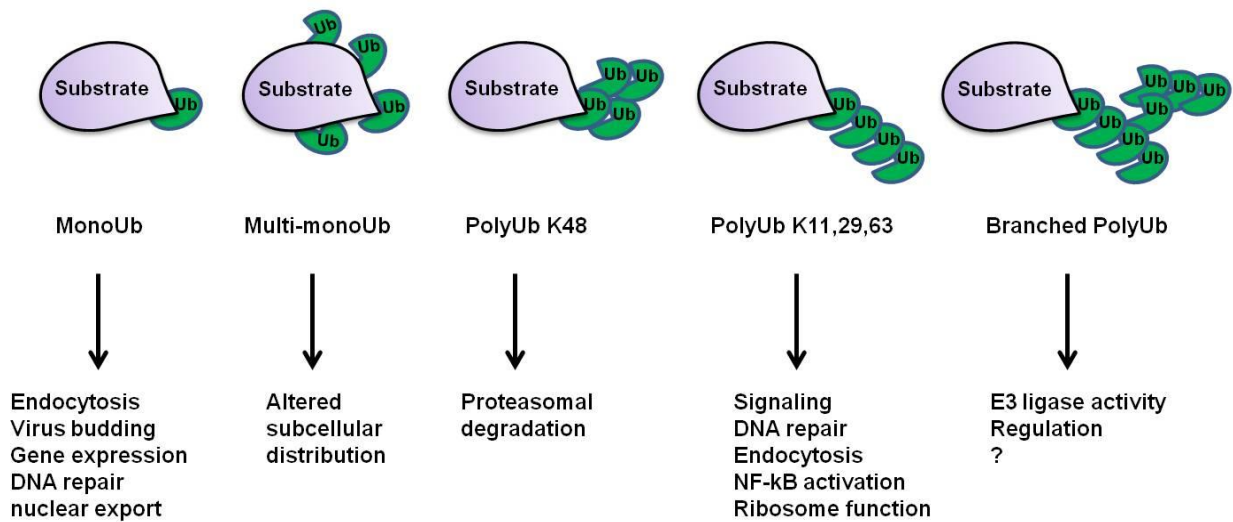


Figure 1.4 Schematic representation of different types of ubiquitin modifications on protein substrate and their functional outcomes.

1.8 The Dual Roles of CBP in p53 Regulation

The tumor suppressor protein, p53 also known as “the guardian of the genome”, is a well-characterized protein whose activation is controlled by interaction with other proteins and also by post-translational modifications [28-30, 164, 165]. Its activation in response to myriad stressors leads to events such as; inhibition of angiogenesis, activation of DNA repair, induction of cell growth arrest or apoptosis depending on the physiological cell condition and cell type [150, 151, 161]. As such, there are multiple layers of regulatory mechanisms involved in p53 signaling pathway.

Under basal cell conditions, the low steady state levels of p53 are maintained by its negative regulator Mdm2, an E3 ligase which ubiquitinates p53 marking it for degradation by the proteasome [144]. The ubiquitination property of Mdm2 depends on its C-terminal RING finger domain by which it catalyzes addition of a single ubiquitin moiety (mono-ubiquitination) on p53 [152]. Monoubiquitinated p53 moieties are exported out of the nucleus into the cytoplasm where polyubiquitination activities by E4 ligases lead to its proteasomal dependent degradation [118, 121]. It is therefore clear that although Mdm2 is required to keep p53 levels low, it may not be sufficient enough for both p53 ubiquitination and degradation [153]. Mdm2 on the other hand, also contributes to the stability and transactivation of p53 via a separate ubiquitination independent mechanism [154].

A. Role of CBP in p53 degradation

The degradation and stability of p53 can be further regulated by the compartmentalized activities of CBP and its paralog, p300 under different cellular conditions. The relationship between p53 and CBP/p300 is therefore quite complex as a result of these compartmentalized activities of CBP/p300 [20, 22]. The N-terminal region of CBP and p300 containing the first 616 amino acids harbor a conserved Zn²⁺-binding Cys-His-rich region which functions as putative E3 and E4 ubiquitin ligases [118]. In vivo and in vitro evidence from previous studies from our laboratory revealed that the intrinsic E3 ligase activity of CBP drives its own ubiquitination while the E4 ligase activity directs p53 polyubiquitination and its subsequent degradation [118]. In unstressed cells, CBP and p300 drive polyubiquitination of Mdm2-mediated monoubiquitinated p53 [118, 121]. As stated earlier, monoubiquitination of p53 by Mdm2 leads to its export from nucleus to cytoplasm. Cytoplasmic CBP and p300 act as E4 ligases by extending the ubiquitin chains on p53 tagging it for degradation [118, 121, 153]. Taken together, Mdm2 co-operates with CBP and p300 to catalyze polyubiquitination and proteasomal degradation of p53.

B. Role of CBP in p53 transactivation

CBP participates in the transcriptional activation of p53 by acetyltransferase activities. CBP/p300 in addition to their intrinsic histone acetyltransferase property, possess the ability to acetylate and modulate transcription of non-histone proteins such as p53. In fact, p53 was the first identified non-histone protein acetylated by CBP/p300 and several initial studies have pointed to the positive role acetylation plays in p53 stability following cellular stress [22, 28, 30]. p53 binds both N and C-termini of CBP under different cellular conditions. Diverse cellular insults can trigger p53 activation that leads to multiple outcomes such as cell cycle arrest, apoptosis, senescence, autophagy [150, 151]. In response to DNA damage, p53 becomes phosphorylated by ATM/ATR in its amino-terminal region and these phosphorylation events are believed to prevent binding by Mdm2 [155]. It has also been shown that phosphorylation of p53 at Ser 15 stimulates its interaction and subsequent acetylation by CBP/p300 on multiple carboxyl-terminal lysine residues which in turn, promotes p53 transcriptional functions [127, 155]. In addition, p53 acetylation is also important in other p53 activities necessary for its checkpoint responses to different stress sensors [156, 157]. In an early study, it was revealed that mutations that abolished phosphorylation at Ser 15 reduced p53 acetylation events and caused p53-dependent transcriptional defects [155]. A separate study also showed that inhibition of p53 deacetylation promotes p53 stability further indicating the importance of CBP/p300 mediated acetylation in p53 stability and transcriptional function [156]. Both CBP and p300 are more abundant in the nucleus where p53 accumulation and acetylation mostly occurs in response to cellular stress.

These dual roles of CBP and p300 in p53 regulation make them important targetable proteins in the p53 pathway and in cancer therapy. It also raises the questions of the mechanism and types of regulators involved in these compartmentalized activities of CBP/p300 towards p53.

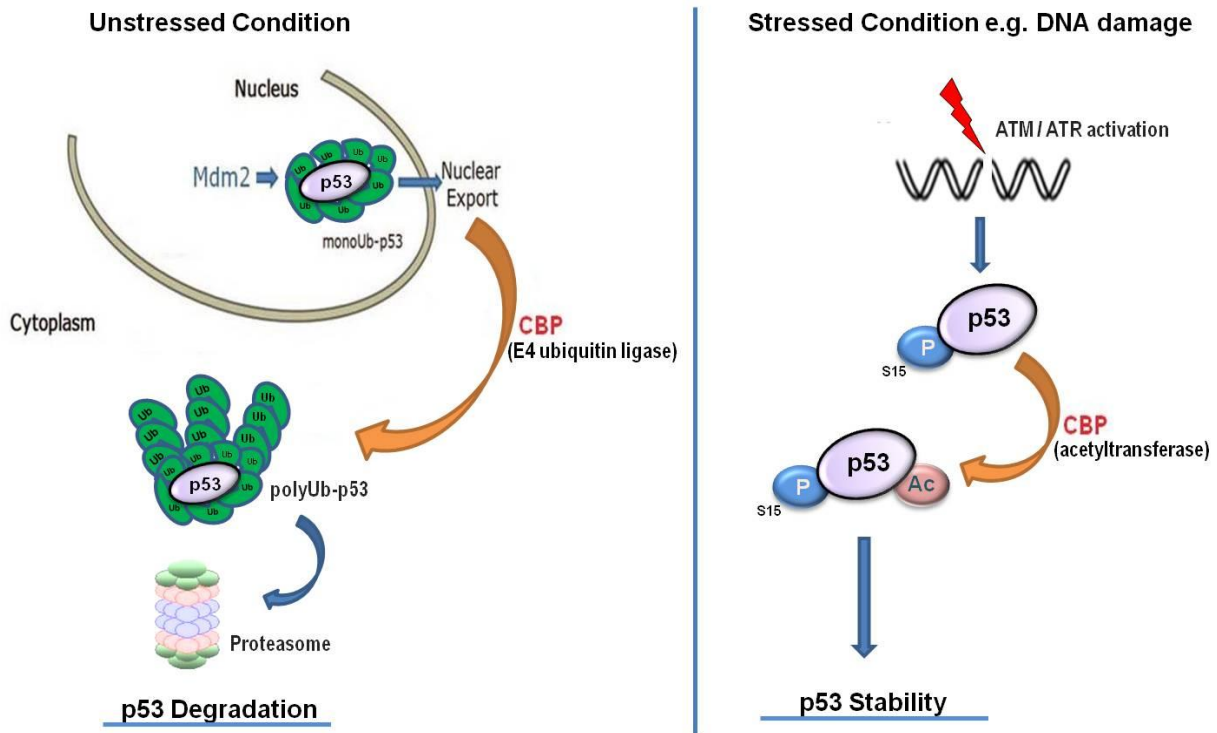


Figure 1.5 Schematic representation of the dual roles of CBP in p53 regulation

1.9 Summary

More than 20 years of research on CBP have produced comprehension of the co-activator role of CBP in the transcription of target genes and the diverse mechanisms that possibly regulate this role. Despite all this work, additional studies are still necessary to further elucidate other evolving underlying factors involved in the modulation of the transcriptional functions of CBP in response to diverse cellular conditions. In addition to its transcriptional roles, CBP participates in a diverse array of other cellular processes such as cell growth and development, cell cycle, apoptosis, and response to cellular stress sensors. It is therefore not surprising that aberrant functioning of CBP is implicated in many human diseases and cancers. As such, CBP has become a promising candidate target for therapeutic strategies. CBP's association with numerous other proteins also adds to the complexity of fully understanding potential regulators of its many functions.

Further, CBP plays vital dual roles in the regulation of one of the most widely and well studied tumor suppressor proteins, p53, which is found to be mutated in more than 50% of human cancers. CBP is required to promote the maintenance of physiologic levels of wild type p53 and is also needed to promote the transactivation of p53 in response to stress. It is known that CBP and its paralogue p300, possess cytoplasmic but not nuclear, E3 autoubiquitination and p53-directed E4 polyubiquitination properties under normal physiologic cell condition. However, the regulation of the compartmentalized ubiquitin properties of CBP has not been examined. What factors

trigger cytoplasmic CBP ubiquitination activities but not nuclear CBP ubiquitination activities? Are there differential CBP interacting partners or differential CBP post-translational modifications involved in these ubiquitination activities? In addition, what effect does DNA damage have on CBP ubiquitination activities? The experiments in this thesis were designed to seek the answers to these questions. Understanding the mechanisms that govern the differential CBP ubiquitin activities, especially towards p53, may provide novel strategic interventions in the p53 signaling pathway of cancer and also shed more light on cancer etiology.

Chapter 2: Activation of Nuclear CBP E3 Autoubiquitination Activity and Differential CBP Post-Translational Modifications in Response to DNA Damage

2.1 Introduction

The transcription of many target genes is dependent on the co-activator function of the histone acetyltransferases, CBP and its paralogue, p300. Different models have described the involvement of CBP and p300 in the modulation of transcription of many target genes. Such models include; histone acetylation through the CBP/p300 intrinsic HAT domain, acetylation of non-histone proteins and transcription factors, physical scaffolds for basal transcription machinery, and recruitment of components of RNA polymerase II machinery [21-27], (Fig. 1.2). The activities of CBP extend to other cellular events such as growth and development, response to stress signals, cell cycle, and apoptosis [36-41].

Previous studies from our laboratory reveal that CBP possesses cytoplasmic, but not nuclear intrinsic E3 ubiquitin ligase autoubiquitination property under physiologic cellular conditions [118]. Interestingly, CBP is more abundant in the nucleus than the cytoplasm; nevertheless, CBP autoubiquitination is exclusively cytoplasmic. The first 451 amino acids of CBP, which includes the C/H1-TAZ1 domain, encode the sequences responsible for this autoubiquitination activity. This domain is one of the Zn²⁺-binding

cys-his-rich regions of CBP and published evidence indicates that Zn-fingerlike domains can function as active E3 ligases [159, 160]. Earlier work indicated that the CBP C/H1-TAZ1 domain encodes an active non-canonical E3 ligase property with no structural similarities with other recognized RING, HECT or U-box E3 domains [118, 159, 160]. Data from previous work also revealed that CBP autoubiquitination does not lead to its degradation but instead, sequences that were found to be required for the autoubiquitination activity were also necessary for the cytoplasmic localized CBP E4 ubiquitin ligase activity, which promotes both in-vivo and in-vitro polyubiquitination and proteasome-dependent degradation of p53 under physiologic cell conditions [118].

Activation of the apical serine/threonine kinases ATM and ATR, in response to DNA damage, leads to phosphorylation of key protein targets that results in activation of checkpoint signaling events which can cause cell cycle arrest, DNA repair, or apoptosis [161-163] (Fig. 1.4). These signaling events are tightly regulated to ultimately assist in maintaining proper cell homeostasis. Distortions and aberrant functioning at any level in these signaling events can cause severe consequences. DNA damage sometimes induces post-translational modifications of proteins which can confer new functions or modulate existing functions of the modified proteins [130,132, 137, 154]. Even though it is known that post-translational modifications such as phosphorylation, acetylation, ubiquitination, sumoylation and methylation influence the co-activation role of CBP under physiologic cellular conditions [112-114, 118-121], the effect of DNA damage on CBP post-translational modification status it is not fully understood. The relevance of these post-translational modifications has been mostly studied in the co-activator role of CBP in the transcription of genes. However, the significance and synergistic effects, if

any, of these modifications in the regulation of other non-transcriptional activities of CBP has not been fully examined.

Based on the observation that CBP engages in compartmentalized ubiquitination activities under physiologic cell conditions, we sought to determine the effect of DNA damage on the compartmentalized CBP autoubiquitination activity. We further determined whether there are differential post-translational modifications between nuclear and cytoplasmic pools of CBP under normal physiologic cell conditions and in response to DNA damage. We show that DNA damage induced by gamma radiation, and also by genotoxic agents, causes activation of the otherwise dormant nuclear CBP E3 autoubiquitination activity. Cytoplasmic CBP E3 autoubiquitination was retained in response to all DNA damaging agents tested. In addition, activation of ATR kinase activity in response to DNA damage was necessary for the activation of the otherwise dormant nuclear CBP E3 autoubiquitination. Further, we identified differential post-translational modifications (PTM) of CBP between the cytoplasmic and nuclear compartments and also differential CBP PTMs in the presence and absence of DNA damage.

2.2 Materials and Methods

Cell Culture, Induction of DNA Damage and Inhibitors

U2OS and H1299 cells were grown and maintained in DMEM and RPMI respectively, supplemented with 10% fetal bovine serum (FBS) and 1% penicillin. Cells were allowed to grow to 90% confluency before treatment with DNA damaging agents. Cells were treated where noted, with 10gray gamma irradiation, 2 μ M doxorubicin or 50 μ M etoposide. All the genotoxic agents were purchased from Sigma Aldrich and reconstituted according to the manufacturer's recommendation.

For inhibition of the kinase activities of ATM and ATR, cells were treated with 3 μ M KU-60019, or 10mM VE-821 (Selleck chemicals) respectively, for 30min prior to DNA damage induction.

Subcellular Fractionation

Cytoplasmic and Nuclear extracts of U2OS and H1299 cells were prepared using the NE-PER Nuclear and Cytoplasmic Extraction kit (Thermo Fisher). Protein concentration was determined using the bicinchoninic acid (BCA) protein assay kit (Thermo Fisher) compared to bovine serum albumin (BSA) protein standards (Thermo Fisher).

siRNA Transfection

U2OS cells were transfected with 30nmoles siRNA (final concentration) using Lipofectamine 2000 (Invitrogen). ATR siRNA was purchased from Ambion Life

Technologies. 72 hours after transfection, cells were either harvested for western blot analysis or treated with etoposide followed by subcellular fractionation and in-vitro E3 assays of CBP.

In vitro E3 Assays of CBP

CBP was immunoprecipitated from 0.8mg cytoplasm or 0.3mg nuclear fractions diluted with NP40 lysis buffer [25mM Tris HCl (pH7.5), 150 mM NaCl, 1µM ZnCl₂, 1% igepal (NP40)], supplemented with protease inhibitors using A-22 antibody (Santa Cruz) followed by protein A agarose. The IPs were washed in NP40 lysis buffer three times followed by two washes in Ub buffer (25mM HEPES, pH7.4, 10mM NaCl, 3mM MgCl₂, 0.05% Triton X-100, 0.5mM DTT, 3mM Mg-ATP). The washed and equilibrated IPs were then incubated with 100ng E1 (rabbit; Boston Biochem), 25ng E2 (UbcH5a, human recombinant; Boston Biochem), and 5µg Ub (human recombinant; Boston Biochem) for 90min at 37°C. Reactions were stopped by the addition of LDS sample buffer, followed by SDS-PAGE and immunoblotting using CBP and Ub antibodies (Santa Cruz).

MudPIT Analysis

U2OS cells were fractionated into cytoplasmic and nuclear fractions followed by CBP immunoprecipitation from both fractions using anti CBP conjugated agarose beads. Eluates were separated by SDS-PAGE followed by coomassie staining. Mass spectrometry analysis was carried out at the proteomics core of the University of Virginia (UVA). Briefly, the gel piece was transferred to a siliconized tube and washed

and destained in 200 μ L 50% methanol for 3hours. The gel pieces were dehydrated in acetonitrile, rehydrated in 30 μ L of 10mM dithiothreitol in 0.1M ammonium bicarbonate and reduced at room temperature for 0.5h. The DTT solution was removed and the sample alkylated in 30 μ L 50mM iodoacetamide in 0.1M ammonium bicarbonate at room temperature for 0.5h. The reagent was removed and the gel pieces dehydrated in 100 μ L acetonitrile. The acetonitrile was removed and the gel pieces rehydrated in 100 μ L 0.1M ammonium bicarbonate. The pieces were dehydrated in 100 μ L acetonitrile, the acetonitrile removed and the pieces completely dried by vacuum centrifugation. The gel pieces were rehydrated in 20ng/ μ L trypsin in 50mM ammonium bicarbonate on ice for 10min. Any excess enzyme solution was removed and 20 μ L 50mM ammonium bicarbonate added. The sample was digested overnight at 37 $^{\circ}$ C and the peptides formed extracted from the polyacrylamide in two 30 μ L aliquots of 50% acetonitrile/ 5% formic acid. These extracts were combined and evaporated to 15 μ L for MS analysis. The LC-MS system consisted of a Thermo Electron Orbitrap Velos ETD mass spectrometer system with a Protana nanospray ion source interfaced to a self-packed 8cm x 75 μ m id Phenomenex Jupiter 10 μ m C18 reversed-phase capillary column. 7 μ L aliquots of the extract were injected and the peptides eluted from the column by an acetonitrile/ 0.1M acetic acid gradient at a flow rate of 0.5 μ L/min over 1.2hours. The nanospray ion source was operated at 2.5kV. The digest was analyzed using the rapid switching capability of the instrument acquiring full scan mass spectra to determine peptide molecular weights followed by product ion spectra [20] to determine amino acid sequence in sequential scans. The data were analyzed by database searching using the Sequest search algorithm against IPI Human.

SDS Gel Band Trypsin Digestion and Peptide Mass Spectrometry Analysis

Gel bands were excised from the SDS PAGE gel, cut into 1mm cubes and washed with 100mM ammonium bicarbonate (AB) pH7.4 (Sigma). The gel cubes were then dehydrated in the speed vac 20minutes and rehydrated in 20µl of 12.5ng/µl trypsin (Promega, Madison WI) in 100mM AB with 1% proteaseMAX surfactant, (Promega, Madison WI) for 2hours at 37°C. The supernatant transferred to a new tube and combined with the supernatant of a 10minutes extraction of the gel pieces with 100% acetonitrile. The peptide solution was then speedvaced to dryness and resuspended in 100mM AB. Peptides were loaded on a self-packed fused silica (polymicro technologies) trap column (360micron o.d. X 100micron i.d.) with a Kasil frit packed with 5-15micron irregular phenyl C-18 YMC packing. The trap column was connected to an analytical column (360micron X 50micron) with a fritted tip at 5 micron or less (New Objective) packed with 5µm phenyl C-18 YMC packing. Peptides were trapped and then eluted into a Thermo Finnigan LCQ deca XP max mass spectrometer with an acetonitrile gradient from 0 % to 80 % over one hour at a flow rate of between 50-150nl/minute. The mass spectrometer was operated in data dependent mode. First a MS scan from mass 300-1600m/z or 400-1800m/z was collected to determine the mass of peptides eluting at that time, then the top five most abundant masses were fragmented into MS/MS scans and placed on an exclusion list for 1minute. This sequence MS followed by 5 MS/MS scans with exclusion was repeated throughout the hour gradient. The approximately 5000 MS² scans were then searched with SEQUEST using a human non-redundant data base down loaded from NCBI. The following variable modifications

was considered for PTM's oxidized (methionine), phosphorylated (serine, threonine and tyrosine), GLC nac modified (threonine) and acetylated (lysine) XCor cut off of (1.25, 1.75, 2.25) for (+1, +2, +3) peptide charge states was applied. MS² scans passing this cut off were manually verified.

PTM's Searches of UVA Data

PTM searches were done at Virginia Commonwealth University at the mass spectrometry core facility. Three SEQUEST searches were performed on each sample to evaluate PTM's and displayed with scaffold. First, acetylated lysine in combination with Glc nac modification of threonine were considered. Secondly, the combination of phosphorylated serine (S), threonine (T) and tyrosine (Y) as well as methylation or acetylation of lysine were considered. Finally, phosphorylation of S, T and Y with methylation of lysine were identified. Spectra scoring above 90% confidence were manually reviewed and confirmed as accurate.

Western Blotting, Immunoprecipitation and Immunofluorescence

For western blot analyses, cytoplasmic and nuclear extracts of cells were prepared using NE-PER fractionation kit followed by SDS-PAGE and immunoblotting with the indicated antibodies. CBP, Ub, ATM, pATM (ser1981), CHK1 antibodies were purchased from Santa Cruz. Tubulin antibody was from Sigma, pCHK1 (ser345) and lamin a/c were from cell signaling.

For CBP immunoprecipitation, cytoplasmic and nuclear extracts were diluted with NP40 lysis buffer [25mM Tris HCl (pH 7.5), 150mM NaCl, 1 μ M ZnCl₂, 1% igepal (NP40)],

supplemented with protease inhibitors followed by overnight incubation with A-22 antibody (Santa Cruz) and protein A agarose. The overnight immunoprecipitates were washed five times in lysis buffer and eluted using LDS loading buffer and DTT. Eluates were subjected to SDS PAGE electrophoresis and western blot signals were quantified after visualization of primary antibody by fluorescent-labeled secondary antibody and detection by Odyssey blot scanner (LiCor), using ImageJ National Institutes of Health (NIH) software.

For Immunofluorescence, cells were seeded in 4 chambered slides for 24hrs followed by treatment with 2 μ M doxorubicin for 3hrs. Cells were fixed in 4% paraformaldehyde (Thermo Scientific) in PBS for 15minutes at room temperature. Following three washes with PBS, cells were permeabilized with 0.2% TritonX-100 in PBS for 10minutes at room temperature. Cells were washed three times with PBS followed by 1hour blocking in Odyssey blocking buffer (Li-Cor, 927-4000) diluted 1:1 with PBS at room temperature. Slides were then incubated overnight at 4°C in primary antibody (anti-CBP, A-22, Santa Cruz) diluted in blocking buffer containing 0.2% TritonX-100. Following three 5 minute washes with PBS, slides were incubated for 1hour at room temperature in the dark in secondary antibody (anti rabbit IgG-CFL 488) diluted in blocking buffer containing 0.2% TritonX-100. Slides were washed three times with PBS followed by mounting with prolong diamond antifade mountant containing DAPI (Life Technologies/Molecular Probes). Images were acquired using the EVOS AMG fluorescent microscope and representative images are shown at the same exposure and magnification.

Statistical Analysis

Statistical comparisons were made using Student's *t*-test; $p < 0.05$ was considered significant and $p < 0.01$ was considered very significant.

2.3 Results

DNA Damage Induces Nuclear CBP Autoubiquitination

CBP has previously been shown to exhibit cytoplasmic but not nuclear E3 autoubiquitination activity under unstressed cellular conditions [118]. The effect of DNA damage on CBP autoubiquitination activity however, was not studied. To assess the effect of DNA damage on CBP E3 autoubiquitination activity, U2OS cells were treated with the following DNA damaging agents; doxorubicin, etoposide, and gamma irradiation for 5hrs, followed by CBP immunoprecipitation and in vitro E3 ligase activity analysis from cytoplasmic and nuclear fractions. Our results revealed activation of the otherwise dormant nuclear CBP E3 autoubiquitination in response to all the different DNA damaging agents, compared with untreated cells (Fig. 2.1, 2.2, 2.3). We however, did not observe any significant changes in cytoplasmic CBP autoubiquitination in response to DNA damage. Demonstrating that these results were not cell-type specific, H1299 cells were treated with doxorubicin for 5hrs followed by CBP immunoprecipitation and in vitro E3 ligase activity. Similar to the observation in U2OS cells, doxorubicin induced activation of nuclear CBP E3 autoubiquitination in H1299 cells (Fig. 2.4).

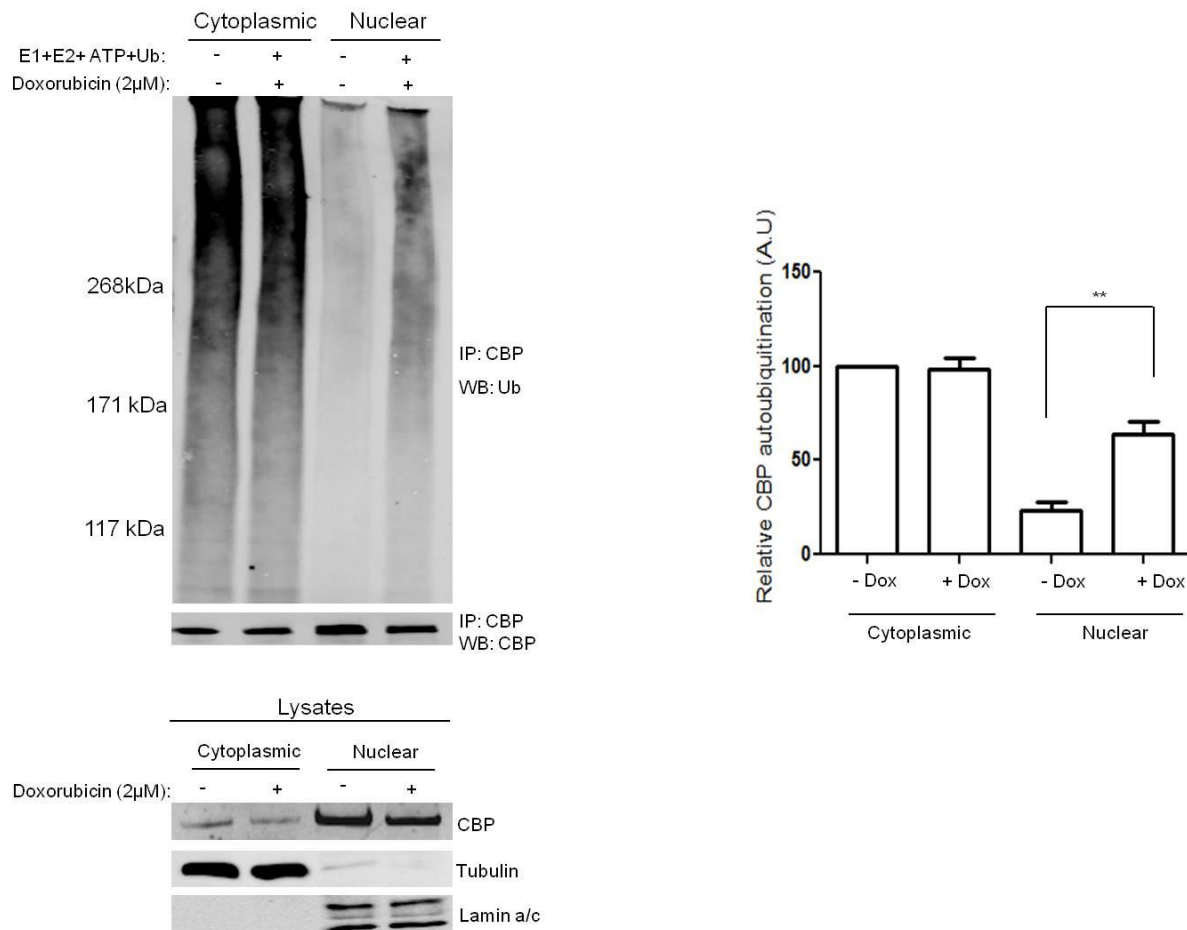


Figure 2.1 Activation of nuclear CBP autoubiquitination in response to doxorubicin. U2OS cells treated with doxorubicin (2 μ M) for 5hrs were harvested for CBP immunoprecipitation from cytoplasmic and nuclear fractions using anti CBP (A-22, Santa Cruz) antibody at 4 $^{\circ}$ C overnight followed by in vitro CBP E3 autoubiquitination assay and immunoblotting with CBP and Ub antibodies. Graph shows quantification of ubiquitination signal by densitometry, normalized to cytoplasmic fraction without doxorubicin. Graph represents mean \pm SEM for three independent experiments. **p<0.01.

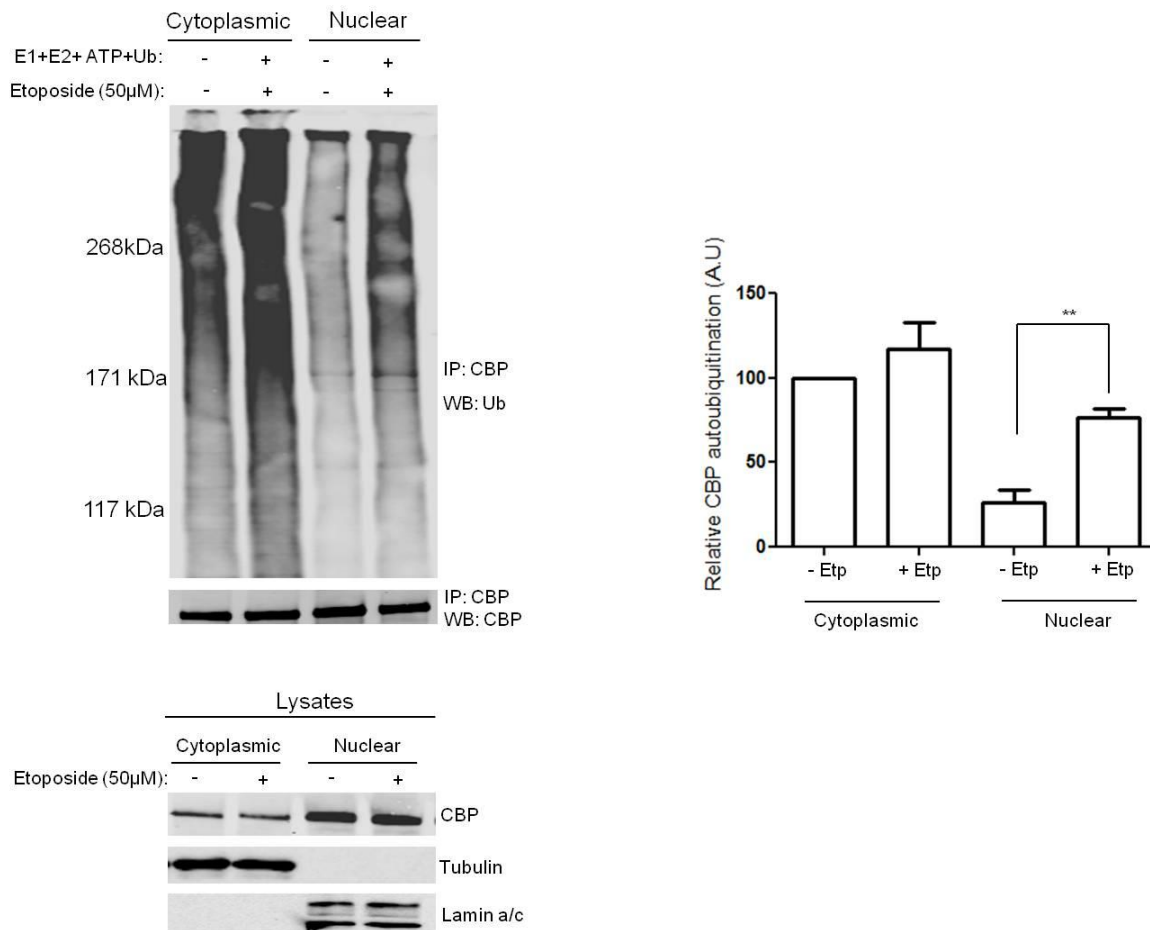


Figure 2.2 Activation of nuclear CBP autoubiquitination in response to etoposide. U2OS cells treated with etoposide (50µM) for 5hrs were harvested for CBP immunoprecipitation from cytoplasmic and nuclear fractions using anti CBP (A-22, Santa Cruz) antibody at 4°C overnight followed by in vitro CBP E3 autoubiquitination assay and immunoblotting with CBP and Ub antibodies. Graph shows quantification of ubiquitination signal by densitometry, normalized to cytoplasmic fraction without etoposide. Graph represents mean ± SEM for three independent experiments. **p<0.01.

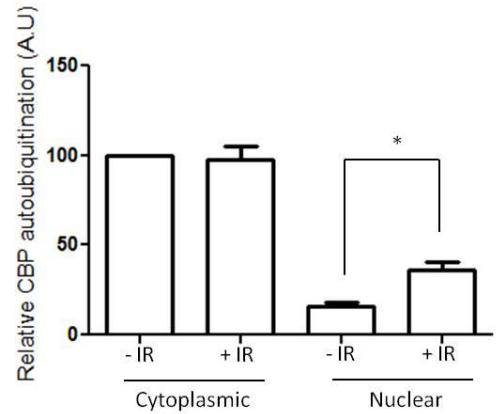
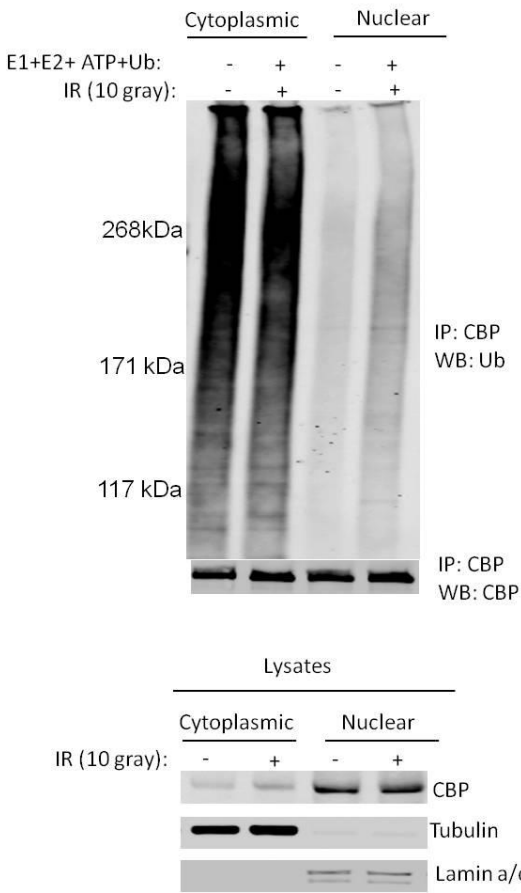


Figure 2.3 Activation of nuclear CBP autoubiquitination in response to gamma irradiation (IR).

U2OS cells were gamma irradiated (10 gray) for 5hrs and harvested for CBP immunoprecipitation from cytoplasmic and nuclear fractions using anti CBP (A-22, Santa Cruz) at 4°C antibody overnight followed by in-vitro CBP E3 autoubiquitination assay and immunoblotting with CBP and Ub antibodies. Graph shows quantification of ubiquitination signal by densitometry, normalized to cytoplasmic fraction without IR. Graph represents mean \pm SEM for three independent experiments. * $p < 0.05$.

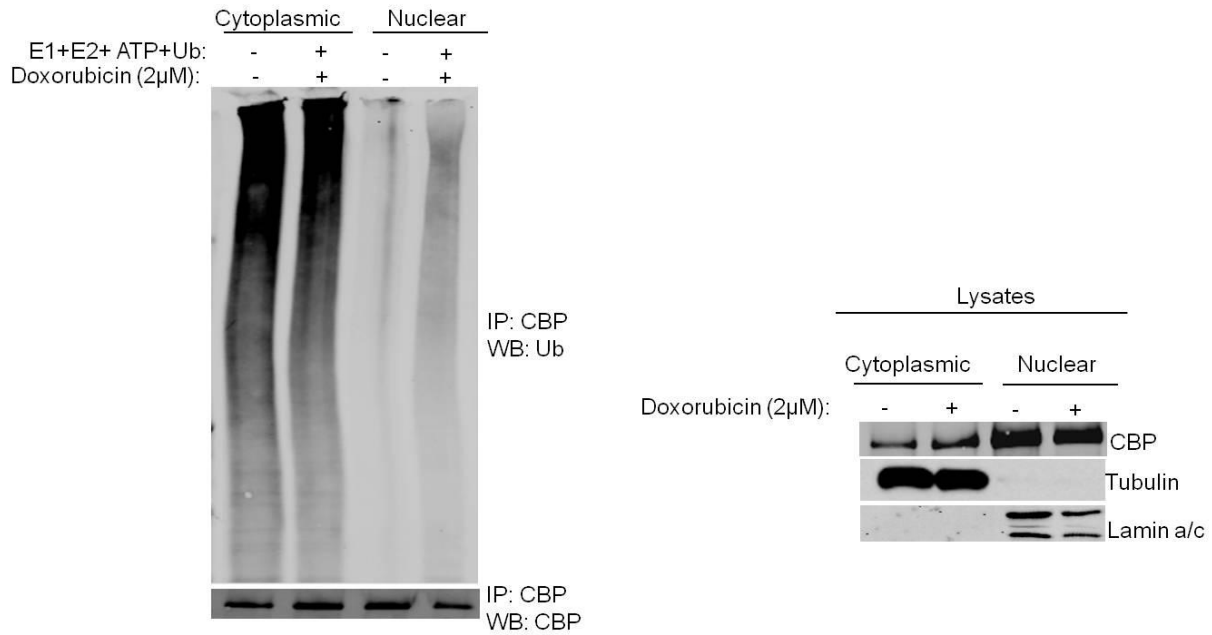


Figure 2.4 Activation of nuclear CBP autoubiquitination in response to doxorubicin in H1299 cells.

H1299 cells were treated with doxorubicin for 5hrs and harvested for CBP immunoprecipitation from cytoplasmic and nuclear fractions using anti CBP (A-22, Santa Cruz) at 4°C antibody overnight followed by in-vitro CBP E3 autoubiquitination assay and immunoblotting with CBP and Ub antibodies. Lysates were immunoblotted with the indicated antibodies.

Activation of ATR Kinase Activity is Necessary for DNA Damage-Induced Nuclear CBP Autoubiquitination

The serine/threonine kinases, ATM and ATR coordinate several signaling cascade events in response to DNA damage. Activation of these kinases result in the phosphorylation of several key proteins that initiate the DNA damage checkpoint, ultimately leading to cell cycle arrest, DNA repair or apoptosis [161, 162], (Fig. 1.4). The ATM-Chk2 signaling pathway is activated in response to ionizing radiation and genotoxic drugs that cause DNA double strand breaks, while the ATR-Chk1 signaling pathway responds to ionizing radiation and agents that cause stalling of replication forks and generation of single stranded DNA breaks [163]. We tested whether the activation of ATM and ATR kinases were necessary for DNA damage induced nuclear CBP E3 autoubiquitination. U2OS cells were treated with vehicle or with either the ATM kinase inhibitor, KU-60019, or the ATR kinase inhibitor, VE-821, for 30 minutes prior to treatment with doxorubicin or etoposide, respectively, followed by CBP immunoprecipitation and in vitro CBP E3 autoubiquitination assay from the nuclear fraction. Inhibition of ATM kinase activity had no effect on DNA damage induced nuclear CBP E3 autoubiquitination (Fig. 2.5). Inhibition of ATR kinase activity however, led to a decrease in the activation of etoposide-induced nuclear CBP E3 autoubiquitination event (Fig. 2.6). To further define the role of ATR signaling in the activation of nuclear CBP E3 autoubiquitination in response to DNA damage, we transiently silenced ATR in U2OS cells using siRNA followed by CBP immunoprecipitation and in vitro CBP E3

ubiquitin ligase assay. Down regulation of ATR using siRNA led to a significant reduction in the activation of nuclear CBP autoubiquitination in response to etoposide-induced DNA damage compared with cells treated with control siRNA (Fig. 2.7).

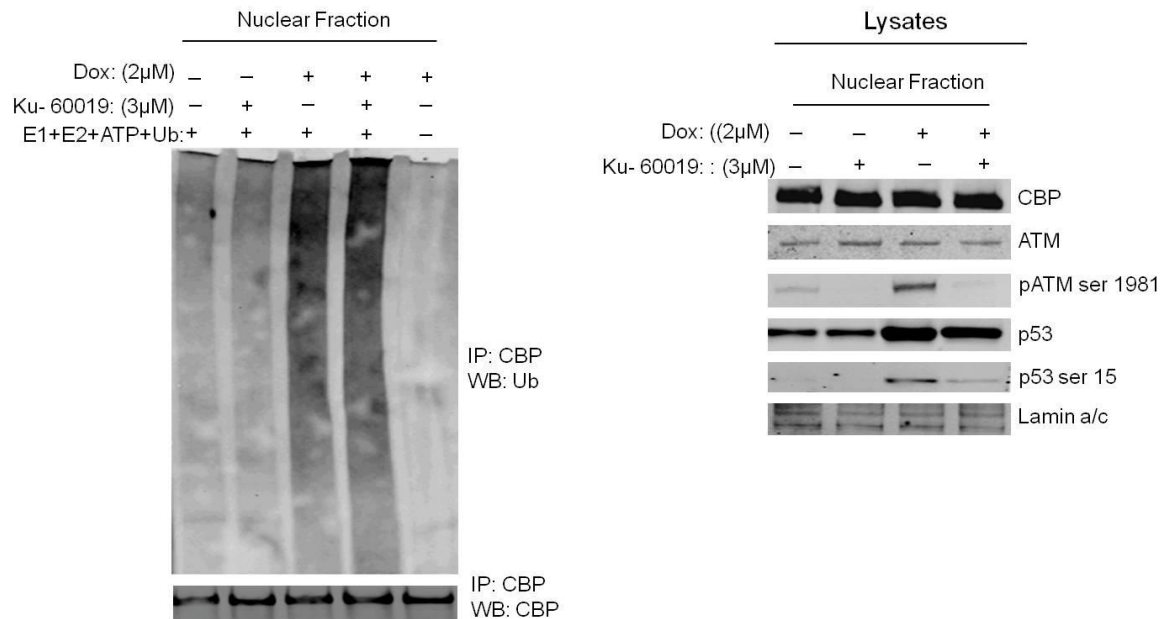


Figure 2.5 ATM kinase activity is not necessary for DNA damage-induced nuclear CBP autoubiquitination. U2OS cells were treated with ATM kinase inhibitor Ku-60019 for 30mins followed by treatment with doxorubicin for 5hrs. Cells were harvested for CBP immunoprecipitation from nuclear fraction using anti-CBP antibody at 4°C overnight. The overnight IPs were washed and incubated with ubiquitin reaction components; E1, E2, Ub, ATP- Mg²⁺ for 90minutes followed by SDS-PAGE and western blot analysis. Lysates from nuclear fraction were immunoblotted with the indicated antibodies.

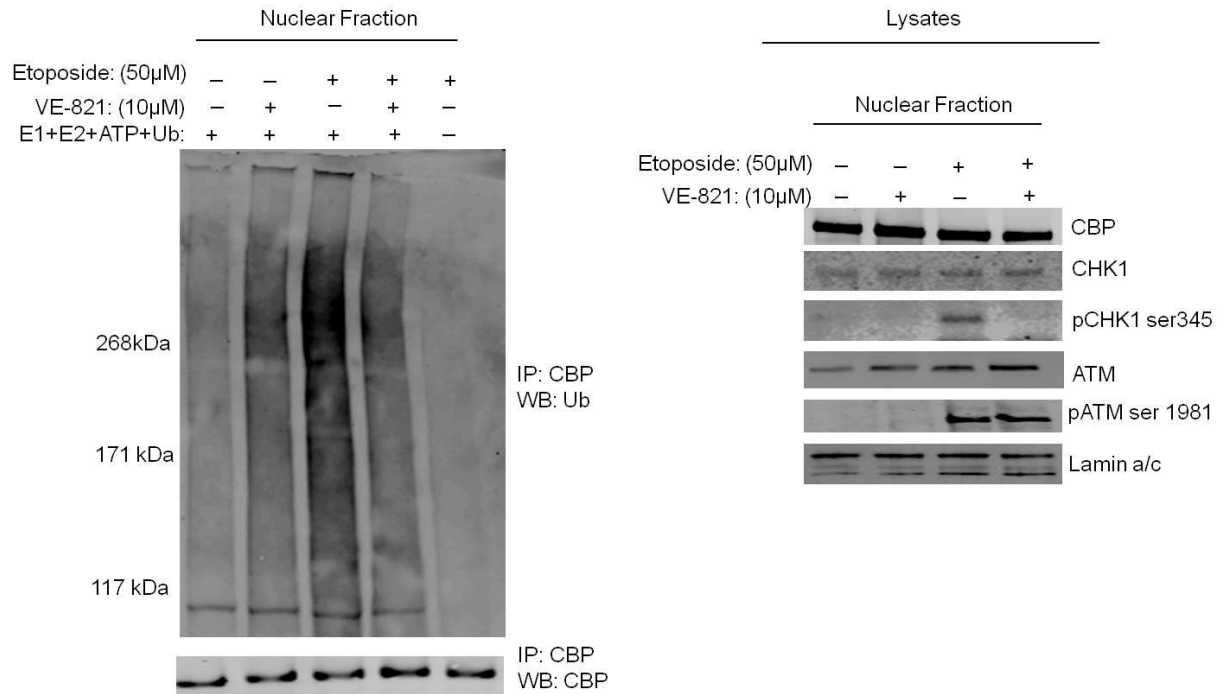


Figure 2.6 Inhibition of ATR kinase activity reduces the DNA damage-induced nuclear CBP autoubiquitination. U2OS cells were treated with ATR kinase inhibitor VE-821 for 30mins followed by treatment with etoposide for 5hrs. Cells were harvested for CBP immunoprecipitation from nuclear fraction using anti-CBP antibody at 4°C overnight. The overnight IPs were washed and incubated with ubiquitin reaction components; E1, E2, Ub, ATP- Mg^{2+} for 90minutes followed by SDS-PAGE and western blot analysis. Lysates from nuclear fraction were immunoblotted with the indicated antibodies.

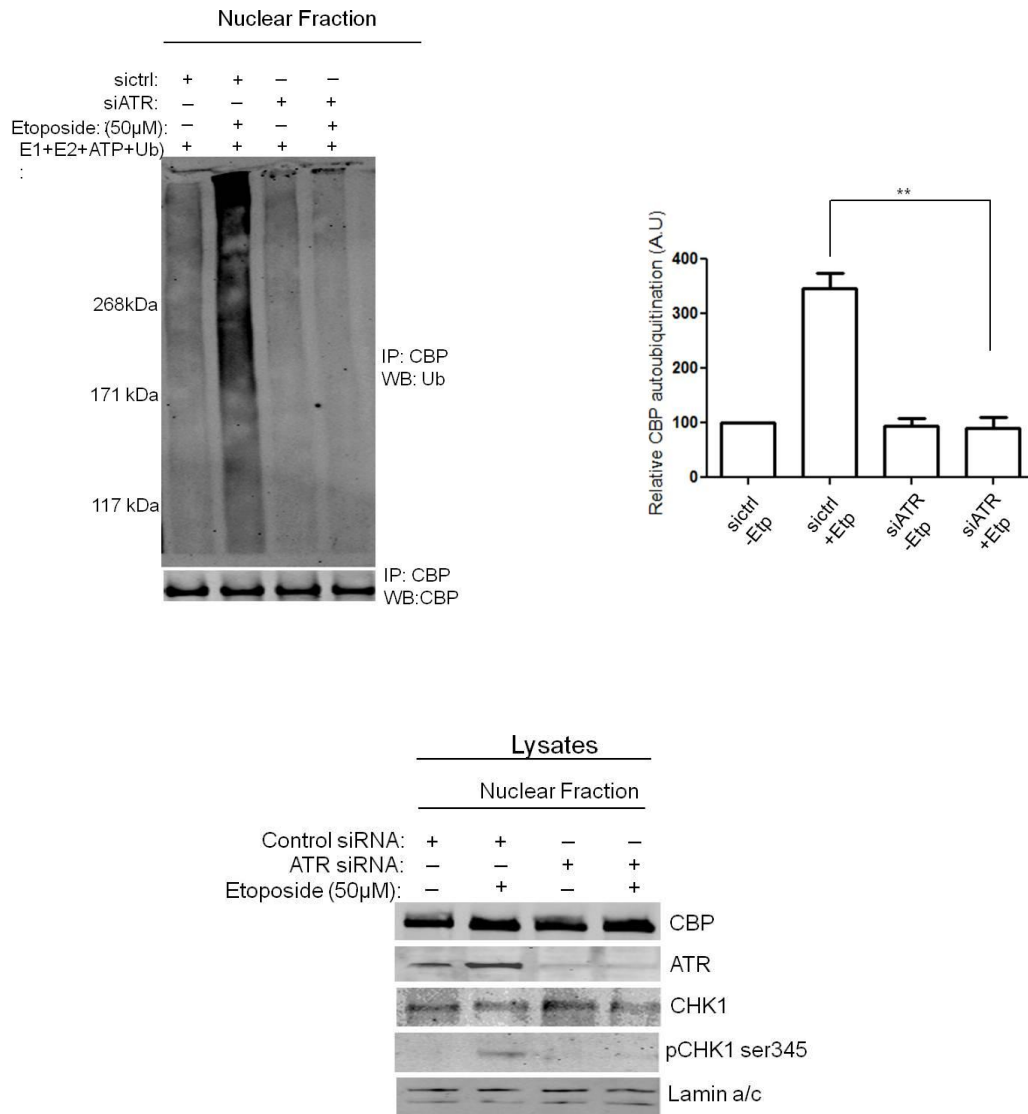


Figure 2.7 ATR depletion reduces the DNA damage-induced nuclear CBP autoubiquitination.

U2OS cells were treated with control siRNA or ATR siRNA for 72hrs followed by etoposide treatment 5hrs before harvest. Cells were harvested for CBP immunoprecipitation from nuclear fraction using anti-CBP antibody at 4°C overnight. The overnight IPs were washed and incubated with ubiquitin reaction components; E1, E2, Ub, ATP- Mg²⁺ for 90 minutes followed by SDS-PAGE and western blot analysis. Lysates from nuclear fraction were immunoblotted with the indicated antibodies.

DNA Damage Redistributes Nuclear CBP Localization

DNA damage induces several signaling events and activities that could influence a protein's stability, cellular localization, and even interaction with other proteins. Endogenous CBP is known to generally have a randomly diffused staining pattern, predominantly in the nucleus, under normal cell condition. To determine the effect of DNA damage on CBP cellular localization, U2OS cells were treated with doxorubicin for 6hrs followed by fixation and staining for immunofluorescence microscopy. In response to doxorubicin treatment, immunofluorescence microscopy of U2OS cells revealed discrete punctuate CBP staining pattern in the nucleus which resembled PML bodies, compared with untreated cells (Fig. 2.8). PML bodies are Some of these punctuate CBP stains co-localized with PML in response to doxorubicin-induced DNA damage (Fig. 2.9).

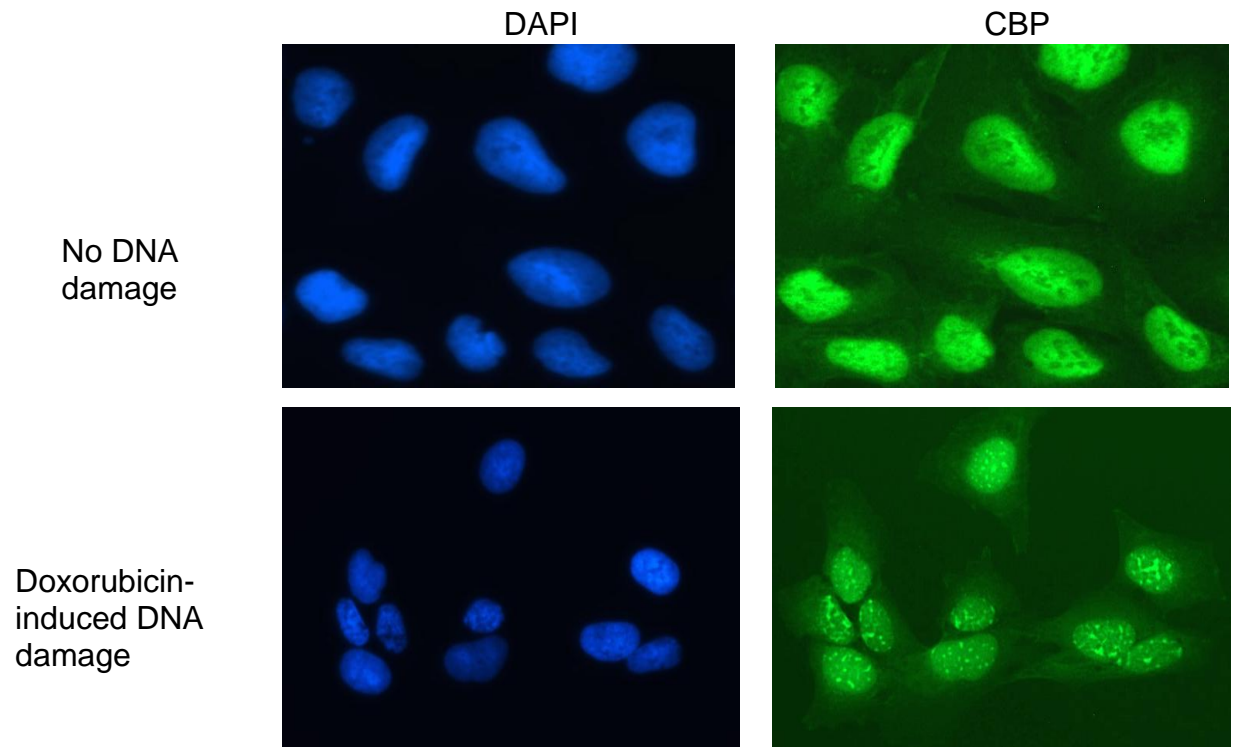


Figure 2.8 Immunofluorescence microscopy of CBP nuclear distribution in the presence and absence of DNA damage. U2OS cells were treated with doxorubicin for 6hrs followed by immunofluorescence microscopy using anti-CBP antibody (Santa Cruz) and DAPI for nuclei staining. Images were acquired using the EVOS AMG fluorescent microscope and representative images are shown at the same exposure and magnification (40X).

Doxorubicin-induced DNA damage

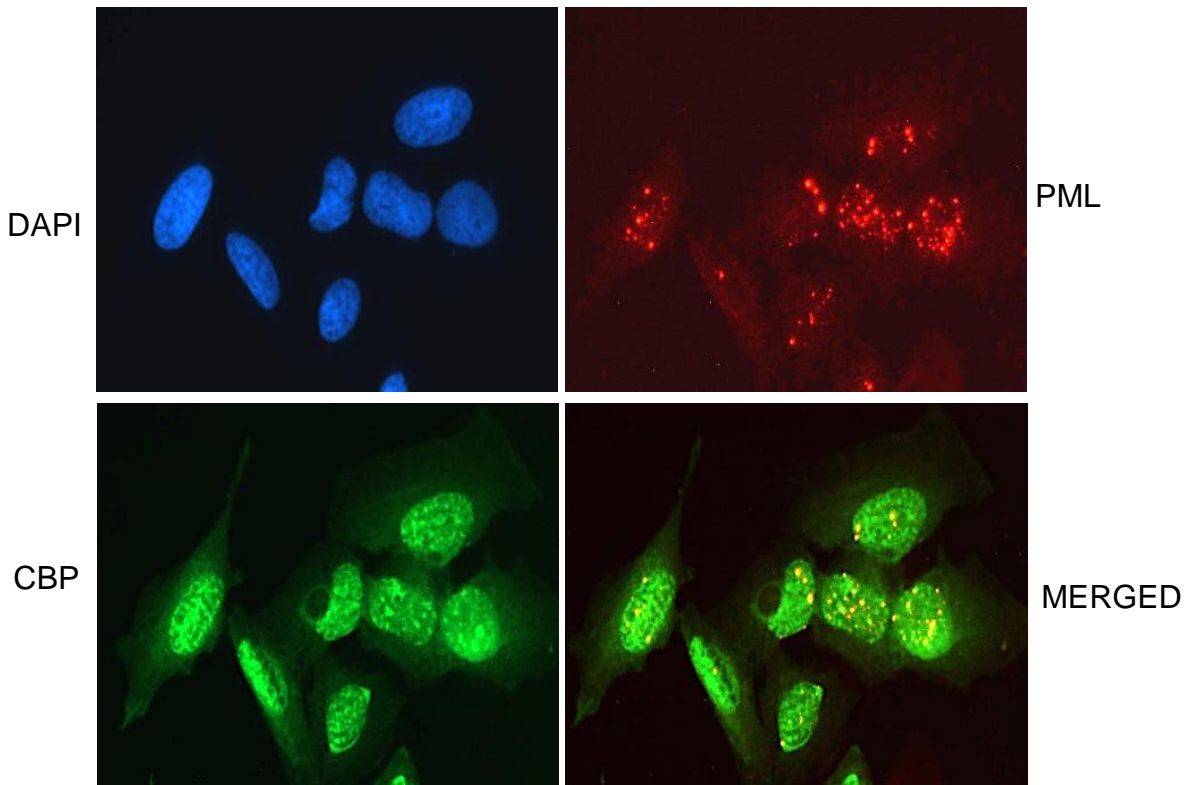


Figure 2.9 Immunofluorescence microscopy of CBP and PML in nuclear bodies in response to doxorubicin. U2OS cells were treated with doxorubicin for 6hrs followed by immunofluorescence microscopy using anti-CBP and PML antibodies (Santa Cruz). DAPI was used for nuclei staining. Images were acquired using the EVOS AMG fluorescent microscope and representative images are shown at the same exposure and magnification (40X).

Post-Translational Modification of Cytoplasmic and Nuclear CBP in Response to DNA Damage

Based on our observation that DNA damage induces the activation of nuclear CBP autoubiquitination, we determined whether differential post translational modifications occur between cytoplasmic and nuclear pools of CBP, in the absence and presence of doxorubicin induced DNA damage. Several studies have indicated the importance of CBP modifications such as phosphorylation, acetylation, ubiquitination, sumoylation, methylation in the regulation of its co-activator role in the transcription of target genes [36, 108, 112-119]. Most of these studies however, investigated CBP post translational modification in the absence of stress conditions and also from whole cell lysates. To identify CBP PTMs in cellular compartments, CBP was immunoprecipitated from cytoplasmic and nuclear fractions of U2OS cells and subjected to mass spectrometry followed by PTM analysis. The following post translational modifications of CBP were detected; acetylation, phosphorylation, methylation and glcNAcylation (Table 1). CBP was found to be differentially acetylated between cytoplasmic and nuclear fractions in the absence of DNA damage. The acetylated sites are consistent with reported sites in the PhosphositePlus database. These acetylated sites were retained in both compartments in response to stress. We confirmed CBP acetylation in the cytoplasmic and nuclear fractions in the absence and presence of doxorubicin-induced DNA damage by reciprocal immunoprecipitations using CBP and acetylated lysine specific antibodies (Figure 2.10).

Also, CBP was methylated only in the nuclear fraction in the absence of DNA damage (Table 1). There's no previous report of this particular methylation site. In addition, glcNAcylation of CBP was detected on the same sites in both cytoplasmic and nuclear fractions in the absence of DNA damage (Table 1). CBP glcNAcylation however, was not detected in response to DNA damage and there is no previous report of this modification.

CBP is Differentially Phosphorylated in Response to DNA Damage

Further, PTM analysis revealed differential CBP phosphorylation between cytoplasmic and nuclear pools in the absence and presence of doxorubicin-induced DNA damage (Table 1). In the absence of doxorubicin-induced DNA damage, phosphorylation was detected only in the nuclear CBP pool, on two different sites; S1763 and S2063. These phosphorylation sites have previously been reported in the PhosphositePlus database. CBP phosphorylation was not detected in the cytoplasmic fraction. In response to DNA damage, nuclear CBP phosphorylation was detected on S124. This site has also been reported in PhosphositePlus and is consistent with a previous work that analyzed ATM/ ATR substrates in response to UV radiation using whole cell lysates [162]. We however, did not detect any cytoplasmic CBP phosphorylation in response to DNA damage.

Table 1: Post-translational Modification (PTM) of cytoplasmic and nuclear CBP identified by mass spectrometry

	Phosphorylation		Acetylation		Methylation		GlcNAcylation	
	Cytoplasm	Nucleus	Cytoplasm	Nucleus	Cytoplasm	Nucleus	Cytoplasm	Nucleus
No DNA damage	None	S1763-p S2063-p	K1937-ac	K1762-ac	None	K420-me	T1927-gl	T1927-gl
Doxoru bicin- induced DNA damage	None	S124	K1937-ac	K1762-ac	None	None	None	None

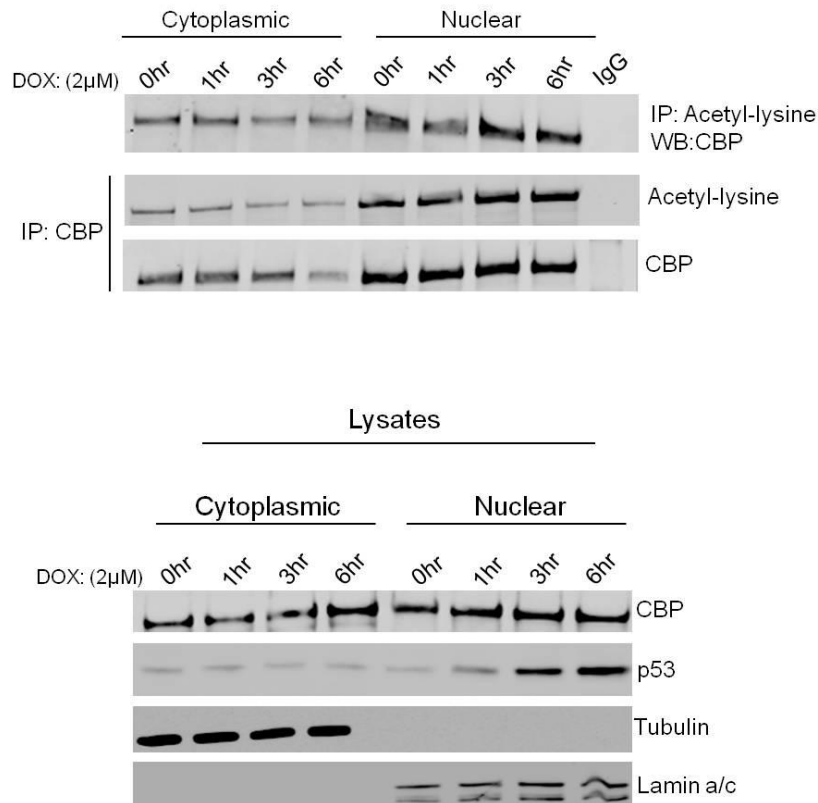


Figure 2.10 Acetylation of CBP in response to Doxorubicin. U2OS cells were treated with Dox over a 6hr time period followed by reciprocal CBP (Santa Cruz) and acetyl lysine (cell signaling) immunoprecipitations from cytoplasmic and nuclear fractions. The IPs were washed and subjected to immunoblotting with CBP (Santa Cruz) and acetyl-lysine (cell signaling) antibodies. Lysates from cytoplasmic and nuclear fractions were immunoblotted with the indicated antibodies.

p53 Ubiquitination in Response to Doxorubicin-Induced DNA Damage

Ubiquitination is an important post-translational modification involved in the regulation of p53 turnover under unstressed cellular condition. In response to various stress signals, p53 is stabilized and its level increases. Post-translational modifications of p53 such as phosphorylation, acetylation, sumoylation have been reported to play roles in p53 stability and transactivation in response to stress [164,165]. Since CBP E3 ubiquitin ligase activity is active in the cytoplasm and in the nucleus, in response to DNA damage (Fig. 2.1-2.3), and based on the fact that CBP is an E4 polyubiquitin ligase for p53 in the absence of stress [118], we examined the endogenous p53 ubiquitination status in response to doxorubicin-induced DNA damage in the cytoplasm and nucleus to determine if there is any correlation between CBP autoubiquitination events and p53 ubiquitination. An early study showed that ubiquitination of p53 is differentially affected by ionizing and UV radiation [168]. We exposed U2OS cells to doxorubicin for 5hrs followed by p53 immunoprecipitation from cytoplasmic and nuclear fractions and immunoblotting with p53 and ubiquitin antibodies. Our results indicated that p53 is ubiquitinated in the cytoplasm with and without DNA damage (Fig 2.11). In the nucleus however, ubiquitin-conjugated p53 were detected more in cells treated with doxorubicin compared with untreated cells (Fig 2.11).

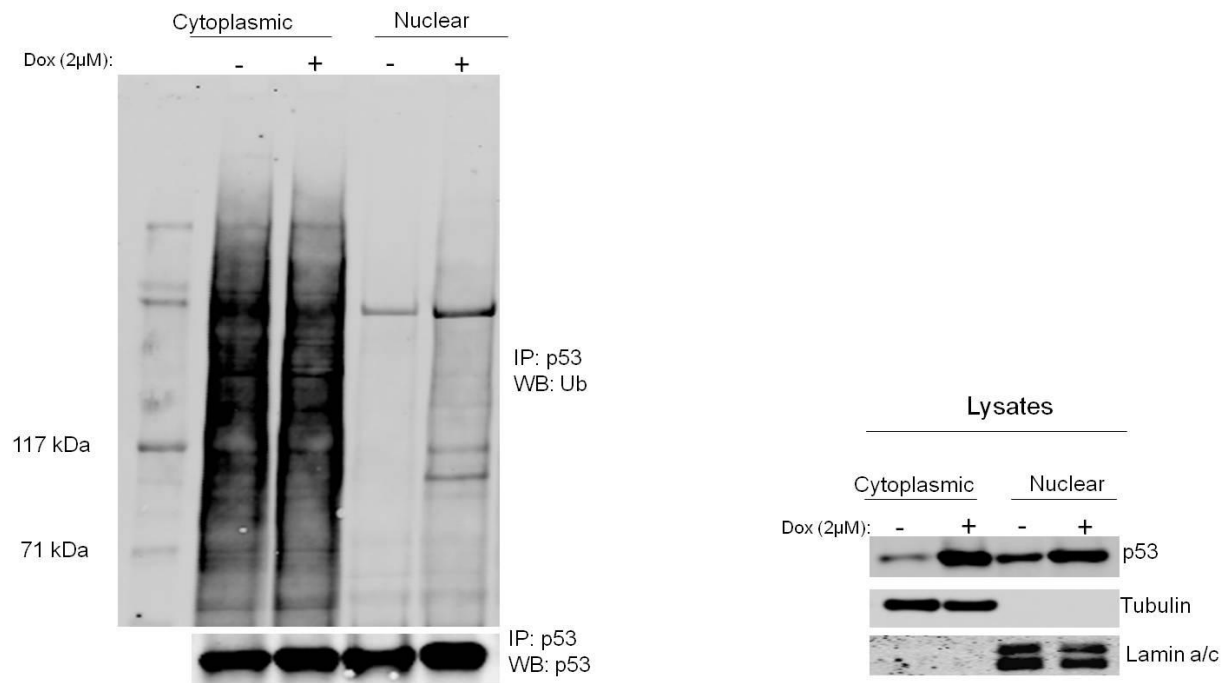


Figure 2.11 Doxorubicin-induced p53 ubiquitination. U2OS cells were treated with 2μM Dox for 5hrs after which p53 was immunoprecipitated from cytoplasmic and nuclear fractions using p53 antibody (DO.1, Santa Cruz) overnight, followed by immunoblotting with p53 (FL-393, Santa Cruz) and ubiquitin (VU-1, Life Sensors) antibodies. Lysates were immunoblotted with the indicated antibodies.

2.4 Summary

The otherwise dormant nuclear CBP E3 autoubiquitination is activated in response to DNA damage induced by gamma radiation and also by genotoxic agents. Cytoplasmic CBP retains its E3 autoubiquitination property in response to DNA damage. Activation of the ATR kinase activity but not ATM kinase activity in response to DNA damage was found necessary to trigger the activation of nuclear CBP autoubiquitination. Knock down of ATR abrogated the DNA damage-induced nuclear CBP E3 autoubiquitination activity. Furthermore, in response to Dox treatment, immunofluorescence microscopy revealed punctuate CBP staining pattern, some of which localized with PML in the nucleus. Post-translational modification (PTM) analysis of CBP revealed differential compartmentalized CBP PTMs in the absence and presence of DNA damage. We found that CBP was methylated on K420 in the nucleus but not in the cytoplasm in the absence of DNA damage but not in response to DNA damage. In addition, nuclear CBP was differentially phosphorylated in the absence versus in response to doxorubicin induced DNA damage. Nuclear CBP was phosphorylated on S1763 and S2063 under unstressed cell condition, but phosphorylated on S124 in response to doxorubicin-induced DNA damage. We however, did not detect any phosphorylation events in cytoplasmic CBP pool with or without genotoxic stress. Also, we found that p53 is polyubiquitinated in response to Dox treatment in both cytoplasmic and nuclear fractions of U2OS cells.

Chapter 3: Novel Interaction between CBP and DBC1 and Regulation of CBP Ubiquitin Ligase Activities

3.1 Introduction

CBP like its paralogue p300, possesses both E3 and E4 ubiquitin ligase activities. Previous work revealed that the N-terminally located conserved Zn²⁺-binding Cys-His-rich region (CH1) of CBP and p300 functions as a putative E3 and E4 ubiquitin ligase domain [118, 121]. We also understand that the intrinsic E3 ubiquitin ligase activity of CBP and p300 drives autoubiquitination while the E4 ubiquitin ligase activity directs p53 polyubiquitination and its subsequent degradation by the 26S proteasomal pathway [118]. E4 enzymes catalyze ubiquitin chain assembly on preformed ubiquitin moieties of substrates, designating them for 26S proteasomal degradation [145, 146]. The E4 ubiquitin ligase activity of CBP and p300 contribute to the mechanisms that maintain the cellular physiologic levels of p53, a tumor suppressor protein frequently mutated in many human cancers, whose activity is controlled by covalent posttranscriptional modifications such as acetylation, methylation, phosphorylation, ubiquitination, neddylation and sumoylation [164, 165]. In the absence of cellular stress, physiologic levels of p53 are primarily maintained by its negative modulator, the Mouse double minute protein 2 (Mdm2), a well characterized ubiquitin E3 ligase enzyme, in conjunction with CBP/p300 which function as ubiquitin E4 conjugation factors [118, 152, 166, 167]. Early studies have indicated that Mdm2 catalyzes multiple

monoubiquitination of p53, a signal for p53 nuclear export [166, 167]. We previously demonstrated that the exported monoubiquitinated p53 is polyubiquitinated by cytoplasmic CBP/p300 targeting p53 for 26S proteasomal degradation [118, 121]. The regulation of the compartmentalized CBP and p300 ubiquitin ligase activities however, was not examined.

Conversely, in response to diverse cellular stress conditions, mechanisms such as MDM2 inactivation, ATM/ATR mediated phosphorylation of p53, and acetylation of specific lysine residues in the C-terminal region of p53 by CBP/p300, have been shown to collectively increase the DNA binding ability, stability and transcriptional activation of p53 [22, 28-30, 131, 132]. CBP and p300 thus play double edged roles in p53 regulation; by promoting p53 polyubiquitination and degradation in the absence of cellular stress and also by promoting p53 stability and transactivation in response to cellular insults.

This chapter describes the experiments carried out in an attempt to understand the regulation of compartmentalized CBP ubiquitin ligase activities in the absence of cellular stress. First, we examined whether there are cytoplasmic activators or nuclear inhibitors of CBP autoubiquitination activity. Using MudPIT and mass spectrometry analyses, we identified CBP binding partners in the cytoplasmic and nuclear fraction of U2OS cells. Our proteomics data revealed that DBC1 is a CBP interacting protein both in the cytosol and nucleus. In addition, our results suggest that DBC1 is involved in the regulation of CBP ubiquitin ligase activities.

3.2 Materials and Methods

Subcellular Fractionation

Cytoplasmic and Nuclear extracts of U2OS and H1299 cells were prepared using the NE-PER Nuclear and Cytoplasmic Extraction kit (Thermo Fisher). Protein concentration was determined using the bicinchoninic acid (BCA) protein assay kit (Thermo Fisher) compared to bovine serum albumin (BSA) protein standards (Thermo Fisher).

In Vitro E3 Assays of CBP

CBP was immunoprecipitated from 0.8mg cytoplasm or 0.3mg nuclear fractions diluted with NP40 lysis buffer [25mM Tris HCl (pH 7.5), 150mM NaCl, 1 μ M ZnCl₂, 1% igepal (NP40)], supplemented with protease inhibitors using A-22 antibody (Santa Cruz) followed by protein A agarose. The IPs were washed in NP 40 lysis buffer three times followed by two washes in Ub buffer (25mM HEPES, pH 7.4, 10mM NaCl, 3mM MgCl₂, 0.05% Triton X-100, 0.5mM DTT, 3mM Mg-ATP). The washed and equilibrated IPs were then incubated with 100ng E1 (rabbit; Boston Biochem), 25ng E2 (Ubch5a, human recombinant; Boston Biochem), and 5 μ g Ub (human recombinant; Boston Biochem) for 90min at 37°C. Reactions were stopped by the addition of LDS sample buffer, followed by SDS-PAGE and immunoblotting using CBP and Ub antibodies (Santa Cruz).

MudPIT Analysis

U2OS cells were fractionated into cytoplasmic and nuclear fractions followed by CBP immunoprecipitation from both fractions using anti CBP conjugated agarose beads. Eluates were separated by SDS-PAGE followed by coomassie staining. Mass spectrometry analysis was carried out at the proteomics core of the University of Virginia (UVA). Briefly, the gel piece was transferred to a siliconized tube and washed and destained in 200 μ L 50% methanol for 3hours. The gel pieces were dehydrated in acetonitrile, rehydrated in 30 μ L of 10mM dithiolthreitol in 0.1M ammonium bicarbonate and reduced at room temperature for 0.5h. The DTT solution was removed and the sample alkylated in 30 μ L 50mM iodoacetamide in 0.1M ammonium bicarbonate at room temperature for 0.5h. The reagent was removed and the gel pieces dehydrated in 100 μ L acetonitrile. The acetonitrile was removed and the gel pieces rehydrated in 100 μ L 0.1M ammonium bicarbonate. The pieces were dehydrated in 100 μ L acetonitrile, the acetonitrile removed and the pieces completely dried by vacuum centrifugation. The gel pieces were rehydrated in 20ng/ μ L trypsin in 50mM ammonium bicarbonate on ice for 10min. Any excess enzyme solution was removed and 20 μ L 50mM ammonium bicarbonate added. The sample was digested overnight at 37°C and the peptides formed extracted from the polyacrylamide in two 30 μ L aliquots of 50% acetonitrile/ 5% formic acid. These extracts were combined and evaporated to 15 μ L for MS analysis. The LC-MS system consisted of a Thermo Electron Orbitrap Velos ETD mass spectrometer system with a Protana nanospray ion source interfaced to a self-packed 8cm x 75 μ m id Phenomenex Jupiter 10 μ m C18 reversed-phase capillary column. 7 μ L aliquots of the extract were injected and the peptides eluted from the

column by an acetonitrile/0.1M acetic acid gradient at a flow rate of 0.5 μ L/min over 1.2hours. The nanospray ion source was operated at 2.5kV. The digest was analyzed using the rapid switching capability of the instrument acquiring full scan mass spectra to determine peptide molecular weights followed by product ion spectra [20] to determine amino acid sequence in sequential scans. The data were analyzed by database searching using the Sequest search algorithm against IPI Human.

SDS Gel Band Trypsin Digestion and Peptide Mass Spectrometry Analysis

Gel bands were excised from the SDS PAGE gel, cut into 1mm cubes and washed with 100mM ammonium bicarbonate (AB) pH 7.4 (Sigma). The gel cubes were then dehydrated in the speed vac 20minutes and rehydrated in 20 μ l of 12.5ng/ μ l trypsin (Promega, Madison WI) in 100mM AB with 1% proteaseMAX surfactant, (Promega, Madison WI) for 2hours at 37 $^{\circ}$ C. The supernatant transferred to a new tube and combined with the supernatant of a 10minute extraction of the gel pieces with 100% acetonitrile. The peptide solution was then speedvaced to dryness and resuspended in 100mM AB. Peptides were loaded on a self-packed fused silica (polymicro technologies) trap column (360micron o.d. X 100micron i.d.) with a Kasil frit packed with 5-15micron irregular phenyl C-18 YMC packing. The trap column was connected to an analytical column (360micron X 50micron) with a fritted tip at 5 micron or less (New Objective) packed with 5 μ m phenyl C-18 YMC packing. Peptides were trapped and then eluted into a Thermo Finnigan LCQ deca XP max mass spectrometer with an acetonitrile gradient from 0% to 80% over one hour at a flow rate of between 50-150nl/minute. The mass spectrometer was operated in data dependent mode. First a MS scan

from mass 300-1600m/z or 400-1800m/z was collected to determine the mass of peptides eluting at that time, then the top five most abundant masses were fragmented into MS/MS scans and placed on an exclusion list for 1 minute. This sequence MS followed by 5 MS/MS scans with exclusion was repeated throughout the hour gradient. The approximately 5000 MS² scans were then searched with SEQUEST using a human non-redundant data base down loaded from NCBI. The following variable modifications was considered for PTM's oxidized (methionine), phosphorylated (serine, threonine and tyrosine), GLC nac modified (threonine) and acetylated (lysine) XCoor cut off of (1.25, 1.75, 2.25) for (+1, +2, +3) peptide charge states was applied. MS² scans passing this cut off were manually verified.

Western Blotting, Immunoprecipitation and Immunofluorescence

For western blot analyses, cytoplasmic and nuclear extracts of cells were prepared using NE-PER fractionation kit followed by SDS-PAGE and immunoblotting with the indicated antibodies.

For immunoprecipitations, cytoplasmic and nuclear extracts were diluted with NP40 lysis buffer [25mM Tris HCl (pH 7.5), 150mM NaCl, 1 μ M ZnCl₂, 1% igepal (NP40)], supplemented with protease inhibitors. Immunoprecipitations from cell lysates were performed at 4°C overnight in the lysis buffer incubated with the indicated antibodies and either Protein A agarose (for antibodies raised in rabbit) or Protein G agarose (for antibodies raised in mouse). The overnight immunoprecipitates were washed five times in lysis buffer and eluted using the LDS loading buffer and DTT. Eluates were subjected to SDS PAGE electrophoresis and western blot signals were quantified after

visualization of primary antibody by fluorescent-labeled secondary antibody and detection by Odyssey blot scanner (LiCor), using ImageJ National Institutes of Health (NIH) software.

For Immunofluorescence, cells were seeded in 4 chambered slides for 24hrs followed by treatment with 2 μ M doxorubicin for 3hrs. Cells were fixed in 4% paraformaldehyde (Thermo Scientific) in PBS for 15 minutes at room temperature. Following three washes with PBS, cells were permeabilized with 0.2% TritonX-100 in PBS for 10 minutes at room temperature. Cells were washed three times with PBS followed by 1hour blocking in Odyssey blocking buffer (Li-Cor, 927-4000) diluted 1:1 with PBS at room temperature. Slides were then incubated overnight at 4⁰C in primary antibody diluted in blocking buffer containing 0.2% TritonX-100. Following three 5 minute washes with PBS, slides were incubated for 1 hour at room temperature in the dark in secondary antibody diluted in blocking buffer containing 0.2% TritonX-100. Slides were washed three times with PBS followed by mounting with prolong diamond antifade mountant containing DAPI (Life Technologies/Molecular Probes). Images were acquired using the EVOS AMG fluorescent microscope and representative images are shown at the same exposure and magnification.

Generation of Knockdown Cell Lines

DBC1 and CBP single or double knockdown stable cell lines were made in the U2OS parent line using Mission shRNA lentiviral vector from Sigma-Aldrich and GIPZ lentiviral shRNA vector from GE Healthcare Dharmacon, respectively. DBC1 Mission shRNA clone IDs were:

NM_021174.4-1597s1c1:

Sequence: 5'-CCGGGCATTGATTTGAGCGGCTGTACTCGAGTACAGCCGCTCAAATCAATGCTTTTTG

and NM_021174.4-1125s1c1:

Sequence: 5'-CCGGCCCATCTGTGACTTCCTAGAACTCGAGTTCTAGGAAGTCACAGATGGGTTTTTG.

GIPZ CREBBP shRNAs tested for knockdown level were: V2LHS_24251, V3LHS_358933, V3LHS_358934, and V3LHS_358935.

Lentiviruses were produced in HEK-293T cells by calcium phosphate mediated transfection using pLKO.1-shRNA or pGIPZ-shRNA plasmid along with pCMV-dR8.9 packaging and pCMV-VSVG envelope plasmids.

HEK-293T cells were cultured in DMEM supplemented with 10% fetal bovine serum and 100 IU/ml penicillin, 100µg of streptomycin, and maintained in a humidified 5% CO₂ incubator at 37°C. HEK-293T cells (5 x 10⁵) were plated in 6-cm plates 24hours before transfection at confluency of 50%. Two hours prior to transfection, medium was removed from cells and replaced with no antibiotic growth medium. CaCl₂-DNAs solution was prepared, added to 2X HBS (HEPES-Buffered Saline), pH 7.1, solution, and incubated for 25minutes at room temperature followed by addition of 0.5ml of calcium phosphate-DNA precipitate to each plate. The culture medium was changed 16hours after transfection. On days 3 and 4, lentivirus supernatant was collected. Virus medium containing 8µg/ml polybrene was used to infect and transduce U2OS cells. Cells were plated in 6-cm plates 24hours before infection at confluency of 60% and infected with 1.0ml of pLKO.1 or pGIPZ lentivirus supernatant. Virus medium was removed the next day and replaced with DMEM. DMEM containing 5µg/ml puromycin was used to select the DBC1sh and CBPsh cells 48hours post-infection. The cells were

collected at 72hours post selection, and lysed for Western blotting. DBC1sh cells were subsequently used to make the DBC1/CBP double knockdown line. Cells were infected with the pGIPZ lentivirus, as previously described, and sorted for TurboGFP.

siRNA Transfection

CBP siRNA and DBC1 SMARTpool ON-TARGET plus siRNA were purchased from Ambion Life Technologies and Dharmacon respectively. U2OS cells were transfected with siRNA (30nM final concentration) using Lipofectamine 2000 (Invitrogen). 72 hours after transfection, cells were harvested and analyzed for the expression level of CBP and DBC1 by western blotting.

Plasmids and Expression of Recombinant proteins

DBC1 was divided into three different regions, DBC1 1-270aa, DBC1 1-470aa and DBC1 697-923aa based on its globular domain structure. The plasmids for overexpressing these truncated DBC1 proteins in mammalian cells were constructed by amplifying DBC1 from the parent plasmid, myc-tagged full length DBC1, which was purchased from Addgene. The following primers were used:

Forward primer for DBC11-270 and DBC1 1-470: 5'-GGATCGAATTCTCCAGTTTAAGCGCCAG

Reverse primer for DBC1 1-270: 5'-GCCATCTCGAGCTAGCTCAGGGGAAGGCTGATAG

Reverse primer for DBC1 1-470: 5'-GCCATCTCGAGCTAGGCATCAGGTGCCTGTTCAG

Forward primer for DBC1 697-923: 5'-GGATCGAATTCTCTGCTGTGCTCCCCTTAGAC

Reverse primer for DBC1697-923: 5'-CCATCTCGAGTCAGTTGCTAGGTGCCGGC

The vector backbone of the parent plasmid has intact *EcoRI* and *XhoI* sites with kozak

sequence, start codon and myc tag upstream of the *EcoRI* site. The parent plasmid and the amplified sequences were double digested with above mentioned restriction endonucleases and ligated with T4 DNA ligase using NEB manufacturer's protocols. DH10B was transformed with the ligated products and transformants were selected overnight on Lysogeny Broth Agar (LBA) plates supplemented with Ampicillin (100 µg/ml). Single colonies were restreaked on Ampicillin supplemented plates to obtain pure clones. Single colonies from the restreaks were grown overnight in LB medium containing Ampicillin (100µg/ml). Plasmid DNA was extracted from the cultures using Qiagen Miniprep kit and verified by Sanger Sequencing (MWG Operon). Full length FLAG-CBP and truncated mutants of CBP were previously made in the Lab.

Generation of shRNA resistant plasmids

shRNA resistant plasmids were constructed by generating silent mutations in the region targeted by Sigma siRNA of the DBC-1 ORF. The silent mutations were generated by Gene Splicing by Overlap Extension (Gene SOEing) method, as described in Chapter 25 of *Methods in Molecular Biology, Vol 15, PCR Protocols Current Methods and Applications*. Briefly, the parent plasmid was amplified with flanking primers containing appropriate restriction sites and complementary overlapping SOEing primers carrying silent mutations to generate DNA fragments with overlapping complementary ends. The final DNA fragment was then generated by amplifying these products with outside flanking primers. The final DNA fragment was digested with *EcoRI* and *XhoI* endonucleases and ligated to the linearized myc tagged vector.

Flanking forward primer: 5'-GGATCGAATTCTCCCAGTTTAAGCGCCAG

Reverse SOEing primer: 5'-CCATTTAGTGCACCCGGAGAGGTCGATGCCAGTCTGGGCCTGCGC

Forward SOEing primer: 5'-ATCGACCTCTCCGGGTGCACTAAATGGTGGCGCTTTGCCGAGTTTCAGTAC

Reverse flanking primer: 5'-CCATCTCGAGTCAGTTGCTAGGTGCCGGC

3.3 Results

A Nuclear Factor Inhibits CBP Autoubiquitination Activity

To define the regulation of the compartmentalized CBP ubiquitin ligase activities in the absence of cellular stress, we first examined whether there are CBP-interacting activators or inhibitors of CBP ubiquitin ligase activities in the cytoplasmic and nuclear compartments, respectively. CBP was first immunoprecipitated from cytoplasmic and nuclear fractions of U2OS cells. Different concentrations of cytoplasmic lysates and of CBP immuno-depleted cytoplasmic lysates were then incubated with nuclear CBP IPs followed by in-vitro CBP E3 autoubiquitination assay performed on the washed nuclear CBP IPs. Similarly, different concentrations of nuclear lysates and of CBP immuno-depleted nuclear lysates were incubated with cytoplasmic CBP IPs followed by in-vitro CBP E3 autoubiquitination assay on the washed cytoplasmic CBP IPs. Our results in Fig. 3.1 indicate that a nuclear factor, depleted with CBP immuno-depletion, inhibits CBP E3 autoubiquitination activity, while a cytoplasmic factor not depleted by a CBP IP promotes CBP autoubiquitination activity.

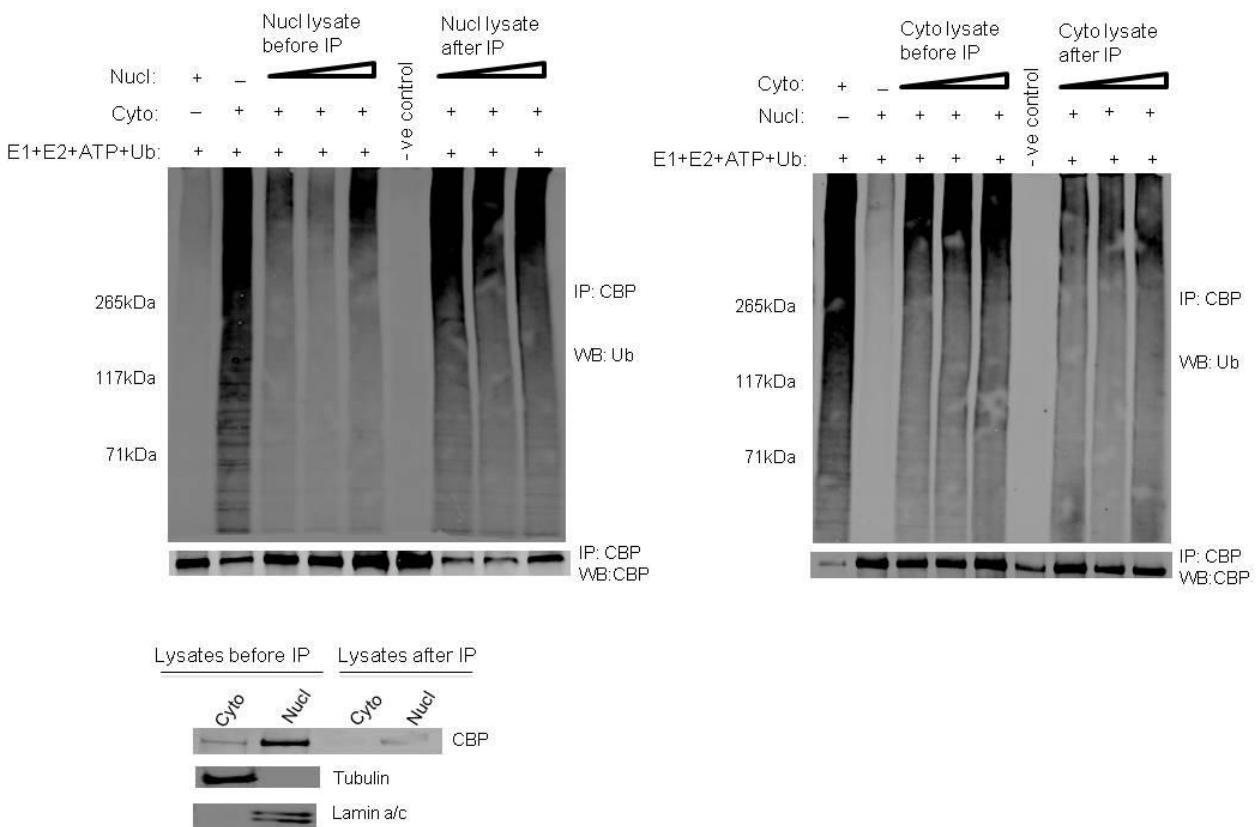


Figure 3.1 Identification of activators and/or inhibitors of CBP E3 autoubiquitination. (Left panel): CBP immunoprecipitation from cytoplasmic and nuclear fractions followed by incubation of cytoplasmic fraction with increasing concentrations of nuclear lysates before IP (0.1mg, 0.2mg, 0.4mg) or with increasing concentration of nuclear lysates after IP (0.1mg, 0.2mg, 0.4mg) for 2hrs followed by in vitro E3 assay and immunoblotting with ubiquitin (Ub) antibody (Santa Cruz). For negative (-) control, cytoplasmic IP was incubated with nuclear extraction buffer. (Right panel): CBP immunoprecipitation from cytoplasmic and nuclear fractions followed by incubation of nuclear fraction with increasing concentration of cytoplasmic lysates before IP (0.1mg, 0.2mg, 0.4mg) or with increasing concentration of cytoplasmic lysates after IP (0.1mg, 0.2mg, 0.4mg) for 2hrs followed by in vitro E3 assay and immunoblotting with ubiquitin (Ub) antibody. For negative control, nuclear IP was incubated with cytoplasmic extraction buffer.

Identification of Nuclear and Cytoplasmic CBP-Interacting Proteins

Using MudPIT analysis, we identified CBP interacting proteins from nuclear, as well as cytoplasmic, fractions of U2OS cells. Silver staining of CBP immunoprecipitations revealed both common and differential protein bands between nuclear and cytoplasmic fractions of U2OS cells (Fig. 3.2), indicating that there are differential CBP binding proteins between both cellular compartments. Nuclear CBP was 3-fold more abundant than cytoplasmic CBP (Fig. 3.3), consistent with previous findings by immunoblot and immunofluorescence [1, 118]. We subtracted from our list of CBP-interacting partners, proteins with only one spectrum count and proteins identified in the IgG control IPs from both cytoplasmic and nuclear fractions. We identified 70 overlapping cytoplasmic CBP-binding proteins and 48 overlapping nuclear CBP-binding proteins from two independent experiments (Fig. 3.4, 3.5) (Tables 2 & 3). Of interest was a 130kDa protein with a total spectra count second to CBP's in the nuclear fraction, but also present in the cytoplasm fraction, identified as Cell Cycle and Apoptosis Regulator protein 2 (CCAR2), otherwise known as Deleted in Breast Cancer 1 (DBC1).

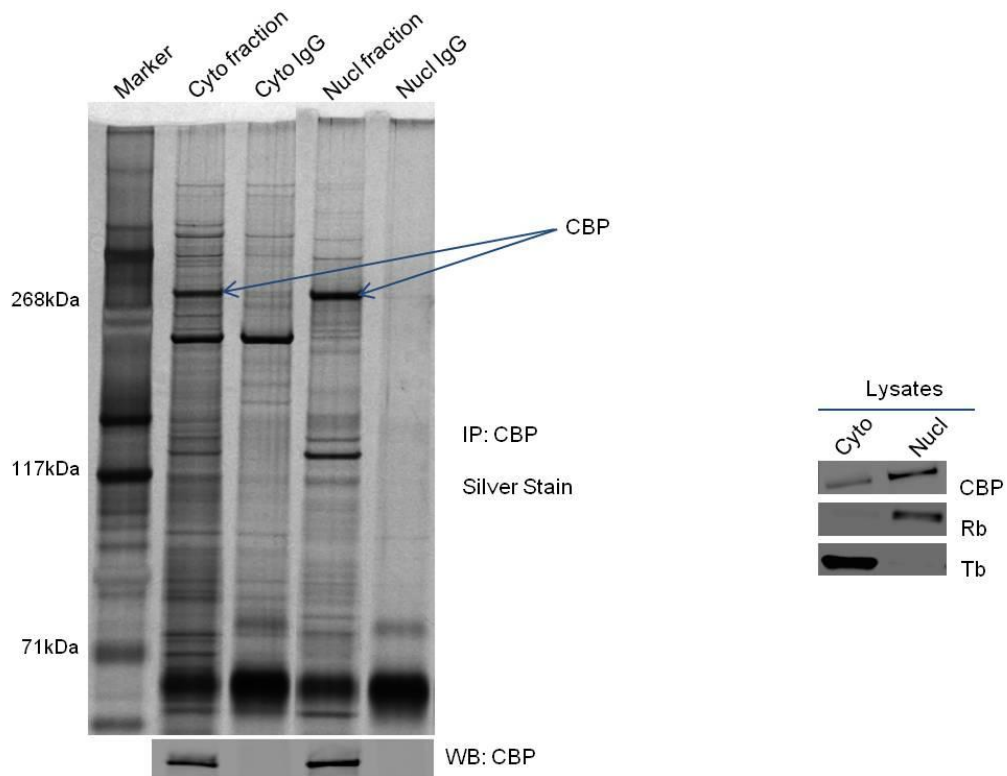


Figure 3.2 Silver staining of CBP immunoprecipitations from cytoplasmic and nuclear fractions of U2OS cells. CBP was immunoprecipitated from cytoplasmic and nuclear fractions of U2OS cells followed by SDS-PAGE electrophoresis and silver staining using the SilverQuest Silver Staining kit from Thermo Fisher Scientific.

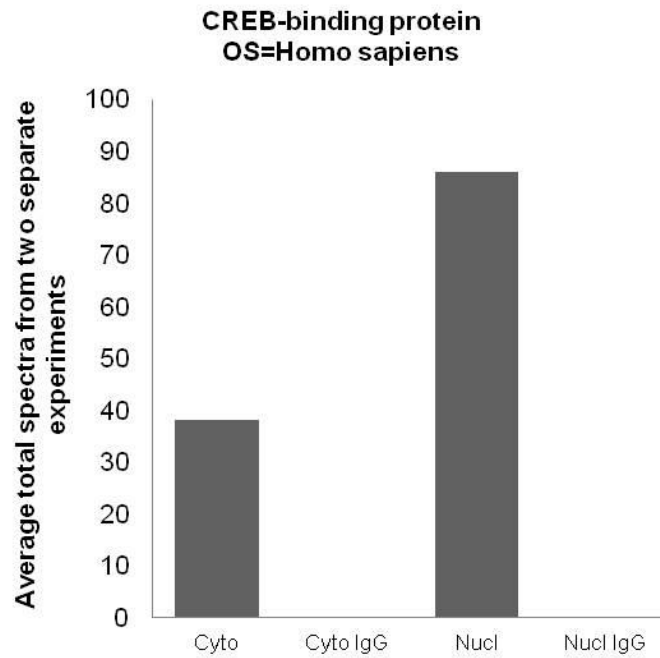


Figure 3.3 Identification of CBP by MudPIT analysis from cytoplasmic and nuclear CBP IPs of U2OS cells. Graph represents the average number of total spectra counts of CBP from two independent experiments.

Table 2: List of cytoplasmic CBP-interacting proteins ranked from highest to lowest total spectrum count. (1-18)

	Description	Gene	Protein accession number	Protein molecular weight (Da)	Protein identification probability	Exclusive unique peptide count	Exclusive unique spectrum count	Total spectrum count
1	CREB-binding protein OS=Homo sapiens GN=CREBBP PE=1 SV=3	CREBBP	Q92793	285,345.4	100.00%	19	25	40
2	Isoform 2 of TBC1 domain family member 15 OS=Homo sapiens GN=TBC1D15	TBC1D15	Q8TC07-2	77,397.4	100.00%	20	26	28
3	Isoform 3 of Protein AHNAK2 OS=Homo sapiens GN=AHNAK2	AHNAK2	Q8IVF2-3	605,647.5	100.00%	21	23	24
4	Cell cycle and apoptosis regulator protein 2 OS=Homo sapiens GN=CCAR2 PE=1 SV=2	CCAR2	Q8N163	102,903.1	100.00%	14	15	21
5	Isoform PML-11 of Protein PML OS=Homo sapiens GN=PML	PML	P29590-11	92,564.5	100.00%	2	2	19
6	Protein TFG OS=Homo sapiens GN=TFG PE=1 SV=2	TFG	Q92734,Q92734-2	43,448.3	100.00%	7	14	18
7	Fatty acid synthase OS=Homo sapiens GN=FASN PE=1 SV=3	FASN	P49327	273,427.1	100.00%	11	11	13
8	Sperm-associated antigen 5 OS=Homo sapiens GN=SPAG5 PE=1 SV=2	SPAG5	Q96R06	134,423.1	100.00%	11	11	13
9	DNA replication licensing factor MCM7 OS=Homo sapiens GN=MCM7 PE=1 SV=4	MCM7	P33993	81,309.0	100.00%	9	10	12
10	Nuclear factor NF-kappa-B p100 subunit OS=Homo sapiens GN=NFKB2 PE=1 SV=4	NFKB2	Q00653,Q00653-4	96,679.6	100.00%	10	11	12
11	Sorting nexin-9 OS=Homo sapiens GN=SNX9 PE=1 SV=1	SNX9	Q8Y5X1	66,592.8	100.00%	9	11	12
12	40S ribosomal protein S4, X isoform OS=Homo sapiens GN=RPS4X PE=1 SV=2	RPS4X	P62701	29,599.3	100.00%	6	7	11
13	U5 small nuclear ribonucleoprotein 200 kDa helicase OS=Homo sapiens GN=SNRNP200 PE=1 SV=2	SNRNP200	O75643	244,513.8	100.00%	9	9	10
14	5-azacytidine-induced protein 1 OS=Homo sapiens GN=AZI1 PE=1 SV=3	AZI1	Q9JPN4,Q9JPN4-2	122,149.9	100.00%	8	8	9
15	Valine-tRNA ligase OS=Homo sapiens GN=VARS PE=1 SV=4	VARS	P26640	140,477.5	100.00%	7	8	9
16	T-complex protein 1 subunit gamma OS=Homo sapiens GN=CCT3 PE=1 SV=4	CCT3	P49368	60,535.4	100.00%	8	8	8
17	Cytoskeleton-associated protein 4 OS=Homo sapiens GN=CKAP4 PE=1 SV=2	CKAP4	Q07065	66,022.2	100.00%	4	4	4
18	Huntingtin-interacting protein 1-related protein OS=Homo sapiens GN=HIP1R PE=1 SV=2	HIP1R	O75146	119,389.7	100.00%	2	2	4

Table 2: List of cytoplasmic CBP-interacting proteins ranked from highest to lowest total spectrum count. (19-36)

	Description	Gene	Protein accession number	Protein molecular weight (Da)	Protein identification probability	Exclusive unique peptide count	Exclusive unique spectrum count	Total spectrum count
19	Constitutive coactivator of PPAR-gamma-like protein 1 OS=Homo sapiens GN=FAM120A PE=1 SV=2	FAM120A	Q9NZB2,Q9NZB2-6	125,273.3	100.00%	7	7	8
20	tRNA (cytosine(34)-C(5))-methyltransferase OS=Homo sapiens GN=NSUN2 PE=1 SV=2	NSUN2	Q08J23,Q08J23-2	86,472.8	100.00%	8	8	8
21	Vigilin OS=Homo sapiens GN=HDLBP PE=1 SV=2	HDLBP	Q00341	141,458.2	100.00%	6	6	7
22	Poly(A) binding protein, cytoplasmic 4 (inducible form), isoform CRA_e OS=Homo sapiens GN=PABPC4 PE=2 SV=1	PABPC4	B1ANR0,Q13310-2,Q13310-3	70,783.8	100.00%	3	3	7
23	DNA-dependent protein kinase catalytic subunit OS=Homo sapiens GN=PRKDC PE=1 SV=3	PRKDC	P78527	469,095.5	100.00%	7	7	7
24	Transferrin receptor protein 1 OS=Homo sapiens GN=TFRC PE=1 SV=2	TFRC	P02786	84,873.6	100.00%	5	5	7
25	Tight junction-associated protein 1 OS=Homo sapiens GN=TJAP1 PE=1 SV=1	TJAP1	Q5JTD0,Q5JTD0-2	61,822.2	100.00%	5	7	7
26	T-complex protein 1 subunit delta OS=Homo sapiens GN=CCT4 PE=1 SV=4	CCT4	P50991	57,926.0	100.00%	5	6	6
27	Eukaryotic translation initiation factor 4 gamma 2 OS=Homo sapiens GN=EIF4G2 PE=1 SV=1	EIF4G2	P78344	102,366.8	100.00%	6	6	6
28	Heterogeneous nuclear ribonucleoprotein M OS=Homo sapiens GN=HNRNPM PE=1 SV=3	HNRNPM	P52272,P52272-2	77,517.3	100.00%	3	3	6
29	Proteasome activator complex subunit 3 OS=Homo sapiens GN=PSME3 PE=1 SV=1	PSME3	P61289,P61289-2	29,507.3	100.00%	4	6	6
30	60S ribosomal protein L7 OS=Homo sapiens GN=RPL7 PE=1 SV=1	RPL7	P18124	29,227.7	100.00%	6	6	6
31	Zyxin OS=Homo sapiens GN=ZYX PE=1 SV=1	ZYX	Q15942	61,276.0	100.00%	5	5	6
32	Kinesin-like protein KIF2A OS=Homo sapiens GN=KIF2A PE=1 SV=3	KIF2A	O00139,O00139-1,O00139-2,O00139-4,O00139-5	77,749.8	100.00%	5	5	5
33	Small kinetochore-associated protein OS=Homo sapiens GN=KNSTRN PE=1 SV=2	KNSTRN	Q9Y448	35,438.8	100.00%	4	4	5
34	AP-2 complex subunit alpha-1 OS=Homo sapiens GN=AP2A1 PE=1 SV=3	AP2A1	O95782,O95782-2	105,364.2	100.00%	3	3	4
35	Hexokinase-1 OS=Homo sapiens GN=HK1 PE=2 SV=1	HK1	E7ENR4	106,316.2	100.00%	3	3	4
36	Isoleucine-tRNA ligase, mitochondrial OS=Homo sapiens GN=IARS2 PE=2 SV=1	IARS2	F6SBX2,Q9NSE4	113,794.1	100.00%	4	4	4

Table 2: List of cytoplasmic CBP-interacting proteins ranked from highest to lowest total spectrum count. (37-55)

	Description	Gene	Protein accession number	Protein molecular weight (Da)	Protein identification probability	Exclusive unique peptide count	Exclusive unique spectrum count	Total spectrum count
37	Monofunctional C1-tetrahydrofolate synthase, mitochondrial OS=Homo sapiens GN=MTHFD1L PE=1 SV=1	MTHFD1L	Q6UB35	105,791.9	100.00%	3	3	4
38	Proliferation-associated protein 2G4 OS=Homo sapiens GN=PA2G4 PE=1 SV=3	PA2G4	Q9UQ80	43,786.7	100.00%	3	3	4
39	Protein-L-isoaspartate(D-aspartate)O-methyltransferase OS=Homo sapiens GN=PCMT1 PE=1 SV=4	PCMT1	P22061, P22061-2	24,636.8	100.00%	4	4	4
40	Isoform 2 of Calcium-binding mitochondrial carrier protein Aralar2 OS=Homo sapiens GN=SLC25A13	SLC25A13	Q9UJ50-2	74,305.3	100.00%	3	3	4
41	WD repeat and HMG-box DNA-binding protein 1 OS=Homo sapiens GN=WDHD1 PE=1 SV=1	WDHD1	O75717	125,970.0	100.00%	4	4	4
42	Zinc finger CCHH-type antiviral protein 1 OS=Homo sapiens GN=ZC3HAV1 PE=1 SV=3	ZC3HAV1	Q7Z2W4	101,432.6	100.00%	4	4	4
43	Alkylidihydroxyacetonephosphate synthase, peroxisomal OS=Homo sapiens GN=AGPS PE=1 SV=1	AGPS	O00116	72,913.3	100.00%	3	3	3
44	Uncharacterized protein C10orf118 OS=Homo sapiens GN=C10orf118 PE=1 SV=2	C10orf118	Q7Z3E2	103,689.8	100.00%	3	3	3
45	F-actin-capping protein subunit alpha-1 OS=Homo sapiens GN=CAPZA1 PE=1 SV=3	CAPZA1	P52907	32,923.2	100.00%	2	2	3
46	Collagen alpha-1(I) chain OS=Homo sapiens GN=COL1A1 PE=1 SV=5	COL1A1	P02452	138,941.4	100.00%	3	3	3
47	Coronin-1C OS=Homo sapiens GN=CORO1C PE=1 SV=1	CORO1C	Q9ULV4, Q9ULV42, Q9ULV4-3	58,948.9	100.00%	3	3	3
48	Developmentally-regulated GTP-binding protein 1 OS=Homo sapiens GN=DRG1 PE=1 SV=1	DRG1	Q9Y295	40,543.8	100.00%	3	3	3
49	Ras GTPase-activating protein-binding protein 1 OS=Homo sapiens GN=G3BP1 PE=1 SV=1	G3BP1	Q13283	52,162.8	100.00%	2	2	3
50	Isoform 3 of Mitochondrial inner membrane protein OS=Homo sapiens GN=IMMT	IMMT	Q16891-3	80,028.2	100.00%	3	3	3
51	Putative helicase MOV-10 OS=Homo sapiens GN=MOV10 PE=1 SV=2	MOV10	Q9HCE1	113,675.5	100.00%	3	3	3
52	SART3 protein OS=Homo sapiens GN=SART3 PE=2 SV=1	SART3	B7ZKM0, Q15020	109,936.4	100.00%	2	2	3
53	Sideroflexin-3 OS=Homo sapiens GN=SFXN3 PE=1 SV=2	SFXN3	Q9BWM7	35,979.1	100.00%	3	3	3
54	FACT complex subunit SPT16 OS=Homo sapiens GN=SUPT16H PE=1 SV=1	SUPT16H	Q9Y5B9	119,917.4	100.00%	3	3	3
55	Isoform 3 of Heterogeneous nuclear ribonucleoprotein Q OS=Homo sapiens GN=SYNCRIP	SYNCRIP	O605063, O60506-4	62,657.2	100.00%	2	2	3

Table 2: List of cytoplasmic CBP-interacting proteins ranked from highest to lowest total spectrum count. (56-70)

	Description	Gene	Protein accession number	Protein molecular weight (Da)	Protein identification probability	Exclusive unique peptide count	Exclusive unique spectrum count	Total spectrum count
56	T-complex protein 1 subunit alpha OS=Homo sapiens GN=TCP1 PE=1 SV=1	TCP1	P17987	60,345.2	100.00%	3	3	3
57	Thrombospondin-1 OS=Homo sapiens GN=THBS1 PE=1 SV=2	THBS1	P07996	129,381.7	100.00%	3	3	3
58	ATP-binding cassette sub-family F member 1 OS=Homo sapiens GN=ABCF1 PE=1 SV=2	ABCF1	Q8NE71, Q8NE71-2	91,682.6	100.00%	2	2	2
59	ATP synthase subunit gamma OS=Homo sapiens GN=ATP5C1 PE=2 SV=1	ATP5C1	B4DL14, P36542, P36542-2	32,882.9	100.00%	2	2	2
60	HLA-B associated transcript 3, isoform CRA_a OS=Homo sapiens GN=BAG6 PE=4 SV=1	BAG6	B0UX83, P46379, P46379-2, P46379-3, P46379-4, P46379-5	119,407.3	100.00%	2	2	2
61	Protein FAM98A OS=Homo sapiens GN=FAM98A PE=1 SV=1	FAM98A	Q8NCA5, Q8NCA5-2	55,401.4	100.00%	2	2	2
62	Fragile X mental retardation syndrome-related protein 1 OS=Homo sapiens GN=FXR1 PE=2 SV=1	FXR1	B4DXZ6, P51114	69,720.9	100.00%	2	2	2
63	Heterogeneous nuclear ribonucleoprotein F OS=Homo sapiens GN=HNRNPF PE=1 SV=3	HNRNPF	P52597	45,671.9	100.00%	2	2	2
64	La-related protein 4 OS=Homo sapiens GN=LARP4 PE=1 SV=3	LARP4	Q71RC2, Q71RC2-3, Q71RC2-4, Q71RC2-5, Q71RC2-7	80,596.3	100.00%	2	2	2
65	Isoform 2 of Palladin OS=Homo sapiens GN=PALLD	PALLD	Q8WX93-2, Q8WX93-5, Q8WX93-9	122,047.9	100.00%	2	2	2
66	Protein PRRC2C OS=Homo sapiens GN=PRRC2C PE=2 SV=1	PRRC2C	E7EPN9, Q9Y520, Q9Y520-0-4, Q9Y520-5, Q9Y520-6, Q9Y520-7	317,078.7	100.00%	2	2	2
67	60S ribosomal protein L14 OS=Homo sapiens GN=RPL14 PE=2 SV=1	RPL14	E7EPB3, P50914	14,557.9	100.00%	2	2	2
68	40S ribosomal protein S9 OS=Homo sapiens GN=RPS9 PE=2 SV=1	RPS9	C9JM19	18,401.5	99.90%	2	2	2
69	Regulator of nonsense transcripts 1 OS=Homo sapiens GN=UPF1 PE=1 SV=2	UPF1	Q92900	124,346.9	100.00%	2	2	2
70	14-3-3 protein zeta/delta (Fragment) OS=Homo sapiens GN=YWHAZ PE=2 SV=1	YWHAZ	E7EX29, P63104	27,745.9	100.00%	2	2	2

Table 3: List of nuclear CBP-interacting proteins ranked from highest to lowest total spectrum count. (1-18)

	Description	Gene	Protein accession number	Protein molecular weight (Da)	Protein identification probability	Exclusive unique peptide count	Exclusive unique spectrum count	Total spectrum count
1	CREB-binding protein OS=Homo sapiens GN=CREBBP PE=1 SV=3	CREBBP	Q92793	265,345.4	100.00%	32	49	84
2	Cell cycle and apoptosis regulator protein 2 OS=Homo sapiens GN=CCAR2 PE=1 SV=2	CCAR2	Q8N163	102,903.1	100.00%	24	34	46
3	Heterogeneous nuclear ribonucleoprotein M OS=Homo sapiens GN=HNRNPM PE=1 SV=3	HNRNPM	P52272, P52272-2	77,517.3	100.00%	9	9	15
4	Heterogeneous nuclear ribonucleoprotein A0 OS=Homo sapiens GN=HNRNPA0 PE=1 SV=1	HNRNPA0	Q13151	30,840.5	100.00%	6	7	13
5	Non-POU domain-containing octamer-binding protein OS=Homo sapiens GN=NONO PE=1 SV=4	NONO	Q15233	54,231.6	100.00%	6	9	13
6	T-complex protein 1 subunit theta OS=Homo sapiens GN=CCT8 PE=1 SV=4	CCT8	P50990	59,621.0	100.00%	11	12	12
7	Isoform 2 of ATP-dependent RNA helicase DDX3X OS=Homo sapiens GN=DDX3X	DDX3X	O00571-2	71,357.4	100.00%	8	9	12
8	Heterogeneous nuclear ribonucleoprotein D0 OS=Homo sapiens GN=HNRNPD PE=1 SV=1	HNRNPD	Q14103, Q14103-3	38,434.5	100.00%	1	2	12
9	Heterogeneous nuclear ribonucleoprotein D-like OS=Homo sapiens GN=HNRNPD PE=1 SV=3	HNRNPD	O14979, O14979-2, O14979-3	46,438.6	100.00%	3	5	9
10	Poly(rC)-binding protein 1 OS=Homo sapiens GN=PCBP1 PE=1 SV=2	PCBP1	Q15365	37,498.2	100.00%	5	7	9
11	Coronin-1C OS=Homo sapiens GN=CORO1C PE=1 SV=1	CORO1C	Q9ULV4, Q9ULV4-2, Q9ULV4-3	58,948.9	100.00%	7	8	8
12	Matrin-3 OS=Homo sapiens GN=MATR3 PE=2 SV=1	MATR3	A8MXP9, P43243	99,970.9	100.00%	8	8	8
13	Heterogeneous nuclear ribonucleoprotein A3 OS=Homo sapiens GN=HNRNPA3 PE=1 SV=2	HNRNPA3	P51991	39,595.1	100.00%	3	5	7
14	Heterogeneous nuclear ribonucleoprotein F OS=Homo sapiens GN=HNRNPF PE=1 SV=3	HNRNPF	P52597	45,671.9	100.00%	3	5	7
15	DNA replication licensing factor MCM7 OS=Homo sapiens GN=MCM7 PE=1 SV=4	MCM7	P33993	81,309.0	100.00%	7	7	7
16	Paraspeckle component 1 OS=Homo sapiens GN=PSPC1 PE=1 SV=1	PSPC1	Q8WXF1	58,744.5	100.00%	5	6	7
17	Nucleolar RNA helicase 2 OS=Homo sapiens GN=DDX21 PE=1 SV=5	DDX21	Q9NR30	87,346.0	100.00%	5	5	6
18	Heterogeneous nuclear ribonucleoprotein L OS=Homo sapiens GN=HNRNPL PE=1 SV=2	HNRNPL	P14866	64,132.8	100.00%	5	5	6

Table 3: List of nuclear CBP-interacting proteins ranked from highest to lowest total spectrum count. (19-33)

	Description	Gene	Protein accession number	Protein molecular weight (Da)	Protein identification probability	Exclusive unique peptide count	Exclusive unique spectrum count	Total spectrum count
19	DNA-dependent protein kinase catalytic subunit OS=Homo sapiens GN=PRKDC PE=1 SV=3	PRKDC	P78527	469,095.5	100.00%	6	6	6
20	GTP-binding nuclear protein Ran OS=Homo sapiens GN=RAN PE=2 SV=1	RAN	B5MDF5, P62826	24,423.1	100.00%	6	6	6
21	Huntingtin-interacting protein 1-related protein OS=Homo sapiens GN=HIP1R PE=1 SV=2	HIP1R	O75146	119,389.7	100.00%	4	4	5
22	PDZ and LIM domain protein 7 OS=Homo sapiens GN=PDLIM7 PE=1 SV=1	PDLIM7	Q9NR12	49,844.4	100.00%	2	2	5
23	40S ribosomal protein S4, X isoform OS=Homo sapiens GN=RPS4X PE=1 SV=2	RPS4X	P62701	29,599.3	100.00%	2	2	5
24	T-complex protein 1 subunit alpha OS=Homo sapiens GN=TCP1 PE=1 SV=1	TCP1	P17987	60,345.2	100.00%	5	5	5
25	Zinc finger protein 185 OS=Homo sapiens GN=ZNF185 PE=1 SV=3	ZNF185	O15231, O15231-3, O15231-4, O15231-6, O15231-7, O15231-8	73,525.4	100.00%	3	4	5
26	Zyxin OS=Homo sapiens GN=ZYG PE=1 SV=1	ZYG	Q15942	61,276.0	100.00%	5	5	5
27	Isoform 3 of Protein_AHNAK2 OS=Homo sapiens GN=AHNAK2	AHNAK2	Q81VF2-3	605,647.5	100.00%	4	4	4
28	Mitotic checkpoint protein BUB3 (Fragment) OS=Homo sapiens GN=BUB3 PE=2 SV=1	BUB3	J3QT28, O43684, O43684-2	37,154.7	100.00%	4	4	4
29	Isoform 2 of 116 kDa U5 small nuclear ribonucleoprotein component OS=Homo sapiens GN=EFTUD2	EFTUD2	Q15029-2	105,385.6	100.00%	2	2	4
30	Trifunctional enzyme subunit alpha, mitochondrial OS=Homo sapiens GN=HADHA PE=1 SV=2	HADHA	P40939	83,001.9	100.00%	4	4	4
31	Heterogeneous nuclear ribonucleoprotein A/B OS=Homo sapiens GN=HNRNPAB PE=2 SV=1	HNRNPAB	D6R9P3.D6 RBZ0.D6RD 18.Q99729-2.Q99729-3	35,967.9	100.00%	2	2	4
32	Heterogeneous nuclear ribonucleoprotein H2 OS=Homo sapiens GN=HNRNP2 PE=1 SV=1	HNRNP2	P55795	49,264.1	100.00%	2	2	4
33	Heterogeneous nuclear ribonucleoprotein H3 OS=Homo sapiens GN=HNRNP3 PE=1 SV=2	HNRNP3	P31942	36,927.6	100.00%	3	4	4

Table 3: List of nuclear CBP-interacting proteins ranked from highest to lowest total spectrum count. (34-48)

	Description	Gene	Protein accession number	Protein molecular weight (Da)	Protein identification probability	Exclusive unique peptide count	Exclusive unique spectrum count	Total spectrum count
34	X-ray repair cross-complementing protein 5 OS=Homo sapiens GN=XRCC5 PE=1 SV=3	XRCC5	P13010	82,707.1	100.00%	4	4	4
35	5-azacytidine-induced protein 1 OS=Homo sapiens GN=AZ11 PE=1 SV=3	AZ11	Q9JPN4, Q9JPN4-2	122,149.9	100.00%	3	3	3
36	Filamin-A OS=Homo sapiens GN=FLNA PE=1 SV=4	FLNA	P21333, P21333-2, Q5HY54	280,008.7	100.00%	3	3	3
37	Huntingtin-interacting protein 1 OS=Homo sapiens GN=HIP1 PE=1 SV=5	HIP1	O00291	116,222.9	100.00%	3	3	3
38	Lamin-B1 OS=Homo sapiens GN=LMBN1 PE=1 SV=2	LMBN1	P20700	66,409.6	100.00%	3	3	3
39	Phostensin OS=Homo sapiens GN=PPP1R18 PE=1 SV=1	PPP1R18	Q6NYC8	67,942.8	100.00%	2	3	3
40	Heterogeneous nuclear ribonucleoprotein U-like protein 1 OS=Homo sapiens GN=HNRNPUL1 PE=2 SV=1	HNRNPUL1	B7Z4B8, Q9BUJ2, Q9BUJ2-2, Q9BUJ2-4	95,739.7	100.00%	2	2	2
41	Nucleolar and coiled-body phosphoprotein 1 OS=Homo sapiens GN=NOLC1 PE=1 SV=2	NOLC1	Q14978, Q14978-2, Q14978-3	74,747.4	100.00%	2	2	2
42	Proliferation-associated protein 2G4 OS=Homo sapiens GN=PA2G4 PE=1 SV=3	PA2G4	Q9UQ80	43,786.7	99.80%	2	2	2
43	Pre-miRNA-processing factor 6 OS=Homo sapiens GN=PRPF6 PE=1 SV=1	PRPF6	O94906	106,927.7	100.00%	2	2	2
44	ATP-dependent DNA helicase Q1 OS=Homo sapiens GN=RECQL PE=1 SV=3	RECQL	P46063	73,458.9	100.00%	2	2	2
45	40S ribosomal protein S3 OS=Homo sapiens GN=RPS3 PE=2 SV=1	RPS3	E9PL09, P23396	26,688.6	99.80%	2	2	2
46	40S ribosomal protein S3a OS=Homo sapiens GN=RPS3A PE=1 SV=2	RPS3A	P61247	29,945.3	100.00%	2	2	2
47	SAFB-like transcription modulator OS=Homo sapiens GN=SLTM PE=1 SV=2	SLTM	Q9NWH9	117,151.1	100.00%	2	2	2
48	WD40 repeat-containing protein SMU1 OS=Homo sapiens GN=SMU1 PE=1 SV=2	SMU1	Q2TAY7	57,544.8	100.00%	2	2	2

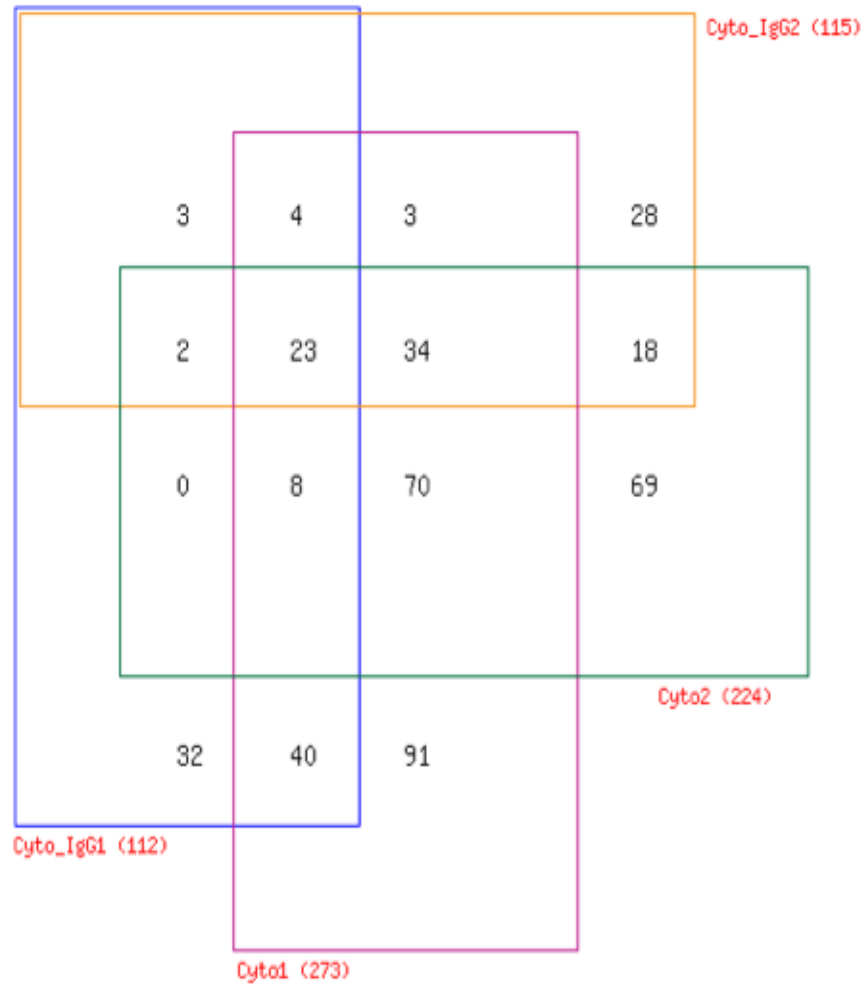


Figure 3.4 Venn diagram representation of cytoplasmic CBP interacting proteins from two independent experiments.

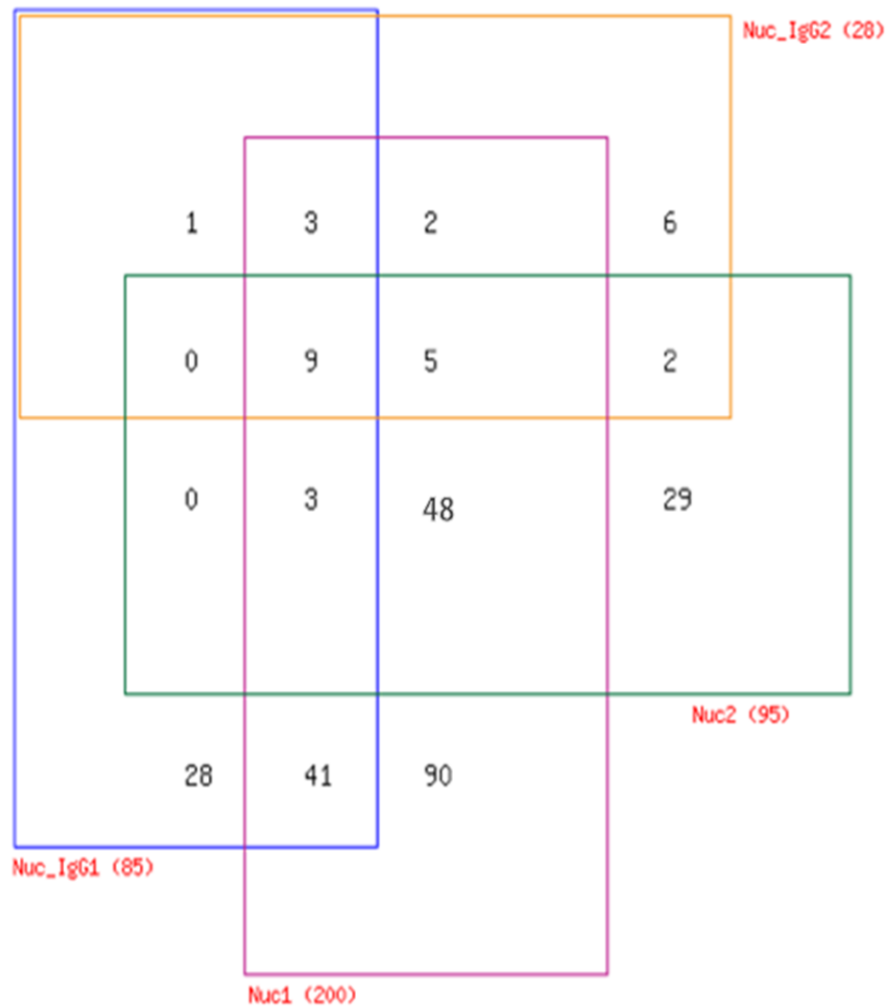


Figure 3.5 Venn diagram representation of nuclear CBP interacting proteins from two independent experiments.

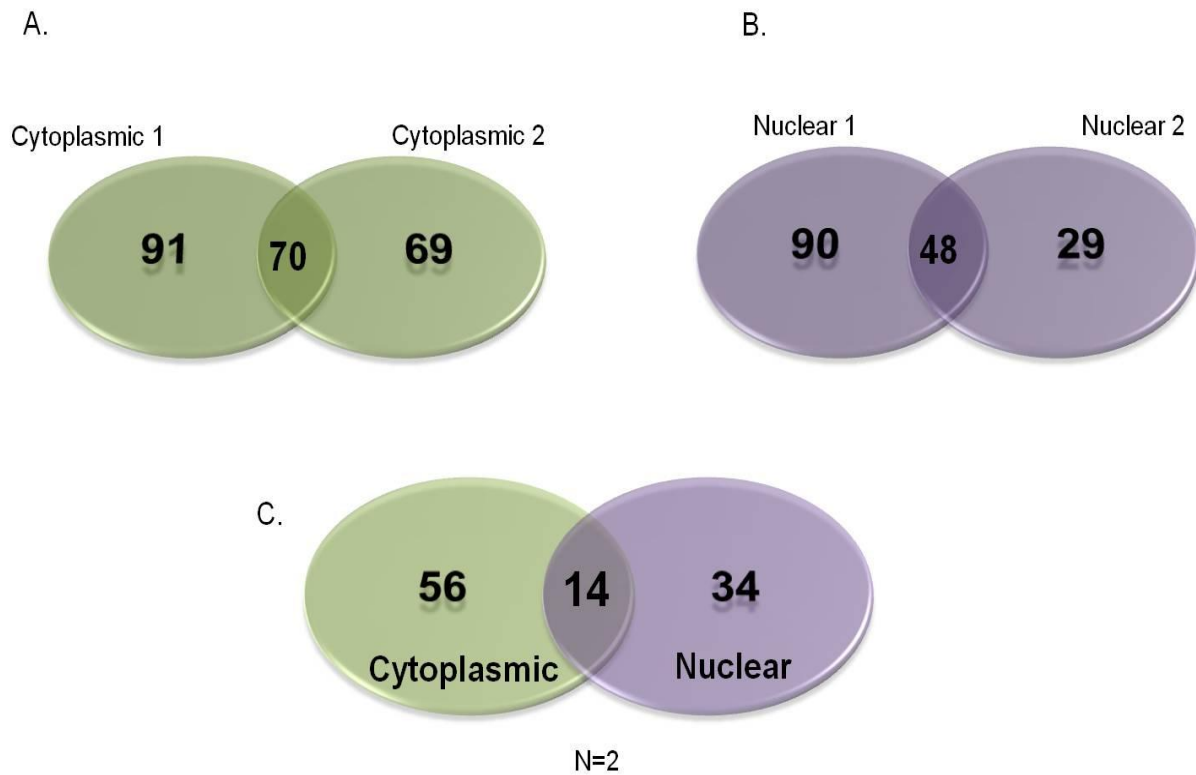


Figure 3.6 Venn diagram representation of CBP-interacting proteins. Proteins were identified by MudPIT analysis from CBP immunoprecipitations from cytoplasmic and nuclear fractions of U2OS cells, from two independent experiments (N=2). **A.** Cytoplasmic CBP- interacting proteins. **B.** Nuclear CBP- interacting proteins. **C.** Overlap between cytoplasmic CBP and nuclear CBP-interacting proteins.

CBP-DBC1 Interaction in Cells

DBC1 was initially mapped to a region homozygously deleted in certain human breast cancers [171, 172], and has previously been shown to modulate the activities of nuclear receptors such as, AR, Rev-erba, ER α , and of epigenetic modifiers such as SIRT1, HDAC3 and SUV39H1 [173-178]. MudPIT data revealed threefold more nuclear DBC1 than cytoplasmic DBC1 from the CBP IPs (Fig. 3.7). To confirm that DBC1 interacts with CBP, we transfected U2OS cells with FLAG-CBP and myc-DBC1 and performed anti-FLAG IP followed by myc or FLAG immunoblotting. As shown in Fig. 3.8 A, myc-DBC1 was observed in the FLAG IP when the two proteins were cotransfected. We further validated the interaction between CBP and DBC1 by endogenous CBP and DBC1 immunoprecipitations from U2OS cells where robust co-immunoprecipitation with each antibody was observed in both nuclear and cytoplasmic lysates, but no signal was seen in control IgG IPs (Fig. 3.8 B). Similar evidence of interaction between endogenous CBP and DBC1 was observed in H1299 cells (Fig. 3.8 C). By immunofluorescence microscopy, both CBP and DBC1 exhibited very similar staining pattern in the nucleus, as that is where the bulk of each protein is localized (Fig. 3.9).

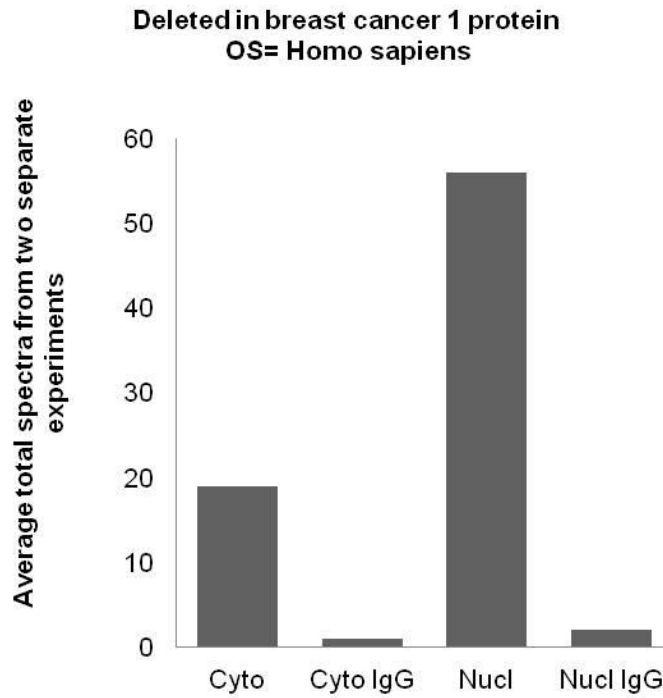


Figure 3.7 Identification of DBC1 by MudPIT analysis from cytoplasmic and nuclear CBP IPs of U2OS cells. CBP was immunoprecipitated from cytoplasmic and nuclear fractions of U2OS cells followed by MudPIT and mass spectrometry analyses. Graph represents the average number of total spectra count from two separate experiments.

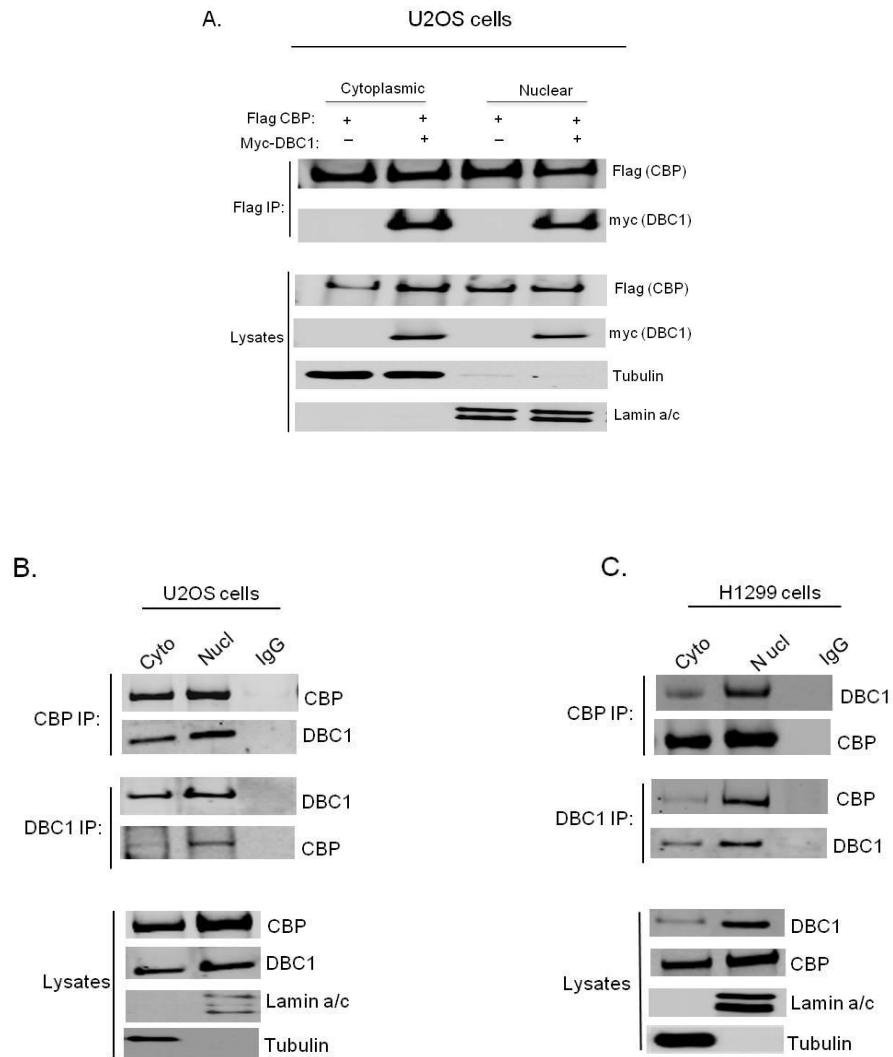


Figure 3.8 DBC1 stably interacts with CBP in cells. **A.** U2OS cells were transfected with flag tagged full length CBP and myc tagged full length DBC1 for 48hrs followed by flag immunoprecipitation and immunoblotting using flag (sigma) and myc (millipore) antibodies. **B. and C.** Endogenous interaction between CBP and DBC1. CBP or DBC1 immunoprecipitations from cytoplasmic and nuclear fractions of U2OS cells (B) and H1299 cells (C) followed by immunoblotting using CBP and DBC1 antibodies.

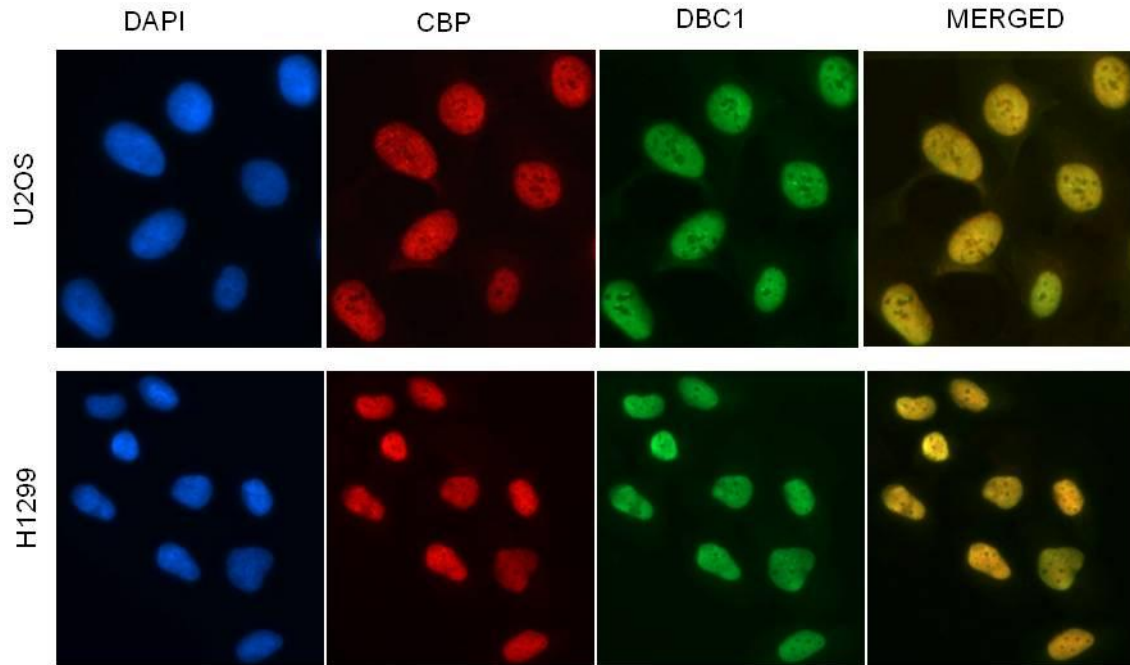


Figure 3.9 Immunofluorescence microscopy of CBP and DBC1 in U2OS and H1299 cells. Images were acquired using the EVOS AMG fluorescent microscope and representative images are shown at the same exposure and magnification (40X).

Mapping the Regions of DBC1 and CBP Required for the CBP-DBC1 Interaction

To identify the regions of DBC1 that are necessary for the CBP-DBC1 interaction, we transfected U2OS cells with full length FLAG-CBP and truncation mutants of myc-DBC1 and performed FLAG IP's followed by FLAG and myc blots. DBC1 protein structure consists of an N-terminal NLS (nuclear localization sequence), LZ (leucine zipper) domain, a centrally located NUDIX domain and a C-terminus coiled-coiled domain. We found that deletion of the N-terminal region of DBC1 (construct 697-923aa) abolished the binding between DBC1 and CBP (Fig. 3.10), while the first 240 amino acids of DBC1 were sufficient for CBP-DBC1 interaction (Fig. 3.11).

To identify the regions of CBP that interact with DBC1, we transfected U2OS cells with full-length myc-DBC1 and the N- and C- terminal deletion constructs of FLAG-CBP followed by FLAG IP's and FLAG and myc blots. CBP consists of three cysteine/histidine domains; CH1, CH2, and CH3 located at the N-terminus transactivation region, the centrally located acetyl-transferase region and the C-terminus transactivation region respectively (Fig. 1.1). The tested constructs deleted all 3 domains (1-351), included CH1 only (1-676), or included CH2/CH3 (Δ 1-665). Our results indicate that DBC1 bound to all the tested CBP constructs, indicating DBC1 interactions with both the extreme N-(1-351) and C-terminal regions (666-2442) of CBP (Fig. 3.12). Notably, p53 also binds to both N- and C- terminal regions of CBP. Binding of p53 to N-terminus of CBP (CH1 domain) promotes p53 polyubiquitination and its subsequent degradation [118] while binding to the C-terminus (CH3 domain) promotes acetylation and transcriptional activation of p53 [157].

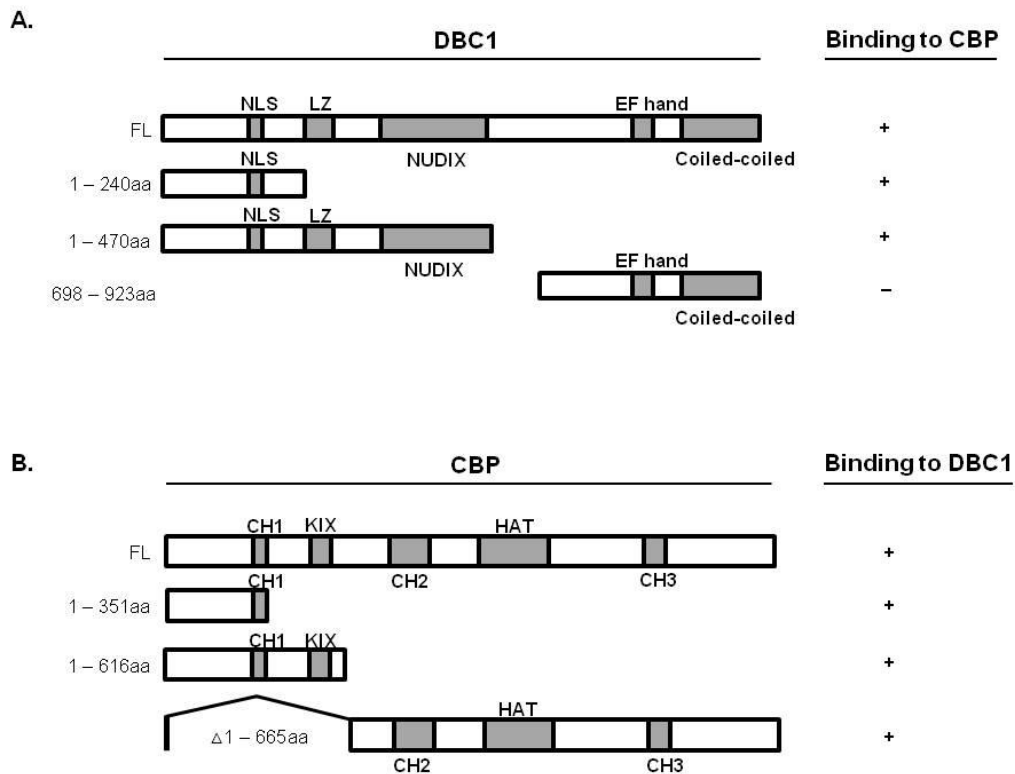


Figure 3.10 Schematic diagram of full-length (FL) DBC1, full-length CBP and deletion mutants of DBC1 and CBP. NLS, nuclear localization sequence; NES, nuclear export sequence; CH1, CH2, CH3, cysteine-histidine regions, LZ; leucine zipper, NUDIX; Nucleoside Diphosphate linked to X, EF; E and F alpha helices of parvalbumin.

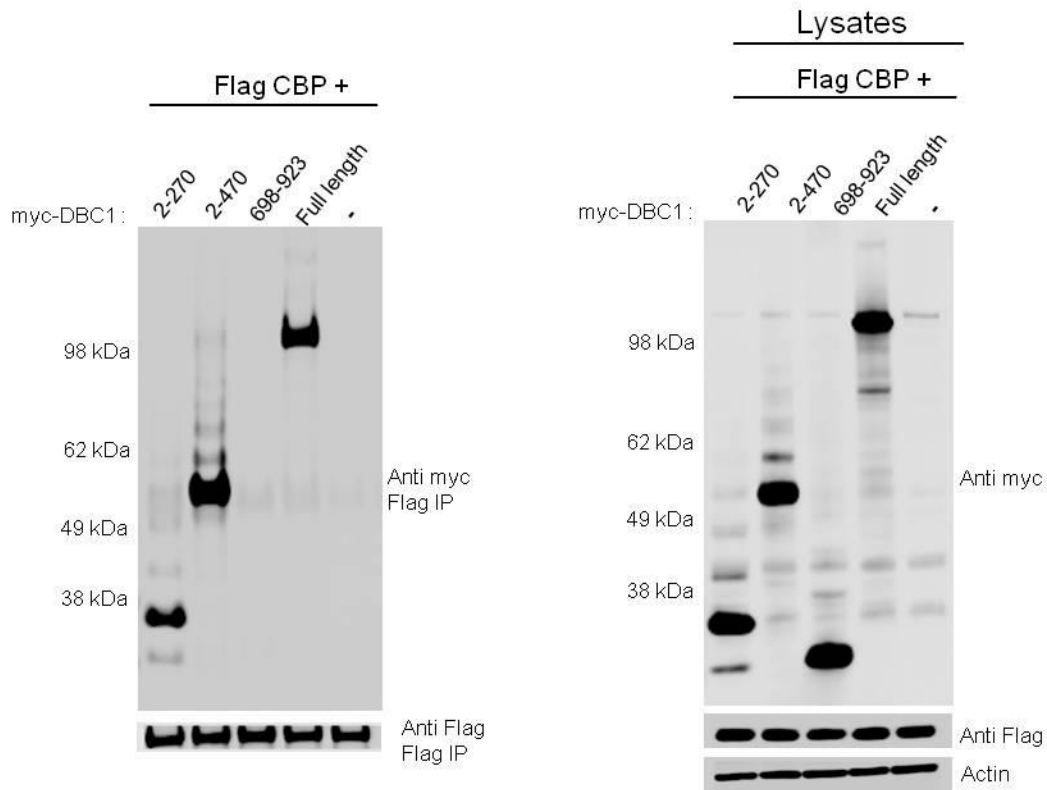


Figure 3.11 N-terminus of DBC1 is required for the CBP-DBC1 interaction. U2OS cells were transfected with full length FLAG-CBP and truncated mutants of myc-DBC1 followed by FLAG IP and immunoblotting with FLAG and myc antibodies.

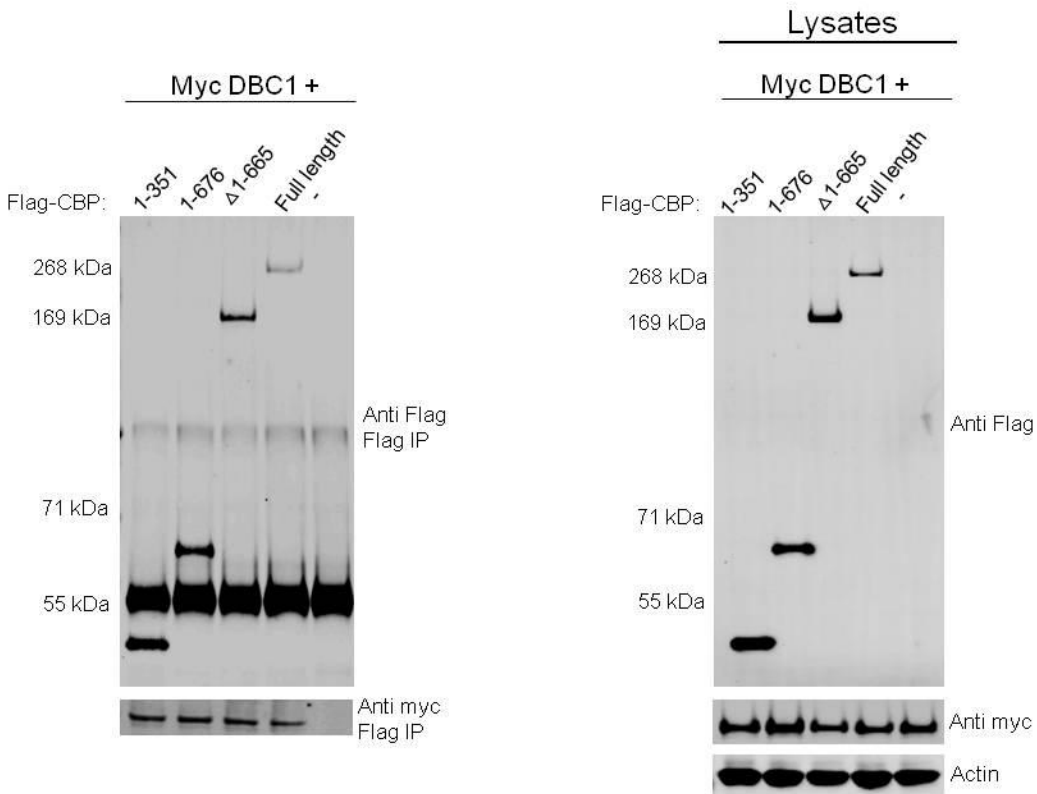


Figure 3.12 Both N- and C- terminal regions of CBP are necessary for the CBP-DBC1 interaction. U2OS cells were transfected with full length myc- DBC1 and truncated mutants of FLAG-CBP followed by FLAG IP and immunoblotting with FLAG and myc antibodies.

Regulation of CBP E3 Autoubiquitination Activity by DBC1

Since DBC1 interacts with CBP in both the nucleus and cytoplasm (Fig. 3.9) and based on our observation that DBC1 binds both N- and C-terminal regions of CBP (Fig. 3.12), we investigated whether DBC1 plays a role in the modulation of compartmentalized CBP ubiquitin activities, which uses CBP N-terminus sequences. U2OS cells were treated with either control siRNA or DBC1 siRNA for 72hrs followed by CBP immunoprecipitation from cytoplasmic and nuclear lysates and in-vitro analysis of CBP E3 autoubiquitination activity. As shown in Fig. 3.13, downregulation of DBC1 led to a significant increase in nuclear CBP E3 autoubiquitination when compared to nuclear fraction of control siRNA. DBC1 depletion modestly increased CBP E3 autoubiquitination in the cytoplasmic compartment when compared to the cytoplasmic control siRNA treated cells. This result confirms our observation that a CBP-dependent nuclear factor inhibits CBP ubiquitin activities (Fig. 3.1).

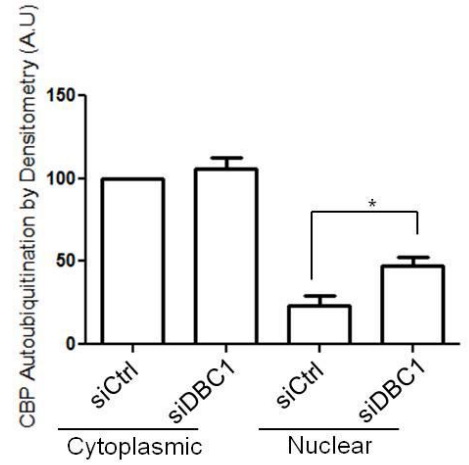
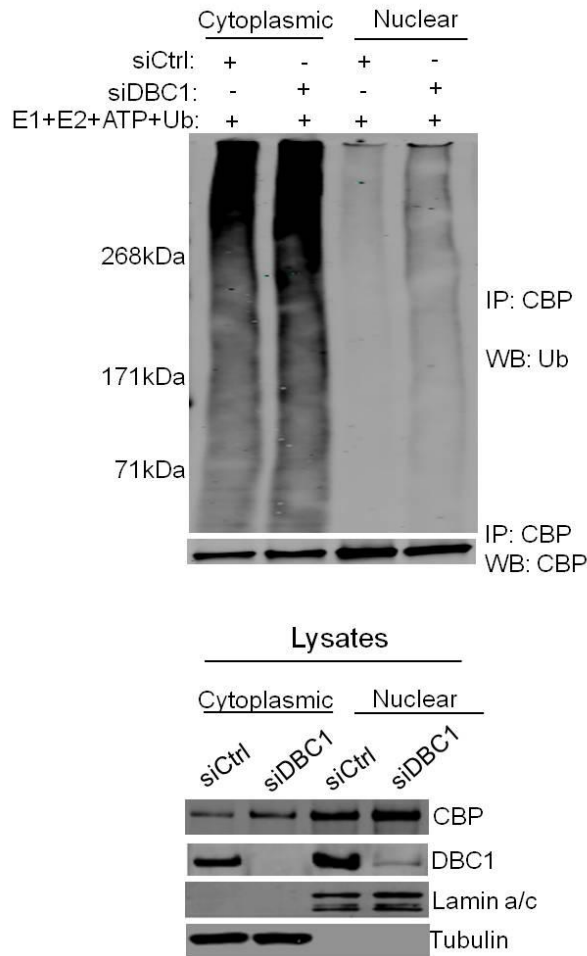


Figure 3.13 DBC1 inhibits nuclear CBP E3 autoubiquitination activity. U2OS cells were transfected with control siRNA or DBC1 siRNA for 72hrs followed by CBP immunoprecipitation from cytoplasmic and nuclear fractions, in-vitro CBP E3 autoubiquitination assay and immunoblotting with CBP and ubiquitin (Ub) antibodies. Graph on the right shows quantification of CBP autoubiquitination by densitometry. Graph represents mean \pm SEM for three independent experiments. * $p < 0.05$. Bottom panel shows immunoblotting of lysates with the indicated antibodies.

Regulation of p53-Directed CBP E4 Ligase Activity by DBC1

Previous work has indicated that the N-terminus sequences of CBP are crucial for its E3 autoubiquitination and p53-directed E4 polyubiquitin ligase activities [118]. Since we found that DBC1 inhibits CBP E3 autoubiquitination, we examined whether DBC1 regulates CBP E4 ligase activity as well. CBP depletion is known to increase p53 half life as previously shown by Shi *et al.*, 2009 [118]. To determine the effect of individual DBC1 loss and CBP/DBC1 loss on p53 stability, U2OS cells transiently expressing either control siRNA, CBP siRNA, DBC1 siRNA or CBP/DBC1 double siRNAs were treated with cycloheximide over a 90 minute time period, followed by p53 immunoblotting. DBC1 depletion led to a decrease in p53 half life compared to control cells while depletion of both CBP and DBC1 rescued the decrease in p53 half life observed in DBC1 depleted cells (Fig. 3.14).

Next, we examined endogenous p53 polyubiquitination status in cells treated with either control siRNA, CBP siRNA, DBC1 siRNA or CBP/DBC1 double siRNAs for 72 hours, followed by p53 immunoprecipitations and immunoblotting with p53 and ubiquitin antibodies. DBC1 depletion caused a moderate increase in p53 polyubiquitination in the cytoplasmic compartment but a more robust increase in p53 polyubiquitination in the nuclear compartment when compared to control siRNA treated cells (Fig. 3.15). As expected, CBP depletion led to a decrease in cytoplasmic p53 polyubiquitination when compared with control siRNA treated cells. CBP/DBC1 double knockdown rescued the increase in p53 polyubiquitination observed in DBC1 depleted cells in both cytoplasmic and nuclear compartments (Fig. 3.15).

To verify whether DBC1 inhibits CBP E4 polyubiquitin activity towards p53, U2OS cells stably expressing DBC1 shRNA were transfected with either empty vector or DBC1 deletion construct, 1-470aa, which we have shown binds CBP (Fig. 3.11). 48hrs post transfection, cells were either treated with cycloheximide over a 90 minute time period to determine p53 stability, or were harvested for p53 immunoprecipitations from cytoplasmic and nuclear compartments to determine p53 polyubiquitination status. We found that re-expression of DBC1 in both cytoplasmic and nuclear compartments led to an increase in p53 half life as compared to DBC1 depleted cells, DBC1 depleted cells transfected with empty vector, as well as cells expressing control shRNA (Fig. 3.16 and 3.17). We also found that DBC1 re-expression rescued the increase in p53 polyubiquitination observed in DBC1 depletion cells (Fig. 3.18).

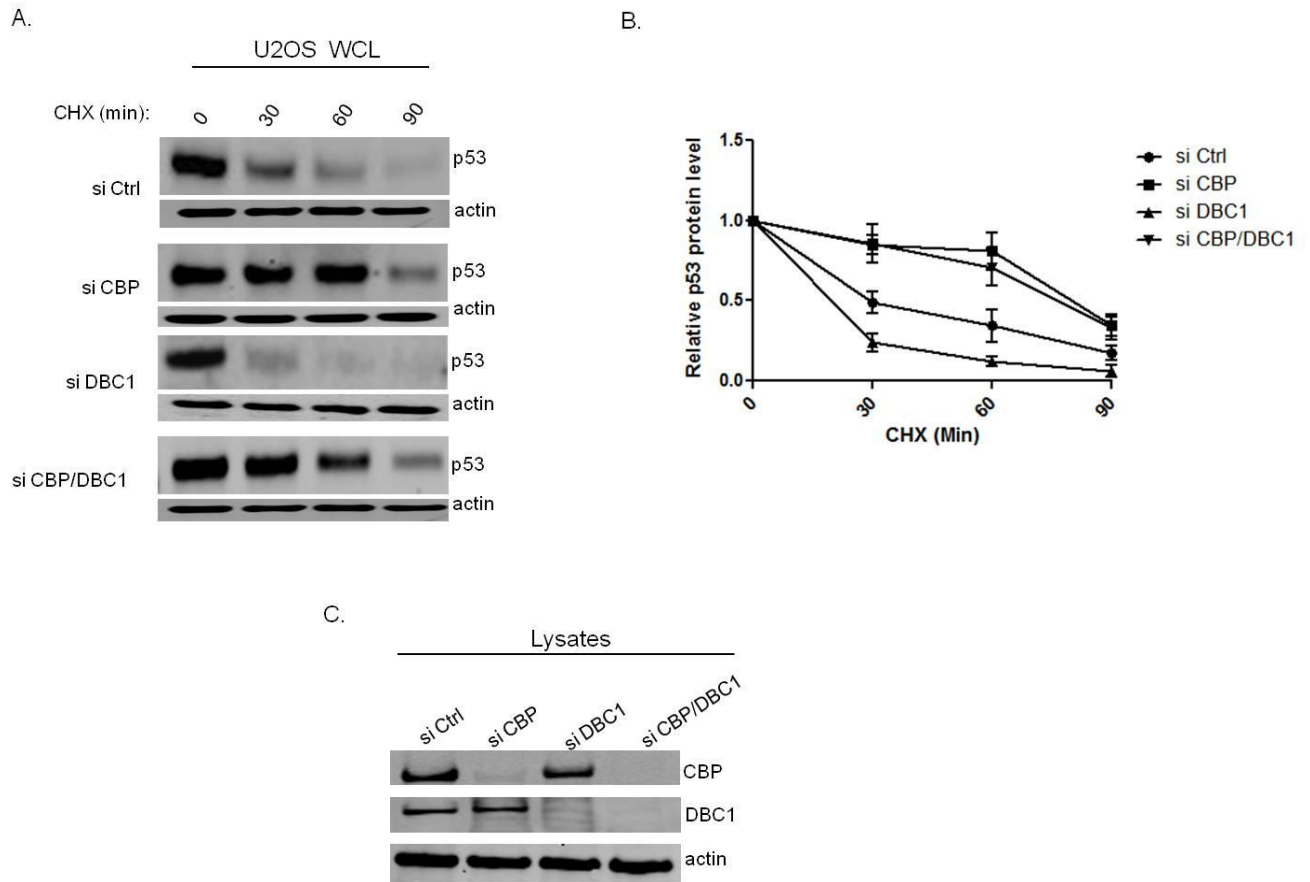


Figure 3.14 DBC1 depletion decreases p53 half life. **A.** U2OS cells treated with 100 μ M cycloheximide (Sigma) for up to 90min were harvested for western analysis using p53 antibody. **B.** Quantification of p53 half life. Graph represents mean \pm S.D from three independent experiments. **C.** Immunoblotting of lysates with the indicated antibodies.

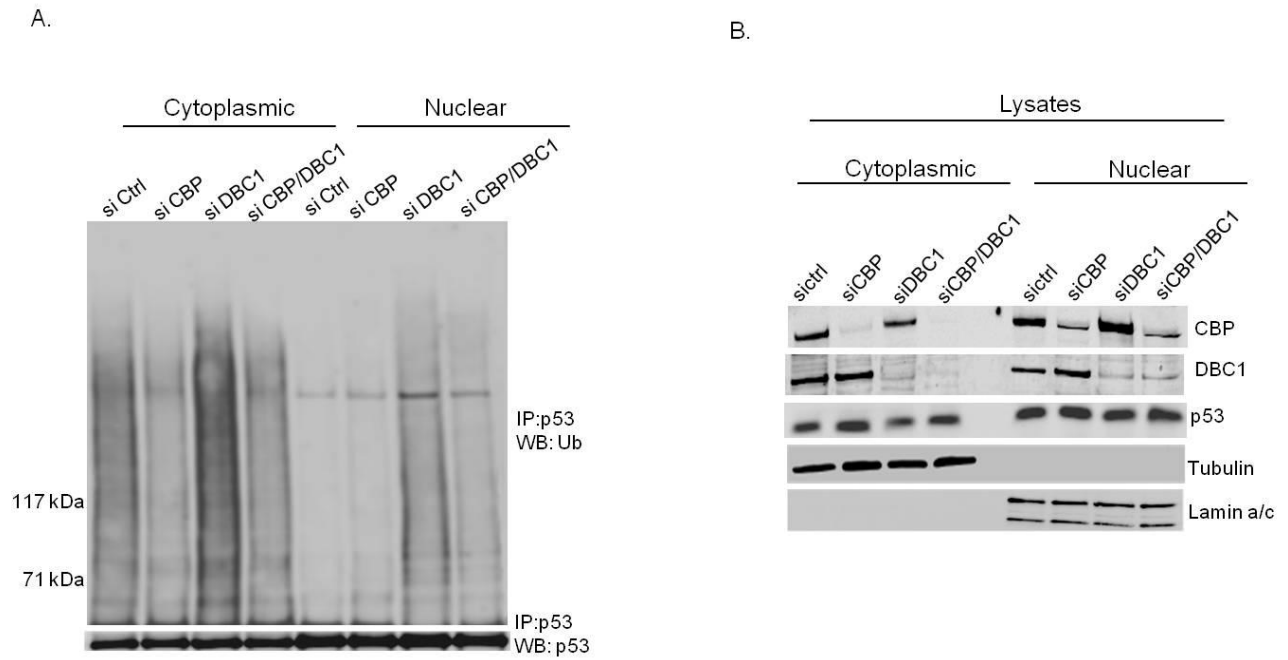


Figure 3.15 DBC1 depletion increases p53 polyubiquitination. **A.** U2OS cells were treated with either control siRNA, CBP siRNA, DBC1 siRNA or double CBP/DBC1 siRNA for 72 hrs followed by p53 immunoprecipitation from cytoplasmic and nuclear fractions and immunoblotting with p53 and ubiquitin antibodies. **B.** Immunoblotting of lysates with the indicated antibodies.

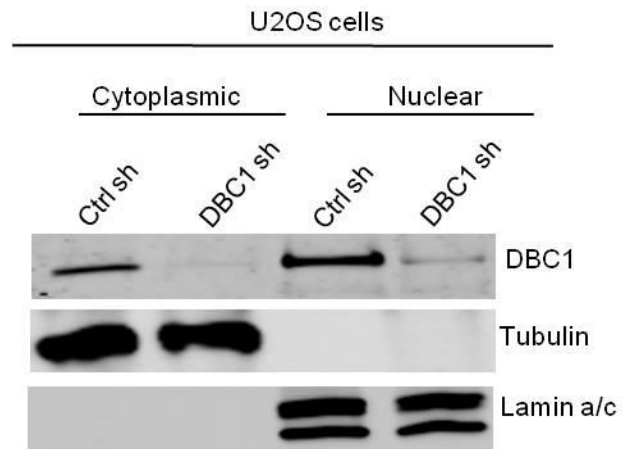


Figure 3.16. U2OS cells expressing DBC1 shRNA. Immunoblot represents cells stably expressing DBC1 shRNA.

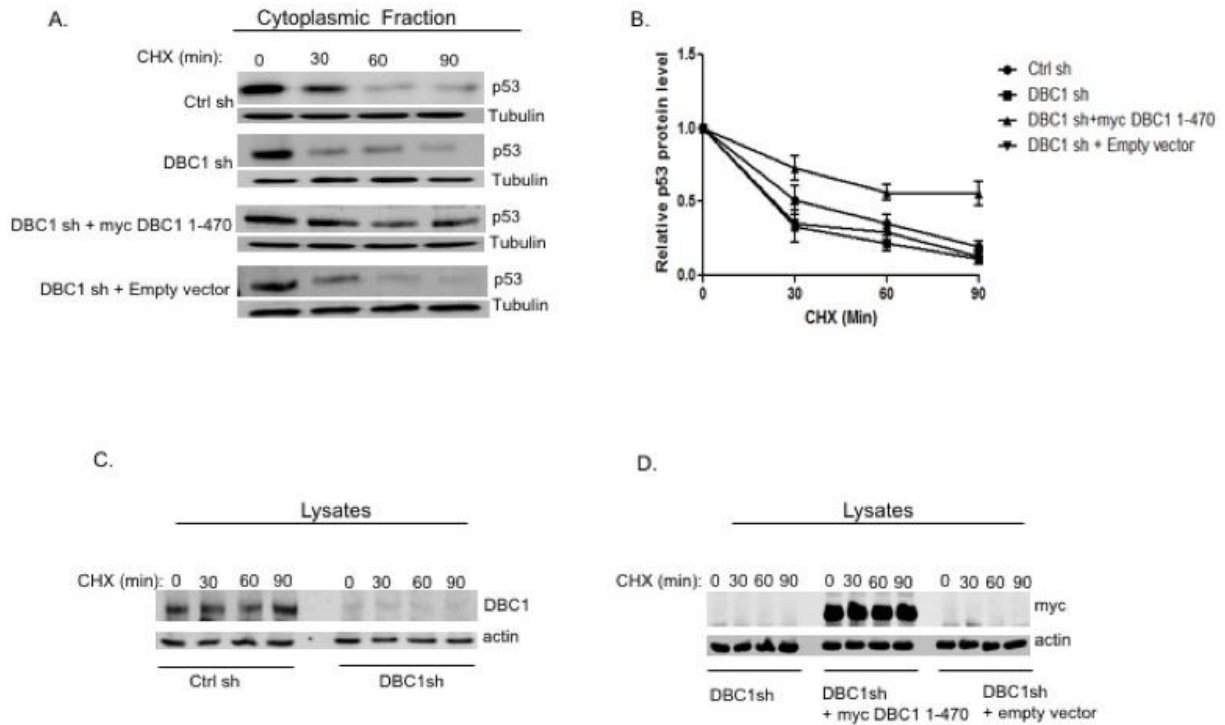


Figure 3.17 Re-expression of DBC1 stabilizes p53 in the Cytoplasmic compartment of DBC1 depleted cells. **A.** U2OS cells expressing DBC1 shRNA were treated with 100 μ M cycloheximide (Sigma) for up to 90min and harvested for subcellular fractionation into cytoplasmic and nuclear fractions followed by immunoblotting with p53 antibody. **B.** Quantification of p53 half life in the cytoplasmic fraction. Graph represents mean \pm S.D from three independent experiments. **C. and D.** Immunoblotting of lysates with the indicated antibodies.

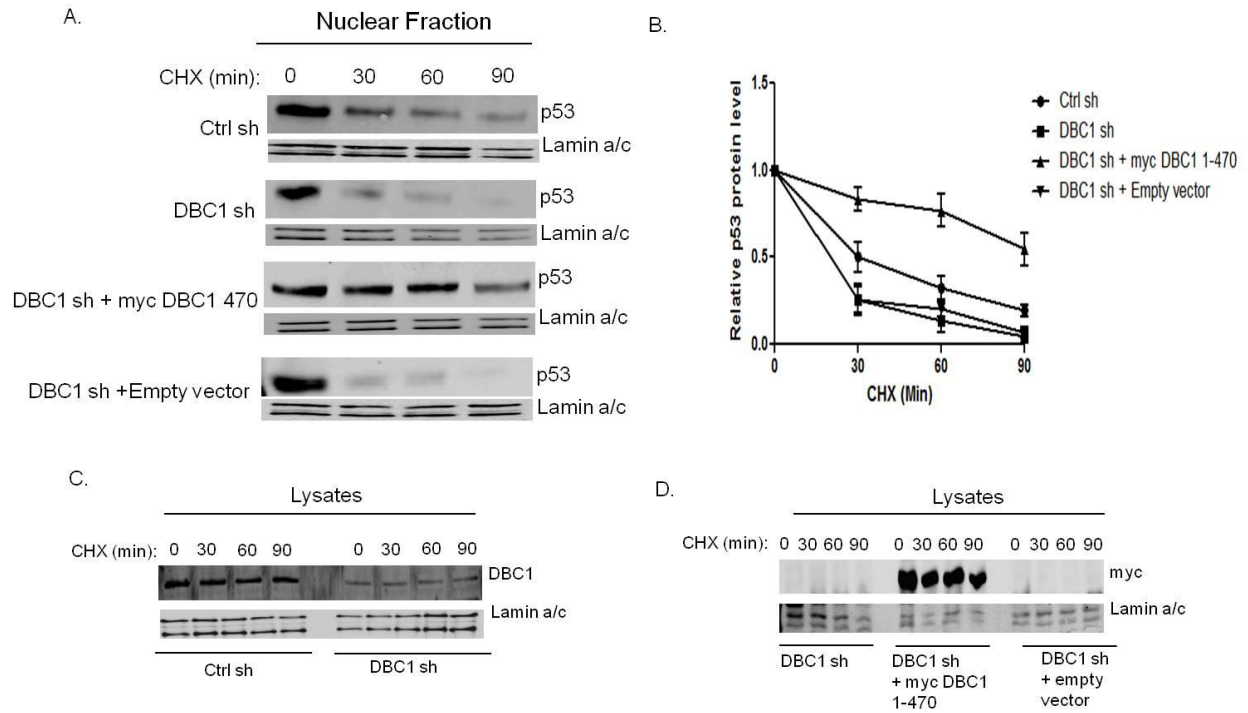


Figure 3.18 Re-expression of DBC1 stabilizes p53 in the Nuclear compartment of DBC1 depleted cells. **A.** U2OS cells expressing DBC1 shRNA were treated with 100 μ M cycloheximide (Sigma) for up to 90min and harvested for subcellular fractionation into cytoplasmic and nuclear fractions followed by immunoblotting with p53 antibody. **B.** Quantification of p53 half life in the nuclear Fraction. Graph represents mean \pm S.D from three independent experiments. **C. and D.** Immunoblotting of lysates with the indicated antibodies.

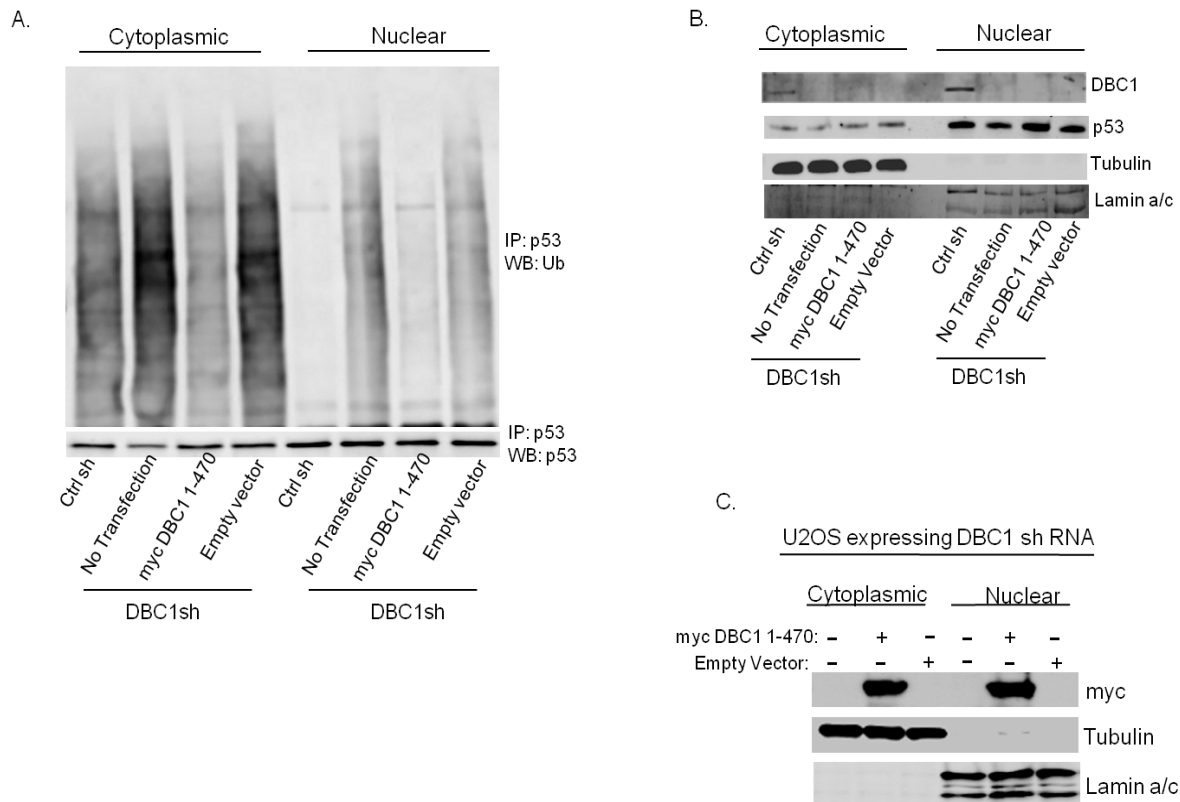


Figure 3.18 Re-expression of DBC1 reduces p53 polyubiquitination in DBC1 depleted cells. A. U2Os cells stably expressing DBC1 shRNA were transfected with either vector only or DBC1 1-470aa construct. 48 hrs after transfection, cells were harvested for p53 immunoprecipitations from cytoplasmic and nuclear fractions followed by immunoblotting with p53 and Ub antibodies. Cells expressing control shRNA were included in this experiment. **B.** immunoblotting of lysates with the indicated antibodies. **C.** Immunoblot represents overexpression of DBC1 1-470aa in DBC1 depleted cells.

Regulation of CBP-DBC1 Interaction by Doxorubicin-Induced DNA Damage

Stressed cells undergo a plethora of activities that could influence signaling events, protein localization, post-translational modifications and even protein-protein interactions. We determined whether DNA damage had any effect on the CBP-DBC1 interaction. U2OS cells were treated with doxorubicin (Dox) over a 6hr time point period, followed by CBP immunoprecipitation and immunoblotting with CBP and DBC1 antibodies. We found that endogenous DBC1 protein level went down in the nucleus in response to Dox-induced DNA damage (Fig. 3.19). We however did not observe any obvious change in cytoplasmic DBC1 protein level in response to Dox. CBP-DBC1 interaction also dissociated in the nucleus over time, in response to Dox-induced DNA damage (Fig. 3.19). By 6hrs Dox treatment, we barely detected any CBP-DBC1 interaction in the nucleus. In the cytoplasm however, we did not observe any obvious change in CBP-DBC1 interaction (Fig. 3.19).

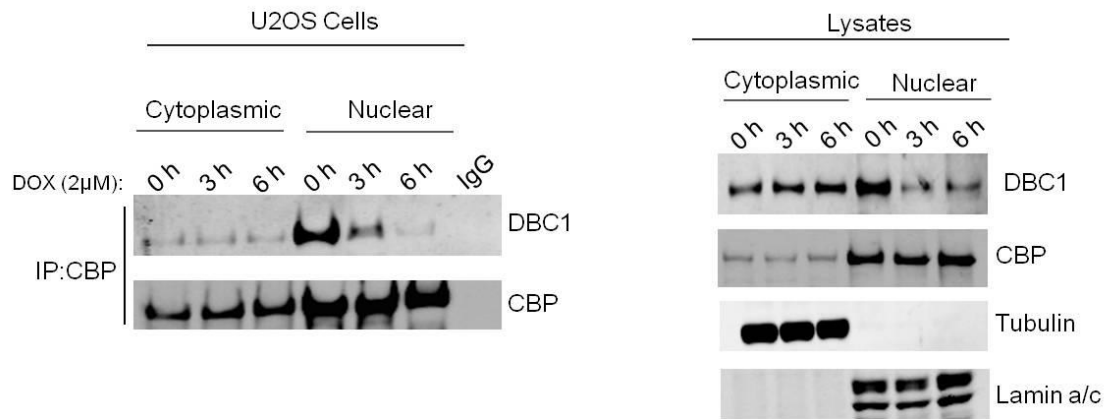


Figure 3.19 Interaction of CBP and DBC1 in response to doxorubicin-induced DNA damage. U2OS cells were treated with 2µM Dox for 1hr, 3hr and 6hr. At the end of the 6hr time point, CBP was immunoprecipitated from cytoplasmic and nuclear lysates using anti CBP A-22 antibody (Santa Cruz) followed by immunoblotting with CBP and DBC1 antibodies (Santa Cruz). Lysates were immunoblotted with the indicated antibodies.

Regulation of p53 Transactivated Targets and Apoptosis by CBP and DBC1

In response to cellular stresses such as DNA damage, CBP functions as a co-activator for p53, thereby promoting p53 transcriptional activities [22, 28]. DBC1 also augments p53 stability by promoting p53 acetylation through inhibition of SIRT1 deacetylase function [175]. To determine if CBP and DBC1 differentially regulate p53 transcriptional activity, we examined the expression of p53-transactivated targets, p21 and PUMA in U2OS cells stably expressing control shRNA, CBP shRNA, DBC1 shRNA and CBP/DBC1 shRNA. In addition, we examined the expression of p53-transactivated apoptotic markers, cleaved caspase 3 and PARP in the stable cells. U2OS cells expressing either control shRNA, CBP shRNA, DBC1 shRNA or CBP-DBC1 shRNA were exposed to doxorubicin (Dox) for 12 hrs for p53-dependent targets, p21 and PUMA protein expression. Augmented p21 and PUMA induction was observed in CBP depleted cells, DBC1 depleted cells and the double CBP/DBC1 depleted cells, compared with cells expressing control shRNA (Fig. 3.20). Overall, p21 and PUMA induction were almost comparable in CBP depleted cells, DBC1 depleted cells, and CBP/DBC1 depleted cells. As expected, individual loss of CBP but not DBC1 resulted in decrease in p53 acetylation on Lys 382 (Fig. 3.20). Furthermore, in response to doxorubicin, CBP deficient cells exhibited elevated cleaved caspase 3 and cleaved PARP protein levels compared with control-sh cells (Fig.3.21). Individual loss of DBC1 caused a slight increase in cleaved caspase 3 compared to control-sh cells. PARP cleavage induction in DBC1 depleted cells was comparable with induction in the control

sh cells. Expression of cleaved caspase 3 and PARP proteins in double CBP/DBC1 depleted cells was comparable with expression in individual loss of CBP.

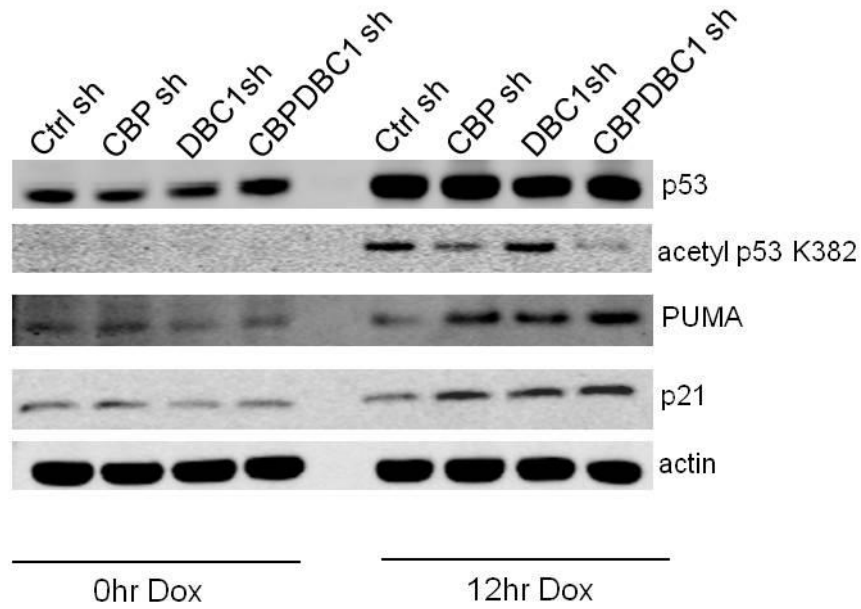


Figure 3.20 Analysis of p53-dependent targets following Dox treatment in CBP and DBC1 stably deficient cells. U2OS cells stably expressing control shRNA, CBP shRNA, DBC1 shRNA or CBP/DBC1 shRNA were Dox treated for followed by cell lysis and immunoblotting with the indicated antibodies.

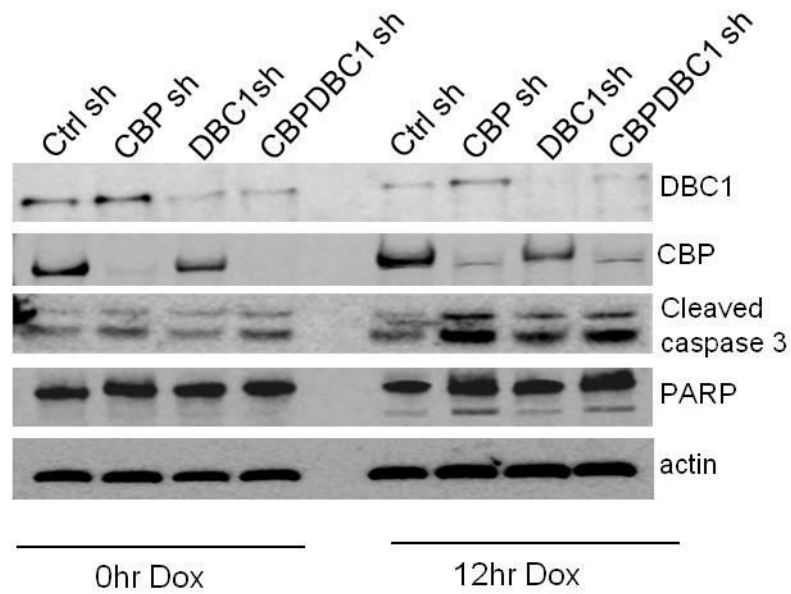


Figure 3.21 Analysis of p53-induced apoptosis in CBP and DBC1 stably deficient cells. U2OS cells stably expressing control shRNA, CBP shRNA, DBC1 shRNA or CBP/DBC1 shRNA were Dox treated followed by cell lysis and immunoblotting with the indicated antibodies.

Table 4: Gene alterations of TP53 and DBC1 obtained from the Cancer Genome Atlas (TCGA) database across cancer types

Cancer Type	Total Number of Patients	% Patients with p53 alterations	% Patients with DBC1 alterations	% of DBC1 alterations with wild type 53	References
Kidney	418	2.2	1.7	100	Nature. 2013 Jul 4; 499(7456):43-9.
Colorectal	212	52	4	100	Nature. 2012 Jul 18; 487(7407):330-7.
Prostate	333	8	16	96	Cell. 2015 Nov 5; 163(4):1011-25.
Stomach	287	48	9	64	Nature. 2014 Sep 11; 513(7517):202-9.
Uterine	240	28	8	58	Nature 2013. May 2; 497(7447):67-73.
Lung	230	46	7	40	Nature. 2014 Jul 31; 511(7511):543-50.
Breast	974	36	7	33	Cell. 2015 Oct 8; 163(2):506-19.
Bladder	127	53	8	30	Nature. 2014 Mar 20; 507(7492):315-22.

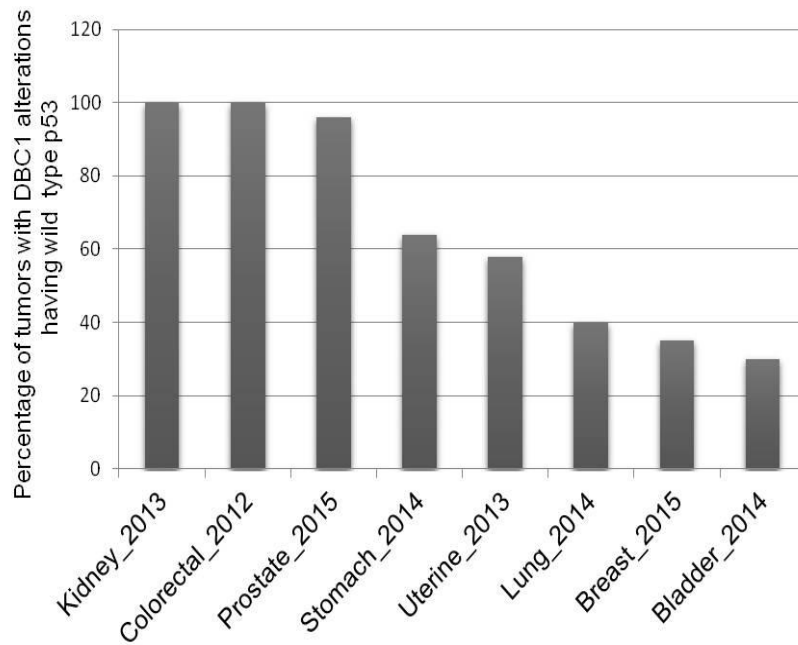


Figure 3.22 TCGA database of tumors with DBC1 alterations retaining wild-type p53 status. Graph shows the percentage of DBC1 deletions or mutations across cancer types that retain wild-type p53 status.

3.4 Summary

CBP was initially identified as possessing cytoplasmic localized but not nuclear intrinsic E3 autoubiquitination and p53-directed E4 ubiquitin ligase activities under physiologic cell conditions. The regulation of the compartmentalized CBP ubiquitin activities was however, not studied. Preliminary studies showed that a CBP-dependent nuclear factor inhibits CBP E3 autoubiquitination while a CBP-independent cytoplasmic factor promotes CBP E3 autoubiquitination. Using MudPIT analysis, we identified DBC1 as a novel CBP-interacting protein in the cytoplasmic and nuclear compartments. Immunofluorescence microscopy revealed that both CBP and DBC1 predominantly localize to the nuclear compartment. The N-terminus of DBC1 associates with both N- and C-terminal regions of CBP. Functional studies indicated that DBC1 inhibits CBP E3 autoubiquitination activity. In addition, we identified that DBC1 depletion caused a decrease in p53 half life and also caused an increase in p53 polyubiquitination. Overexpression of DBC1 in DBC1 depleted cells rescued both the decrease in p53 half life and the increase in p53 polyubiquitination. Furthermore, we found that DNA damage abrogated the CBP-DBC1 interaction in the nuclear compartment, possibly a factor in DNA damage induction of CBP E3 activity. CBP and DBC1 deficient cells caused augmented p21 and PUMA expression compared with control-sh cells. CBP depletion caused an increased cleaved caspase 3 /PARP induction compared with DBC1 depleted cells and control cells.

Chapter 4: Discussion and Future Perspective

Apart from its co-activator role in the transcription of target genes, CBP is involved in many other cellular pathological and physiological processes, such as cell growth and differentiation, cell transformation and development, response to stress, cell cycle regulation and apoptosis [36-44]. Given these pleiotropic cellular roles of CBP, it is oftentimes implicated in several human diseases and cancers and as such, a complete comprehension of the mechanisms that regulate its multifaceted functions is imperative, especially in the development of new strategies for therapeutic interventions.

Since the identification of CBP/ p300 as possessing intrinsic cytoplasmic E3 ubiquitin ligase activity and also as physiological cytoplasmic but not nuclear E4 ligases for p53, the mechanism of the compartmentalized CBP/p300 ubiquitin ligase activities has not been investigated. Also, the effect of DNA damage on the ubiquitin ligase activities of CBP and p300 was not examined. Both CBP and p300 mostly reside in the nucleus with some amount in the cytoplasm. CBP however, is readily detected in the cytoplasm compared to p300. Based on previous knowledge, the model for p53 degradation indicates that p53 is first monoubiquitinated by its well studied E3 ligase, MDM2, leading to its export from nucleus to cytoplasm. In the cytoplasm, CBP/p300 function as E4 ubiquitin ligases, catalyzing the conjugation of polyubiquitin chains unto the already monoubiquitinated p53 species. Polyubiquitinated p53 is then subsequently targeted for proteasomal degradation by the 26S proteasome in the cytoplasm.

CBP/p300 are therefore clearly necessary for the maintenance of physiologic p53 levels in the absence of cellular stress.

The studies within this dissertation have provided insight into the regulation of the compartmentalized CBP ubiquitin ligase activities both in the absence and in response to DNA damage. The main findings are recapitulated here. As described in chapter two, gamma irradiation and genotoxic-induced DNA damage augmented the otherwise dormant nuclear CBP E3 autoubiquitination activity. Also, activation of ATR kinase was necessary for the DNA damage-induced nuclear CBP E3 autoubiquitination. In addition, CBP exhibited differential post translational modification in the cytoplasm versus nucleus in response to DNA damage. In chapter three, DBC1 was identified as a novel CBP interacting partner in both cytoplasmic and nuclear compartments. In the absence of DNA damage, knockdown of DBC1 resulted in the activation of nuclear CBP E3 and p53-directed E4 ubiquitin ligase activities. DBC1 depletion also led to increased p53 polyubiquitination.

Implications From Chapter 2 and Future Perspectives: Activation of Nuclear CBP E3 Autoubiquitination and Differential CBP Post-translational Modifications in Response to DNA Damage

In this chapter, the effect of DNA damage on CBP E3 autoubiquitination was investigated. In the absence of cellular stress, cytoplasmic CBP E3 ubiquitin ligase activity is active while nuclear CBP E3 ubiquitin ligase activity is dormant. We found that gamma irradiation, doxorubicin, and etoposide treatments all induced the activation of the dormant nuclear CBP E3 autoubiquitination activity in U2OS and H1299 cells (Fig.

2.2, 2.3, 2.4). These DNA damaging agents have different mechanisms of action to induce damage. Regardless of the mechanism, our data revealed that DNA damage causes activation of nuclear CBP E3 autoubiquitination in vitro. Even though at this point we do not understand the in vivo relevance of the ubiquitination modification of CBP in response to DNA damage, it is possible that certain CBP activities, in response to DNA damage and other stress signals are augmented as a result of this modification. Different biological outcomes can occur from the different types of ubiquitin chain topologies. For example, ubiquitination of proteins via Lys48 generally leads to proteasomal degradation while Lys63 linkage has been linked to signal transduction, subcellular localization and DNA repair [135, 137,147]. Lys63-linked ubiquitination has also been shown to be important in the stability and scaffolding functions of some proteins [169]. Since the DNA damage-induced ubiquitination of CBP does not lead to CBP degradation, other ubiquitin linkages other than Lys48 may be present which may contribute to CBP's re-localization in response to damage, its stability or other damage - induced functions. One mechanism by which CBP modulates transcription of target genes is by forming a scaffold for DNA-binding and general transcription factors [25, 26], (Fig. 1.2). Since ubiquitination via Lys63-linkages has been shown to mediate the scaffolding function of some proteins [169], it will be necessary to determine if the ubiquitin conjugates on CBP in response to DNA damage are linked through Lys63 and to also determine if CBP forms a scaffold for certain signaling events that occur in response to damage.

Chromatin remodeling and modifications culminate in access to DNA damage sites for repair, and CBP is known to be recruited to DSBs for histone acetylation [170]. There

could possibly be crosstalk between CBP ubiquitination and its HAT function such that autoubiquitination of CBP induces some sort of conformational change that promotes CBP HAT activities. An earlier report showed that CBP autoacetylation was important in positioning the CBP HAT and bromo domains for recognition by binding partners [117]. One question is whether CBP autoubiquitination in response to stress signals also facilitates easy recognition by binding partners. Much evidence exists for the effect of post-translational modifications such as acetylation, phosphorylation, methylation on CBP transcriptional co-activator and HAT functions [108, 112, 115-117, 120, 122, 128]. Further investigation will be necessary to examine the non-proteolytic effects of CBP autoubiquitination and to also determine whether CBP autoubiquitination has regulatory roles on its co-activator and HAT activities.

We found that activation of ATR kinase activity was necessary for the DNA damage-induced activation of nuclear CBP E3 ubiquitin ligase activity (Fig. 2.5, 2.6). Activation of the apical kinases, ATM and ATR, in response to DNA damage, activate checkpoint signaling through phosphorylation of substrate proteins. Indeed, our observation that nuclear CBP is phosphorylated on S124 only in the nucleus in response to DNA damage, indicates that CBP maybe a direct target of ATR kinase activation (Table 2.1). This result is consistent with a prior study that identified several novel proteins phosphorylated by ATM/ATR on SQ/TQ motifs in response to UV radiation [162]. The study, using whole cell lysates, reported phosphorylation of CBP on S124 in response to UV radiation at the SQ/TQ motif [162]. Phosphorylation is known to regulate the co-activator role of CBP in the transcription of certain gene targets [112-114]. Is nuclear CBP phosphorylation on S124 necessary for the DNA damage-induced

nuclear CBP autoubiquitination or is it necessary for CBP acetyltransferase or co-activator function post DNA damage? Recruitment of CBP to promoters of target genes is transient and occurs in response to different cellular signals, implying tight regulation of CBP mobility. Since CBP is subjected to diverse post-translational modifications, the future direction for this part of the project would be to determine if there are cross talks between all these DNA damage-induced CBP modifications and to fully understand how this may contribute to CBP functions in response to DNA damage.

Under physiologic cell conditions, CBP has a diffuse nuclear staining pattern when examined by immunofluorescence. We found that in response to genotoxic stress, CBP localizes to discrete nuclear bodies, some of which localize with PML bodies (Fig. 2.7). It is known that CBP is recruited to PML bodies in response to RAS oncogenic stress, where a trimeric p53-PML-CBP complex is formed, which facilitates p53 acetylation by CBP, thereby promoting p53 stability [158]. One vital question is whether CBP autoubiquitination regulates CBP nuclear mobility and association with these discrete nuclear bodies in response to stress.

DNA-damage induced CBP autoubiquitination could also possibly have role in p53 regulation post DNA damage. We have previously established that under physiologic conditions, CBP is a p53-directed E4 ubiquitin ligase and that the N-terminal region of CBP required for its E3 autoubiquitination are also important for its E4 activity [118]. In response to cellular stress, it is known that mechanisms such as ATM/ATR phosphorylation of p53 on S15 and S20, ATM/ATR phosphorylation of Mdm2, and sequestration of Mdm2 into the nucleolus by p14ARF, abrogate the p53-Mdm2 interaction, thereby stabilizing p53 to initiate DNA damage repair [155, 161, 165]. The

same lysine residues on p53 that are ubiquitinated in the absence of stress are also acetylated in response to stress. In response to DNA damage, p53 ubiquitination is transiently suppressed and once repair is completed, p53 levels must return to homeostatic level, but exactly how this is accomplished is not completely understood. Since CBP polyubiquitinates p53 in the absence of stress and also acetylates p53 in response to stress, it is efficient for CBP to be involved in the mechanism that returns p53 to homeostatic levels once repair is completed. We have shown in this work in consistent with previous data, that p53 is ubiquitinated in the nucleus, in response to doxorubicin (Fig. 2.9). DNA damage-induced CBP autoubiquitination could therefore prime activation of CBP E4 activity towards p53, providing a mechanism by which p53 is degraded after DNA damage repair. Mdm2-p53 interaction is disrupted in response to DNA damage, and so some other p53 E3 ligases may function in conjunction with CBP in regulating p53 degradation post DNA damage. On the other hand, since p53 and Mdm2 form a negative feedback loop such that p53 transactivation leads to Mdm2 transcription, it is also possible that once repair is achieved, Mdm2 is available to cooperate with CBP to destabilize p53. Further investigation is required to fully elucidate this complicated mechanism in the p53 regulatory pathway.

Implications From Chapter 3 and Future Perspectives: Novel Interaction Between CBP and DBC1 and Regulation of CBP Ubiquitin Ligase Activities

In this chapter, the regulation of CBP ubiquitin ligase activities by binding partners was investigated under unstressed cell conditions. CBP, as expected, has many binding partners as a result of its transcriptional role and also because of its involvement in many other cellular activities. Interestingly, and despite all previous studies and available information on CBP-binding proteins, there was no report of CBP-DBC1 interaction. MudPIT studies revealed that DBC1 stably interacts with CBP in the nuclear and cytoplasmic compartments. DBC1 was first identified as being deleted in certain breast cancers but there is evidence that it is also implicated in other cancer types such as prostate cancer [171-173]. Its role in tumorigenesis is however, still controversial, playing either a tumor suppressor or a tumor promoting role [172]. The mechanism of DBC1 function is therefore expected to be pleiotropic and may be dependent on the cancer type and/or the cancer-inducing signals. We found that the N-terminus of DBC1 interacts with both N- and C- termini of CBP (Fig. 3.13 and 3.14). The N-terminus of DBC1 is known to interact with the deacetylases SIRT1 and HDAC3, thereby inhibiting their functions [176, 177]. In addition, the N-terminal region of DBC1 binds to and regulates the epigenetic modifier SUV3H1 and certain nuclear receptors [173-175, 178]. Both N- and C- terminal regions of CBP are functional. For example, binding of N-terminus of p53 to the N-terminus of CBP promotes p53 degradation while binding to the C-terminus of CBP is necessary for p53 stabilization [156, 157]. The fact that the N-terminus of DBC1, which has been shown to possess inhibitory ability on the

functioning of binding partners, binds both terminal regions of CBP, which are functional in p53 regulation, suggests that DBC1 may play a role in the regulation of CBP activities towards p53. In this study, depletion of DBC1 using siRNA robustly increased CBP E3 autoubiquitination activity in the nucleus and modestly in the cytoplasm (Fig. 3.15). It was previously shown that the N-terminus of CBP is required for CBP E3 autoubiquitination and p53-directed E4 ubiquitin activities [118]. The simple explanation for inhibition of CBP E3 ubiquitin ligase activity by DBC1 is most likely as a result of its binding to the N-terminal region of CBP. At this point, we do not know the relevance of DBC1 binding to the C-terminal region of CBP, and if there are any regulatory roles involved. It will be interesting to determine the importance of DBC1 interaction with C-terminal region of CBP.

We understand from previous studies that both Mdm2 and CBP cooperate to maintain physiologic p53 levels under unstressed cell conditions [118, 152, 166, 167]. Evidence indicates that p53 is first monoubiquitinated in the nucleus by its E3 ubiquitin ligase, Mdm2, signaling p53 export into the cytoplasm, where it becomes polyubiquitinated by cytoplasmic CBP and degraded by the 26S proteasome [118, 121, 166, 167]. CBP loss has been shown to stabilize p53 [118]. In this present work, we identified that DBC1 loss led to a decrease in p53 half life in U2OS cells and also promoted p53 polyubiquitination (Fig. 3.16 and 3.17.). In addition, we found that re-expression of DBC1 rescued the decrease in half life and the increase in p53 polyubiquitination observed in DBC1 depleted cells. These observations suggest that DBC1 likely promotes p53 stability by inhibiting CBP E4 polyubiquitin activity towards p53. These findings may help provide an explanation for why monoubiquitinated

species of p53 cannot be polyubiquitinated by nuclear CBP but instead, are exported from the nucleus to the cytoplasm for polyubiquitination by cytoplasmic CBP, followed by proteasomal dependent p53 degradation. So, DBC1 binds tightly with CBP in the nucleus and inhibits CBP E4 polyubiquitination ability. In the cytoplasm however, CBP polyubiquitinates p53, mediating p53 degradation, despite the CBP-DBC1 interaction in the cytoplasm. Even though DBC1 inhibits CBP ubiquitin ligase activities in the cytoplasm and nucleus, the inhibition is more profound in the nucleus than in the cytoplasm. This could be as a result of differential CBP and DBC1 PTMs in the nucleus vs. cytoplasm, DBC1 interacting proteins in the nucleus and cytoplasm, stoichiometry of CBP and DBC1 in the nucleus and cytoplasm, or as a result of other cytoplasmic entities that promote CBP ubiquitin ligase activities. It will be therefore necessary to determine if any of these stated factors contribute to DBC1 inhibitory function towards CBP.

A recent work demonstrated the tumor suppression activity of DBC1 through the regulation of p53 stability in mouse embryonic fibroblasts [180]. They showed that the N-terminus of DBC1 interacts with the N-terminus of p53 but does not interact with Mdm2. Their work also indicated that DBC1 stabilizes p53 through competition with Mdm2 [180]. Since CBP, Mdm2 and DBC1 bind the N-terminus of p53, there is therefore an intriguing possibility that these proteins could exist in some sort of complex that co-operatively regulates p53 turn over and stability in cells.

In response to doxorubicin-induced DNA damage, endogenous DBC1 protein levels decreased in the nuclear compartment resulting in a dissociation of CBP-DBC1 interaction (Fig. 3.19). An early study showed caspase- dependent amino

terminally truncated versions of DBC1 in response to tumor necrosis factor (TNF) - α -mediated apoptosis, resulting in decreased level of endogenous nuclear DBC1 protein [181]. Their data indicated that deletion of the amino -terminus of DBC1 led to cytoplasmic localization. They also showed a decrease in DBC1 protein level in response to staurosporine and the genotoxic agent, etoposide [181], to indicate that apoptotic pathway inducers generate this amino terminally truncated DBC1. This finding may therefore explain the reason for the dissociation of nuclear CBP-DBC1 interaction in response to DNA damage we observed (Fig. 3.19). We have shown in this work that the N-terminus of DBC1 is required for interaction with CBP (Fig. 3.11). This simply means that in response to DNA damage, the DBC1 N-terminus region is truncated and so cannot effectively interact with CBP. Also, it is known that in response to DNA damage, DBC1 is phosphorylated by ATM/ATR, promoting its binding with the p53 deacetylase protein, SIRT1[179]. DBC1/SIRT1 interaction inhibits the deacetylase function of SIRT1, promoting p53-dependent apoptosis [179].

The physiologic role of CBP and DBC1 in the regulation of p53 biologic responses after DNA damage is not completely understood. Individual losses of CBP and DBC1 caused p21 and PUMA induction suggesting that individually, physiologic levels of neither CBP nor DBC1 are required for the p53-dependent transactivation of p21 and PUMA in response to doxorubicin in U2OS cells. Also, p21 and PUMA induction do not require acetylation of p53 on Lysine 382 as CBP deficient cells with decreased p53 Lys 382 acetylation, and DBC1 depleted cells showing p53 acetylation on Lysine 382, exhibited p21 and PUMA induction (Fig. 3.20). In addition, CBP and DBC1 seem to regulate apoptotic response differently. While individual loss of CBP

augmented cleaved caspase 3/PARP protein expression, DBC1 deficient cells only showed a slight increase in cleaved caspase 3/PARP compared with CBP deficient cells. Further work will be necessary to fully elucidate the role of DBC1 in p53-induced apoptosis. DBC1 has been shown to be involved in TNF- α -mediated apoptosis [181]. In response to TNF- α -mediated death signaling and etoposide induced apoptosis, DBC1 is processed in a caspase dependent manner into carboxyl-terminally containing forms. These proteolytically processed DBC1 forms were shown to be necessary for sensitizing cells to TNF- α -mediated apoptosis [181]. CBP and DBC1 may therefore engage in different pathways to regulate biologic responses to apoptosis.

Our data support the proposed tumor suppression function of DBC1, via inhibition of CBP-dependent p53 polyubiquitination in the absence of cellular stress. Frequently, p53 regulators that are altered in cancers are usually involved in the maintenance of physiologic p53 levels. This could possibly be a factor in the loss of DBC1 in some human cancers. For instance, according to The Cancer Genome Atlas (TCGA) database, a study carried out in 2015 on breast invasive carcinoma revealed that 33% of patients with DBC1 homozygous deletion or mutations retained wild type p53 (Table 4 and Fig 3.22) [182]. Also according to TCGA, a separate study carried out in 2015 on prostate adenocarcinoma revealed that 96% of patients with DBC1 homozygous deletion or mutations had wild type p53 status. Other cancer types with DBC1 alterations but retaining the wild-type p53 status were also reported in TCGA database (Table 4 and Fig 3.22) [183].

Final Thoughts

The work described within this dissertation, for the first time, reveals that DBC1 interacts with CBP, in the cytoplasm and nucleus. In the absence of DNA damage, DBC1 negatively regulates CBP E3 autoubiquitination, and p53-directed, CBP E4 ubiquitin ligase activities in cells. Physiologic p53 levels are primarily maintained by ubiquitination activities coordinated by Mdm2, an E3 ubiquitin ligase, and CBP, an E4 ubiquitin ligase. CBP-DBC1 interaction, thus, participates in the complex pathway, that regulates p53 turnover and stability in cells.

In response to DNA damage, the CBP-DBC1 interaction is disrupted in the nucleus, and nuclear CBP ubiquitin ligase activity is induced following ATR kinase activation. CBP is modified, in response to DNA damage, and also recruited to PML bodies, where it acetylates p53, contributing to p53 stability. Once DNA damage is repaired, the active CBP ubiquitin ligase activity possibly participates in the reset of p53 levels to homeostatic levels. DBC1 is also known to be modified, in response to DNA damage, leading to its tight interaction with SIRT1, and subsequent inhibition of the deacetylase function of SIRT1.

All in all, this study provides insights into the mechanism of differential CBP ubiquitin ligase activities, in the absence and presence of DNA damage, in the cytoplasm versus nucleus. The significance of this thesis work is that it may open up avenues for the development of novel cancer therapeutic strategies, that target the p53 degradation pathway, to cause p53 stabilization and activation in tumors that retain wild type p53.

Normal condition

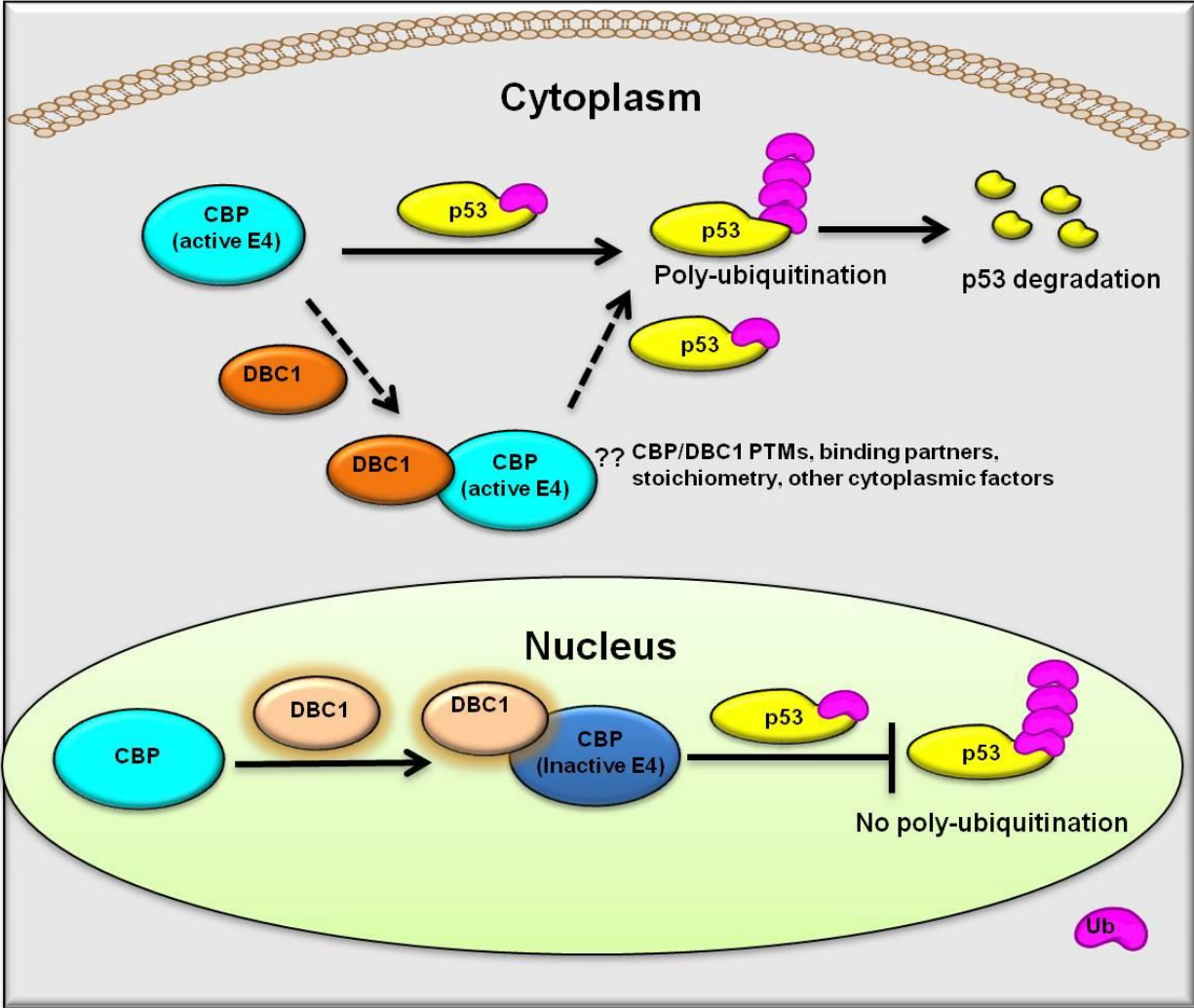


Figure 4.1 Graphic summary of CBP-DBC1 interaction and p53 degradation in the absence of cellular stress. DBC1 interacts with CBP in cytoplasm and nucleus. Cytoplasmic CBP E4 polyubiquitin activity towards p53 is active with or without interaction with DBC1. CBP-DBC1 interaction in nucleus inhibits CBP E4 polyubiquitin activity towards p53.

Appendix

CBP-Interacting Proteins in Response to Doxorubicin-Induced DNA Damage

CBP possesses cytoplasmic restricted E3 autoubiquitination and p53-directed E4 ubiquitin ligase activities in the absence of cellular stress. These CBP ubiquitin ligase activities are dormant in the nucleus, in the absence of stress. The studies within Chapter 2 of this dissertation examined the effect of DNA damage on CBP ubiquitin ligase activities. We showed that DNA damage can induce the activation of the otherwise dormant nuclear CBP E3 autoubiquitination while cytoplasmic CBP E3 autoubiquitination remained active. The next step was to identify CBP-interacting proteins in the cytoplasm and nucleus, in response to DNA damage. CBP was immunoprecipitated from cytoplasmic and nuclear fractions of U2OS cells treated with doxorubicin for 3 hrs, followed by MudPIT analysis. After subtracting non-specific proteins that bound IgG controls for IPs, MudPIT data revealed 97 cytoplasmic CBP-interacting proteins, and 38 nuclear CBP-interacting proteins (Table 5). We identified 11 overlapping CBP-interacting proteins between cytoplasm and nucleus, amongst which was PML (Table 5). This is consistent with studies that showed that CBP interacts with PML, and that CBP can be recruited to PML nuclear bodies, in response to DNA damage (122, 158). Notably, PML was also identified by MudPIT analysis as cytoplasmic CBP-interacting protein in the absence of DNA damage. PML protein is crucial for the formation of PML nuclear bodies and there are 7 known PML isoforms

designated PMLI to PMLVII. PML1-VI are mostly found in the nucleus while PML VII is cytoplasmic. We identified interaction between CBP and PML-II, in the absence of DNA damage, in the cytoplasm, and also in response to DNA damage, in the cytoplasm and nucleus. This observation is based on data obtained from one MudPIT analysis in response to DNA damage. It will be therefore necessary to repeat the MudPIT analysis in response to DNA damage, in order to confirm this observation. Also, it will be interesting to examine the effect of PML-II and other candidate CBP-interacting proteins, on CBP ubiquitin ligase activities, in response to DNA damage.

Table 5: List of cytoplasmic-interacting CBP proteins after DNA damage ranked from highest to lowest total spectrum count. (1-20)

	Description	Gene	Protein accession number	Protein Molecular weight (Da)	Protein identification probability	Exclusive unique peptide count	Exclusive unique spectrum count	Total spectrum count
1	CREB-binding protein	CREBBP	Q92793	265,345.4	100.00%	13	14	21
2	Fatty acid synthase	FASN	P49327	273,427.1	100.00%	25	28	33
3	Cell cycle and apoptosis regulator protein 2	CCAR2	Q8N163	102,903.1	100.00%	10	10	15
4	Isoform PML-2 of Protein PML	PML	P29590-8	90,719.2	100.00%	1	1	17
5	WD repeat and HMG-box DNA-binding protein 1	WDHD1	O75717	125,970.0	100.00%	12	12	13
6	Constitutive coactivator of PPAR-gamma-like protein 1	FAM120A	Q9NZB2-6	125,273.3	100.00%	10	10	13
7	Protein AHNAK2	AHNAK2	Q81VF2-3	616,628.3	100.00%	11	11	13
8	Zinc finger CCH domain-containing protein 7A	ZC3H7A	Q81WR0	110,540.1	100.00%	9	9	11
9	Heat shock protein beta-1	HSPB1	P04792	22,782.6	100.00%	8	9	10
10	E3 ubiquitin-protein ligase TRIM21	TRIM21	F5H012	54,081.4	100.00%	1	2	10
11	CCR4-NOT transcription complex subunit 1	CNOT1	A5YKK6	266,944.7	100.00%	6	6	9
12	Sperm-associated antigen 5	SPAG5	Q98R06	134,423.1	100.00%	7	7	8
13	Protein TFG	TFG	Q92734-2	43,448.3	100.00%	6	6	8
14	Vigilin	HDLBP	Q00341	141,458.2	100.00%	2	2	8
15	Leucine-rich PPR motif-containing protein, mitochondrial	LRPPRC	P42704	157,912.2	100.00%	5	5	8
16	Keratin, type I cytoskeletal 18	KRT18	P05783	48,059.0	100.00%	3	3	7
17	TBC1 domain family member 15	TBC1D15	Q8TC07-2	79,493.2	100.00%	3	3	7
18	Nuclear factor NF-kappa-B p100 subunit	NFKB2	Q00653-4	96,679.6	100.00%	7	7	7
19	Moloney leukemia virus 10, homolog	MOV10	Q9HCE1	113,675.5	100.00%	6	7	7
20	Tankyrase-1-binding protein	TNKS1BP1	Q9C0C2	181,795.0	100.00%	2	3	7

Table 5: List of cytoplasmic-interacting CBP proteins after DNA damage ranked from highest to lowest total spectrum count. (21-40)

	Description	Gene	Protein accession number	Protein Molecular weight (Da)	Protein identification probability	Exclusive unique peptide count	Exclusive unique spectrum count	Total spectrum count
21	Staphylococcal nuclease domain-containing protein 1	SND1	Q7KZF4	101,998.5	100.00%	5	5	7
22	Major vault protein	MVP	Q14764	99,326.0	100.00%	7	7	7
23	U5 small nuclear ribonucleoprotein 200 kDa helicase	SNRNP200	O75643	244,513.8	100.00%	6	6	6
24	Isoform 2 of Polyadenylate-binding protein 4	PABPC4	Q13310-3	69,579.5	100.00%	2	2	6
25	60S ribosomal protein L4	RPL4	P36578	47,699.1	100.00%	3	3	6
26	Clustered mitochondria protein homolog	CLUH	K7EIG1	139,625.5	100.00%	6	6	6
27	Isoform 3 of Heterogeneous nuclear ribonucleo protein Q	SYNCRIP	O60506-3	62,657.2	100.00%	2	2	5
28	Tight junction-associated protein 1	TJAP1	Q5JTD0-2	61,822.2	100.00%	4	4	5
29	Splicing factor, proline- and glutamine-rich	SFPQ	P23246	76,149.5	100.00%	4	4	5
30	ELAV-like protein 1	ELAVL1	B4DVB8	38,997.0	100.00%	3	4	5
31	FK506-binding protein 15	FKBP15	Q5T1M5	133,630.3	100.00%	5	5	5
32	Microtubule-associated protein	MAP4	E7EVA0	245,445.5	100.00%	2	2	5
33	Matrin-3	MATR3	A8MXP9	99,970.9	100.00%	4	4	5
34	Polyubiquitin-C (Fragment)	RPS2	F5H2Z3	15,310.2	72.40%	0	0	4
35	T-complex protein 1 subunit theta	CCT8	P50990	59,621.0	100.00%	4	4	4
36	Eukaryotic translation initiation factor 3	EIF3A	Q14152	166,574.9	100.00%	4	4	4
37	Sorting nexin-9	SNX9	Q9Y5X1	66,592.8	100.00%	3	4	4
38	60S ribosomal protein L7a	RPL7	P18124	29,227.7	100.00%	3	4	4
39	La-related protein 4	LARP4	Q71RC2-4	80,596.3	100.00%	4	4	4
40	Tubulin beta-4B chain	TUBB	P88371	49,830.7	99.80%	1	1	4

Table 5: List of cytoplasmic-interacting CBP proteins after DNA damage ranked from highest to lowest total spectrum count. (41-60)

	Description	Gene	Protein accession number	Protein Molecular weight (Da)	Protein identification probability	Exclusive unique peptide count	Exclusive unique spectrum count	Total spectrum count
41	Poly [ADP-ribose] polymerase 1	PARP1	P09874	113,087.8	100.00%	4	4	4
42	Serine/arginine-rich-splicing factor 1	SRSF1	Q07955	27,745.1	100.00%	3	3	3
43	Nucleolar RNA helicase 2	DDX21	Q9NR30	87,346.0	100.00%	2	2	3
44	Zinc finger CCHH-type antiviral protein 1	ZC3HAV1	Q7Z2W4	101,432.6	100.00%	3	3	3
45	Transferrin receptor protein 1	TFRC	P02786	84,873.6	100.00%	3	3	3
46	Elongation factor Tu, mitochondrial	TUFM	P49411	49,542.4	100.00%	3	3	3
47	Y-box-binding protein 3	YBX3	P16989	40,089.4	100.00%	2	2	3
48	Monofunctional C1-tetrahydrofolate synthase, mitochondrial	MTHFD1L	Q6UB35	105,791.9	100.00%	2	2	3
49	Ribosomal protein L19	RPL19	P84098	23,467.4	100.00%	3	3	3
50	Phosphorylase b kinase regulatory subunit alpha, skeletal muscle isoform	PHKA1	P46020-2	137,315.6	100.00%	3	3	3
51	Isoform Short of Cold shock domain-containing protein E1	CSDE1	O75534-3	85,747.8	100.00%	3	3	3
52	Alpha-enolase	ENO1	P06733	47,170.2	100.00%	2	2	3
53	Isoform 2 of Filamin-A	FLNA	P21333-2	280,008.7	100.00%	3	3	3
54	DNA replication licensing factor MCM3	MCM3	B4DWW4	95,910.3	100.00%	3	3	3
55	MKL/myocardin-like protein 1	MKL1	Q969V6	98,921.1	100.00%	3	3	3
56	Proteasome activator complex subunit 3	PSME3	P61289	29,507.3	100.00%	1	2	2
57	DNA-dependent protein kinase catalytic subunit	PRKDC	P78527	469,095.5	100.00%	2	2	2
58	Zyxin	ZYX	Q15942	61,276.0	100.00%	2	2	2
59	Isoform 6 of Ataxin-2-like protein	ATXN2L	Q8VWWM7-6	102,894.9	100.00%	1	2	2
60	Interleukin enhancer-binding factor 2	ILF2	Q12905	43,062.7	100.00%	2	2	2

Table 6: List of nuclear CBP-interacting proteins after DNA damage ranked from highest to lowest total spectrum count. (1-19)

	Description	Gene	Protein accession number	Protein Molecular weight (Da)	Protein identification probability	Exclusive unique peptide count	Exclusive unique spectrum count	Total spectrum count
1	CREB-binding protein	CREBBP	Q92793	265,345.4	100.00%	31	46	69
2	Cell cycle and apoptosis regulator protein 2	CCAR2	Q8N163	102,903.1	100.00%	18	25	27
3	Keratin, type II cytoskeletal 6A	KRT6A	P02538	60,046.4	100.00%	2	2	12
4	Spectrin alpha chain, non-erythrocytic 1	SPTAN1	Q13813-2	284,542.7	100.00%	11	13	13
5	Huntingtin-interacting protein 1-related protein	HIP1R	O75146	119,389.7	100.00%	8	9	11
6	Keratin, type I cytoskeletal 16	KRT16	P08779	51,269.0	99.80%	0	0	8
7	Paraspeckle component 1	PSPC1	Q8WXF1	58,744.5	100.00%	6	6	7
8	Major vault protein	MVP	Q14764	99,326.0	100.00%	7	7	7
9	Desmoplakin	DSP	P15924	331,781.4	100.00%	5	5	5
10	60S acidic ribosomal protein	RPLP0	P05388	34,274.3	100.00%	4	5	5
11	Keratin, type I cytoskeletal 18	KRT18	P05783	48,059.0	100.00%	2	2	5
12	Ig gamma-1 chain C region	IGHG1	P01857	36,105.0	100.00%	2	2	5
13	Spectrin beta chain, non-erythrocytic 1	SPTBN1	Q01082	274,613.4	100.00%	4	4	4
14	Isoform 3 of Coronin-1C	CORO1C	Q9JULV4-3	58,948.9	100.00%	3	3	4
15	Heterogenous nuclear ribonucleoprotein A3	HNRNPA3	P51991	39,595.1	100.00%	2	2	4
16	Phostensin	PPP1R18	Q6NYC8	67,942.8	100.00%	3	4	4
17	Serine/arginine-rich-splicing factor 1	SRSF1	Q07955	27,745.1	100.00%	4	4	4
18	Nucleolar RNA helicase 2	DDX21	Q9NR30	87,346.0	100.00%	4	4	4
19	G2/mitotic-specific cyclin-B3	CCNB3	Q8WWML7	157,923.0	100.00%	3	3	3

Table 6: List of nuclear CBP-interacting proteins after DNA damage ranked from highest to lowest total spectrum count. (20-37)

	Description	Gene	Protein accession number	Protein Molecular weight (Da)	Protein identification probability	Exclusive unique peptide count	Exclusive unique spectrum count	Total spectrum count
20	ELM2 and SANT domain-containing protein 1	ELMSAN1	Q6PJG2	114,989.3	100.00%	3	3	3
21	Protein S100-A7	S100A7	P31151	11,471.7	100.00%	3	3	3
22	Protein AHNAK2	AHNAK2	Q8IVF2-3	616,628.3	100.00%	3	3	3
23	5-azacytidine-induced protein 1	AZ11	Q9JPN4-2	122,149.9	100.00%	3	3	3
24	Heterogeneous nuclear ribonucleoprotein M	HNRNPM	P52272-2	77,517.3	100.00%	3	3	3
25	Nucleolar and coiled-body phosphoprotein 1	NOLC1	Q14978-3	74,747.4	100.00%	3	3	3
26	Androgen receptor	AR	E9PEG3	77,015.4	100.00%	2	2	2
27	Cleavage and polyadenylation specificity factor subunit 1	CPSF1	Q10570	160,885.9	100.00%	2	2	2
28	rRNA 2'-O-methyltransferase fibrillarin (Fragment)	FBL	M0R2Q4	29,182.2	99.90%	2	2	2
29	Filamin-C	FLNC	Q14315-2	291,015.0	100.00%	2	2	2
30	Serine/threonine-protein phosphatase PP1-alpha catalytic subunit	PPP1CA	P62136	37,513.9	100.00%	2	2	2
31	Protein S100-A8	S100A8	P05109	10,835.0	99.90%	2	2	2
32	Nucleolar transcription factor 1	UBTF	E9PKP7	87,440.5	100.00%	2	2	2
33	GTP-binding nuclear protein Ran	RAN	P62826	24,423.1	100.00%	2	2	2
34	SAFB-like transcription modulator	SLTM	Q9NWH9	117,151.1	100.00%	2	2	2
35	Isoform 2 of Nucleophosmin	NPM1	P06748-2	29,464.9	100.00%	2	2	2
36	DNA mismatch repair protein Msh2	MSH2	P43246	104,745.8	100.00%	2	2	2
37	Isoform PML-2 of Protein PML	PML	P29590-8	90,719.2	79.90%	0	0	1

List of References

1. Chrivia, J. C., Kwok, P. S., Lamb, N., Hagiwara, M., Montminy, M. R., & Goodman, R. H. (1993). Phosphorylated CREB binds specifically to the nuclear protein CBP. *Nature*, 365, 855-859. 2.
2. Arany, Z., Sellers, W.R., Livingston, D.M., Eckner, R. (1994). E1A-associated p300 and CREB-associated CBP belong to a conserved family of coactivators. *Cell*, 77, 799-800.
3. Lewis, J. B., & Mathews, M. B. (1980). Control of adenovirus early gene expression: a class of immediate early products. *Cell*, 21, 303-313.
4. Egan, C., Jelsma, T. N., Howe, J. A., Bayley, S. T., Ferguson, B., & Branton, P. E. (1988). mapping of cellular protein-binding sites on the products of early region 1A of human adenovirus type 5. *Molecular and Cellular Biology*, 8, 3955-3959.
5. Dyson, N. (1992). Adenovirus E1A targets key regulators of cell proliferation. *Cancer surveys*, 12, 161-195.
6. Marmorstein, R. (2001). Structure and function of histone acetyltransferases. *Cell Mol Life Sci*, 58, 693-703.
7. Bannister, A. J., & Kouzarides, T. (1996). The CBP co-activator is a histone acetyltransferase. *Nature*, 384, 641-643.

8. Ogryzko, V. V., Schiltz, R. L., Russanova, V., Howard, B. H., & Nakatani, Y. (1996). The transcription coactivators p300 and CBP are histone acetyltransferase. *Cell*, 87, 953–959.
9. Chakravarti, D., Ogryzko, V., Kao, H. Y., Nash, A., Chen, H., Nakatani, Y., & Evans, R. M. (1999). A viral mechanism for inhibition of p300 and PCAF acetyltransferase activity. *Cell*, 96, 393-403.
10. Chen, C. J., Deng, Z., Kim, A. Y., Blobel, G. A., & Lieberman, P. M. (2001). Stimulation of CREB binding protein nucleosomal histone acetyltransferase activity by a class of transcriptional activators. *Mol Cell Biol*, 21, 476-487.
11. Lau, O. D., Kundu, T. K., Soccio, R. E., Ait-Si-Ali, S., Khalil, E. M., Vassilev, A., Wolffe, A. P., Nakatani, Y., Roeder, R. G., & Cole, P. A. (2000). HATs off: Selective synthetic inhibitors of the histone acetyltransferases p300 and PCAF. *Molecular Cell*, 5(3), 589-595.
12. Balasubramanyam, K., Varier, R. A., Altaf, M., Swaminathan, V., Siddappa, N. B., Ranga, U., & kundu, T. K. (2004). Curcumin, a novel p300/CREB-binding protein-specific inhibitor of acetyltransferase, represses the acetylation of histone/non-histone proteins and histone acetyltransferase-dependent chromatin transcription. *Journal of Biological Chemistry*, 279(49), 51163-51171.
13. Santer, F. R., Hoschele, P. P., Oh, S. J., Erb, H. H., Bouchai, J., Cavarretta, I. T., Parson, W., Meyers, D. J., Cole, P. A., & Culig, Z. (2011). Inhibition of the acetyltransferases p300 and CBP reveals a targetable function of p300 in the survival and invasion pathways of prostate cancer cell lines. *Molecular Cancer Therapeutics*, 10, 1644-1655.

14. Yan, G., Eller, M. S., Elm, C., Larocca, C. A., Ryu, B., Panova, I. P., Dancy, B. M., Bowers, E. M., Meyers, D., Lareau, L., Cole, P. A., Taverna, S. D., & Alani, R. M. (2013). Selective Inhibition of p300 HAT blocks cell cycle progression, induces cellular senescence, and inhibits the DNA damage response in melanoma cells. *Journal of Investigative Dermatology*, 133, 2444-2452.
15. Korsus, E., Rosenfeld, M. G., & Mayford, M. (2004). CBP histone acetyltransferase activity is a critical component of memory consolidation. *Neuron*, 42(6), 961-967.
16. Janknecht, R., & Hunter, T. (1996). A growing coactivator network. *Nature*, 383, 22–23.
17. Onate, S. A., Tsai, S. Y., Tsai, M.J., & O'Malley, B. W. (1995). Sequence and characterization of a coactivator for the steroid hormone receptor superfamily. *Science*, 270, 1354–1357.
18. Kamei, Y., Xu, L., Heinzel, T., Torchia, J., Kurokawa, R., Gloss, B., Lin, S. C., Heyman, R. A., Rose, D.W., Glass, C. K., & Rosenfeld, M.G. (1996). A CBP integrator complex mediates transcriptional activation and AP-1 inhibition by nuclear receptors. *Cell*, 85, 403–414
19. Swope, D. L., Mueller, C. L., & Chrivia, J. C. (1996). CREB-binding protein activates transcription through multiple domains. *J Biol Chem*, 271(45), 28138–28145.
20. Teufel, D. P., Freund, S. M, Bycroft, M., & Fersht, A. R. (2007). Four domains of p300 each bind tightly to a sequence spanning both transactivation subdomains of p53. *Proc Natl Acad Sci USA*, 104(17), 7009–7014.

21. Martinez-Balbas, M. A., Bannister, A. J., Martin, K., Haus-Seuffert, P., Meisterernst, M., & Kouzarides, T. (1998). The acetyltransferase activity of CBP stimulates transcription. *EMBO J*, 17, 2886-2893.
22. Lill, N. L., Grossman, S. R., Ginsberg, D., DeCaprio, J., & Livingston, D. M. (1997). Binding and modulation of p53 by p300/CBP coactivators. *Nature*, 387(6635), 823–827.
23. Martinez-Balbas, M., Bauer, U., Nielsen, S., Brehm, A., Kouzarides, T. (2000). Regulation of E2F1 activity by acetylation. *EMBO* 19(4), 662-671.
24. Ma, K., Chan, J. K., Zhu, G., & Wu, Z. (2005). Myocyte enhancer factor 2 acetylation by p300 enhances its DNA binding activity, transcriptional activity, and myogenic differentiation. *Mol Cell Biol*, 25, 3575–3582.
25. Kalkhoven, E. (2004). CBP and p300: HATs for different occasions. *Biochemical Pharmacology*, 68, 1145-1155.
26. Chan, H., & La Thangue, N. B. (2001). P300/CBP proteins: HATs for transcriptional bridges and scaffolds. *Journal of Cell Science*, 114, 2363-2373.
27. Dilworth, F. J., & Chambon, P. (2001). Nuclear receptors coordinate the activities of chromatin remodeling complexes and coactivators to facilitate initiation of transcription. *Oncogene*, 20, 3047-3054.
28. Gu, W., & Roeder, R. G. (1997). Activation of p53 sequence-specific DNA binding by acetylation of the p53 C-terminal domain. *Cell*, 90, 595-606.
29. Meek, D. W. (1994). Post-translational modification of p53. *Semin. Cancer Biol*, 5, 203-210.

30. Feng, L., Lin, T., Uranishi, H., Gu, W., & Xu, Y. (2005). Functional Analysis of the roles of posttranslational modifications at the p53 C terminus regulating p53 stability and activity. *Mol Cell Biol*, 25(13), 5389-5395.
31. Thompson, M. A., & Ramsay R. G. (1995). Myb: an old oncoprotein with new roles. *Bioessays*, 17, 341-350.
32. Tomita, A., Towatari, M., Tsuzuki, S., Hayakawa, F., Kosugi, H., Tamai, K., Miyazaki, T., Kinoshita, T., & Saito, H. (2000). c-Myb acetylation at the carboxy-terminal conserved domain by transcriptional co-activator p300. *Oncogene*, 19, 444-451.
33. Hung, H. L., Lau, J., Kim, A. Y., Weiss, M. J., & Blobel, G. A. (1999). CREB-binding protein acetylates hematopoietic transcription factor GATA-1 at functionally important sites. *Mol Cell Biol*, 19, 3496-3505.
34. Miller, I. J., & Bieker, J. J. (1993). A novel, erythroid cell-specific murine transcription factor that binds to the CACCC element and is related to the Kruppel family of nuclear proteins. *Mol Cell Biol*, 13, 2776-2786.
35. Zhang, W., & Bieker, J. J. (1998). Acetylation and modulation of erythroid Kruppel-like factor (EKLF) activity by interaction with histone acetyltransferases. *Proc Natl Acad Sci USA*, 95, 9855-9860.
36. Goodman, R. H., & Smolik, S. (2000). CBP/p300 in cell growth, transformation, and development. *Genes & Development*, 14, 1553-1577.
37. Gallimore, P.H., Turnell, A.S. (2001). Adenovirus E1A: remodeling the host cell, a life or death experience. *Oncogene* 20: 7824-7835.

38. Arany, Z., Huang, E., Eckner, R., Bhattacharya, S., Jiang, C., Goldberg, M., Bunn, F., & Livingston, D. (1996). An essential role for p300/CBP in the cellular response to hypoxia. *Proc Natl Acad Sci USA*, 93, 12969–12973.
39. Turnell, A. S., Stewart, G. S., Grand, R. J. A., Rookes, S. M., Martin, A., Yamano, H., Elledge, S. J., & Gallimore, P. H. (2005). The APC/C and CBP/p300 cooperate to regulate transcription and cell-cycle progression. *Nature*, 438, doi:10.1038/Nature04151.
40. Gao, X. N., Lin, J., Ning, Q. Y., Gao, L., Yao, Y. S., Zhou, J. H., Li, Y. H., Wang, L. L., & Yu, L. (2013). A Histone Acetyltransferase p300 Inhibitor C646 Induces Cell Cycle Arrest and Apoptosis Selectively in AML1-ETO- Positive AML Cells. *PLoS One*, 8(2), e55481. doi:10.1371/journal.pone.0055481.
41. Dietze, E., Bowie, M., Mrozek, K., Caldwell, E., Neal, C., Marjoram, R., Troch, M., Bean, G., Yokoyama, K., Ibarra, C., & Seewaldt, V. (2005). CREB-binding protein regulates apoptosis and growth of HMECs grown in reconstituted ECM via laminin-5. *Journal of Cell Science*, 118, 5005-5022.
42. Rebel, V. I., Kung, A., Tanner, E., Yang, H., Bronson, R., & Livingston, D. (2002). Distinct roles for CREB-binding protein and p300 in hematopoietic stem cell self-renewal. *PNAS*, 99, 14789-14794.
43. Ait-Si-Ali, S., Polesskaya, A., Filleur, S., Ferreira, R., Duquet, A., *et al.* (2000). CBP/ p300 histone acetyl- transferase activity is important for the G1/S transition. *Oncogene*, 19, 2430–2437.
44. Yuan, Z., Huang, Y., Ishiko, T., Nakada, S., Utsugisawa, T., Shioya, H., utsugisawa, Y., Shi, Y., Weichselbaum, R., & Kufe, D. (1999). Function for p300

- and not CBP in the apoptotic response to DNA damage. *Oncogene*, 18, 5714 - 5717.
45. Avantaggiati, M. L., Ogryzko, V., Gardner, K., Giordano, A., Levine, A. S., & Kelly, K. (1997). Recruitment of p300/CBP in p53- dependent signal pathways. *Cell*, 89, 1175-1184.
 46. Pao, G. M., Janknecht, R., Ruffner, H., Hunter, T., & Verma, I. M. (2000). CBP/p300 interact with and function as transcriptional coactivators of BRCA1. *Proc. Natl Acad Sci*, 97, 1020-1025.
 47. Oelgeschlager, M., Janknecht, R., Krieg, J., Schreek, S., & Luscher, B. (1996). Interaction of the co-activator CBP with Myb proteins: Effects on Myb-specific transactivation and cooperativity with NF-M. *EMBO J*, 15, 101-110.
 48. Lee, J. S., See, R. H., Deng, T., & Shi, Y. (1996). Adenovirus E1A downregulates c-Jun and Jun-B mediated transcription by targeting their coactivator p300. *Mol Cell Biol*, 16, 4312-4326.
 49. Bannister, A. J., oehler T., Wilhelm, D., Angel, P., & Kouzarides, T. (1995). Stimulation of c-Jun activity by CBP: c-Jun residues Ser63/73 are required for CBP induced stimulation in vivo and CBP binding in vitro. *Oncogene*, 11(12), 2509-2514.
 50. Felts, S. J., Stang, M. T., & Getz, M. J. (1997). A c-Fos- and E1A-interacting component of the tissue factor basal promoter complex mediates synergistic activation of transcription by transforming growth factor- β 1. *Oncogene*, 14, 1679-1685.

51. Nissen, L. J., Gelly, J. C., & Hipkind, R. A. (2001). Induction-independent Recruitment of CREB-binding Protein to the c-fos Serum Response Element through Interactions between the Bromodomain and Elk-1. *Jour of Biol Chem*, 276(7), 5213-5221.
52. Kwok, R. P., Laurance, M. E., Lundblad, J. R., Goldman, P. S., Shih, H., Connor, L. M., Marriott, S. J., & Goodman, R. H. (1996). Control of cAMP-regulated enhancers by the viral transactivator Tax through CREB and the co-activator CBP. *Nature*, 380, 642-646.
53. Harrod, R., Tang, Y., Nicot, C., Lu, H. S., Vassilev, A., Nakatani, Y., & Giam, C.Z. (1998). An exposed KID-like domain in human T-cell lymphotropic virus type 1 Tax is responsible for the recruitment of coactivators CBP/p300. *Mol Cell Biol*, 18, 5052-5061.
54. Van Orden, K. V., Yan, J. P., & Nyborg, J. K. (1999). Binding of the human T-cell leukemia virus Tax protein to the coactivator CBP interferes with CBP-mediated transcriptional control. *Oncogene*, 18, 3766-3772.
55. Yang, X. J., Ogryzko, V. V., Nishikawa, J., Howard, B. H., & Nakatani, Y. (1996). A p300/CBP associated factor that competes with the adenoviral oncoprotein E1A. *Nature*, 382, 319-324.
56. Patel, D., Huang, S. M., Bagila, L. A., & McCance, D. J. (1999). The E6 protein of human papillomavirus type 16 binds to and inhibits co-activation by CBP and p300. *EMBO J*, 18, 5061-5072.

57. Eckner, R., Ludlow, J. W., Lill, N. L., Oldread, E., Arany, Z., Modjtahedi, N., DeCaprio, J. A., Livingston, D. M., & Morgan, J. A. (1996). Association of p300 and CBP with simian virus 40 large T antigen. *Mol Cell Biol*, 16, 3454-3464.
58. Grossman, S. R., & Laimins, L. A. (1989). E6 protein of human papillomavirus type 18 binds zinc. *Oncogene*, 4, 1089-1093.
59. Scheffner, M., Huibregtse, J. M., Vierstra, R. D., & Howley, P. M. (1993). The HPV-16 E6 and E6-AP complex functions as a ubiquitin protein ligase in the ubiquitination of p53. *Cell*, 75, 495-505.
60. Zimmermann, H., Degenkolbe, R., Bernard, H. U., & O'Connor, M. (1999). The HPV-16 E6 oncoprotein can down-regulate p53 activity by targeting the transcriptional co-activator CBP/p300. *Journal of Virology*, 73, 6209-6219.
61. Zimmermann, H., Koh, C. H., Degenkolbe, R., O'Connor, M. J., Muller, A., Steger, G., Chen, J., Lui, Y., Androphy, E., & Bernard, H. U. (2000). Interaction with CBP/p300 enables the bovine papillomavirus type 1 E6 oncoprotein to down-regulate CBP/p300-mediated transactivation by p53. *Journal of General Virology*, 81, 2617-2623.
62. Rubinstein, J. H., & Taybi, H. (1963). Broad thumbs and toes and facial abnormalities. *Am J Dis Child*, 105, 588-608.
63. Petrij, F., Giles, R. H., Dauwerse, H. G., Saris, J. J., Hennekam, R. C. M., Masuno, M., Tommerup, N., Ommen, G. J, Goodman, R. H., & Peters, D. J. (1995). Rubinstein-Taybi syndrome caused by mutations in transcriptional co-activator CBP. *Nature*, 376, 348-351.

64. Miller, R. W., & Rubinstein, J. H. (1995). Tumors in Rubinstein-Taybi syndrome. *Am J med Genet*, 56(1), 112-115.
65. Taine, L., Goizet, C., Wen, Z. Q., Petrij, F., Breuning, M. H., Ayme, S., Saura, R., Arveiler, B., & Lacombe, D. (1998). Submicroscopic deletion of chromosome 16p13.3 in patients with Rubinstein-Taybi syndrome. *Am J Med Genet*, 78, 267-270.
66. Petrij, F., Dauwerse, H. G., Blough, R. I., Giles, R. H., van der Smagt, J. J., Maaswinkel-Mooy, P. D., van Karnebeek, C. D., van Ommen, G. J. B., & van Haeringen, A. (2000). Diagnostic analysis of the Rubinstein-taybi syndrome: Five cosmids should be used for microdeletion and low number of protein truncating mutations. *J Med Genet*, 37, 168-176.
67. Bartsch, O., Wagner, A., Hinkel, G. K., Krebs, P., Stumm, M., Schmalenberger, B., Bohm, S., Balci, S., & Majewski, F. (1999). FISH studies in 45 patients with Rubinstein-Taybi syndrome: Deletions associated with polysplenia, hypoplastic left heart and death in infancy. *Eur J Hum Genet*, 7, 748-756.
68. Tanaka, Y., Naruse, I., Maekawa, T., Masuya, H., Shiroishi, T., & Ishii, S. (1997). Abnormal skeletal patterning in embryos lacking a single Cbp allele: a partial similarity with Rubinstein-Taybi syndrome. *Proc Natl Acad Sci*, 94, 10215-10220.
69. Oike, Y., Hata, A., Mamiya, T., Kaname, T., Noda, Y., Suzuki, M., Yasue, H., Nabeshima, T., Araki, K., & Yamamura, K. (1999). Truncated CBP protein leads to classical Rubinstein-Taybi syndrome phenotypes in mice: implications for a dominant-negative mechanism. *Hum Mol Genet*, 8, 387-396.

70. Borrow, J., Stanton, V. P. Jr., Andresen, J. M., Becher, R., Behm, F. G., Chaganti, R. S., Civin, C. I., Distech, C., Dube, I., Frischauf, A. M., Horsman, D., Mitelman, F., Volinia, S., Watmore, A. E., & Housman, D. E. (1996). The translocation t(8;16)(p11;p13) of acute myeloid leukemia fuses a putative acetyl transferase to the CREB-binding protein. *Nat Genet*, 14, 33-41.
71. Taki, T., Sako, M., Tsuchida, M., & Hayashi, Y. (1997). t(11;16)(q23;p13) translocation in myelodysplastic syndrome fuses the MLL gene to the CBP gene. *Blood*, 89, 3945-3950.
72. Sobulo, O. M., Borrow, J., Tomek, R., Reshmi, S., Harden, A., Schlegelberger, B., Housman, D., Dogget, N. A., Rowley, J. D., & Zeleznik-Le, N. J. (1997). MLL is fused to CBP, a histone acetyltransferase, in therapy-related acute myeloid leukemia with a t(11;16)(q23;p13). *Proc Natl Acad Sci USA*, 94, 8732-8737.
73. Giles, R. H., Dauwerse, J. G., Higgins, C., Petrij, F., Wessels, J. W., Beverstock, G. C., Dohner, H., Jotterand-Bellomo, M., Falkenburg, J. H., Slater, R. M., van Ommen, G. J., Hagemeijer, A., van der Reijden, B. A., & Breuning, M. H. (1997). Detection of CBP rearrangements in acute myelogenous leukemia with t(8;16). *Leukemia*, 11, 2087-2096.
74. Panagopoulos, I., Fioretos, T., Isaksson, M., Samuelsson, U., Billstrom, R., Strombeck, B., Mitelman, F., & Johansson, B. (2000). Fusion of the MORF and CBP genes in acute myeloid leukemia with the t(10;16)(q22;p13). *Hum Mol Genet*, 10, 395-404.
75. Borrow, J., Stanton, V. P., Andresen, J. M., Becher, R., Behm, F. G., Chaganti, R. S., Civin, C. I., Distech, C., Dube, I., Frischauf, A. M., Horsman, D.,

- Mitelman, F., Volonia, S., Watmore, A. E., & Housman, D. E. (1996). The translocation t(8;16)(p11;p13) of acute myeloid leukaemia fuses a putative acetyltransferase to the CREB-binding protein. *Nat Genet*, 14(1), 33-41.
76. Horwitz, K. B., Jackson, T. A., Bain, D. L., Richer, J. K., Takimoto, G. S., & Tung, L. (1996). Nuclear receptor coactivators and corepressors. *Mol Endocrinol*, 10(10), 1167-77.
77. Fu, M., Wang, C., Reutens, A. T., Wang, J., Angeletti, R. H., Siconolfi-Baez, L., et al. (2000). p300 and p300/cAMP-response element –binding protein-associated factor acetylate the androgen receptor at sites governing hormone-dependent transactivation. (2000). *J Biol Chem*, 275, 20853-60.
78. Fu, M., Rao, M., Wang, C., Sakamaki, T., Wang J., Di Vizio, D., Zhang, X., Albanese, C., Balk, S., Chang, C., Fan, S., Rosen, E., Palvimo, J., Ja"nne, O., Muratoglu, S., Avantaggiati, M., & Pestelli, R. (2003). Acetylation of androgen receptor enhances coactivator binding and promotes prostate cancer cell growth. *Mol Cell Biol*, 23(23), 8563-8575.
79. Comuzzi, B., Lambrinidis, L., Rogatsch, H., Godoy-Tundidor, S., Knezevic, N., Krhen, I., Marekovic, Z., Bartsch, G., Klocker, H., Hobisch, A., & Culig, Z. (2003). The Transcriptional Co-Activator cAMP Response Element-Binding Protein-Binding Protein Is Expressed in Prostate Cancer and Enhances Androgen- and Anti-Androgen-Induced Androgen Receptor Function. *Am J Pathol*, 162, 233-241.
80. Ianculescu, I., Wu, D., Siegmund, K., Stallcup, M. (2011). Selective roles for CBP and p300 as coregulators for androgen-regulated gene regulated gene

- expression in advanced prostate cancer cells. *Journal of Biological Chemistry*, 287(6), 4000-4013.
81. Gao, Y., Geng, J., Hong, X., Qi, J., Teng, Y., Yang, Y., Qu, D., & Chen, G. (2014). Expression of p300 and CBP is associated with poor prognosis in small cell lung cancer. *Int J Clin Exp Pathol*, 7(2), 760-767.
82. Steffan, J. S., Kazantsev, A., Spasic-Boskovic, O., Greenwald, M., Zhu, Y. Z., Gohler, H., *et al.* (2000). The Huntington's disease protein interacts with p53 and CREB-binding protein and represses transcription. *Proc Natl Acad Sci USA*, 97, 6763-6768.
83. Rouaux, C., Jokic, N., Mbebi, C., Boutillier, S., Loeffler, J. P., & Boutillier, A. L. (2003). Critical loss of CBP/p300 histone acetylase activity by caspase-6 during neurodegeneration. *Embo J*, 22, 6537-6549.
84. Dupuis, I., Tapia, M., Rene, F., Lutz-Bucher, B., Gordon, L., Mercken, L., *et al.* (2000). *Neurobiol Dis*, 7, 274-285.
85. Hughes, R. E. (2002). Polyglutamine disease: acetyltransferases awry. *Curr Biol*, 12, 141-143.
86. Takahashi, J., Fujigasaki, H., Zander, C., El Hachimi, K. H., Stevanin, G., Durr, A., *et al.* (2002). Two populations of neuronal intranuclear inclusions in SCA7 differ in size and promyelocytic leukaemia protein content. *Brain*, 125, 1534-1543.
87. McCampbell, A., Taylor, J. P., Taye, A. A., Robitschek, J., Li, M., Walcott, J., *et al.* (2000). CREB-binding protein sequestration by expanded polyglutamine. *Hum Mol Genet*, 9, 2197-2202.

88. Nucifora, F. C., Sasaki, M., Peters, M. F., Huang, H., Cooper, J. K., Yamada, M. *et al.* (2001). Interference by huntingtin and atrophin-1 with cbp-mediated transcription leading to cellular toxicity. *Science*, 291, 2423-2428.
89. McCampbell, A., Taye, A. A., Whitty, L., Penney, E., Steffan, J. S., & Fischbeck, K. H. (2001). Histone deacetylase inhibitors reduce polyglutamine toxicity. *Proc Natl. Acad. Sci. USA*, 98, 15179-15184.
90. Jiang, H., Nucifora, Jr. F. C., Ross, C. A., & DeFranco, D. B. (2003). Cell death triggered by polyglutamine-expanded huntingtin in a neuronal cell line is associated with degradation of CREB-binding protein. *Hum Mol Genet*, 12, 1-12.
91. Rouaux, C., Loeffler, J., & Boutillier, A. L. (2004). Targeting CREB-binding protein (CBP) loss of function as a therapeutic strategy in neurological disorders. *Biochem Pharm*, 68(6), 1157-1164.
92. He, L., Sabet, A., Djedjos, S., Miller, R., Sun, X., Hussain, M. A., Radovick, S., & Wondisford F.E (2009). Metformin and Insulin Suppress Hepatic Gluconeogenesis by Inhibiting cAMP Signaling Through Phosphorylation of CREB-Binding Protein (CBP). *Cell*, 137(4), 635-646.
93. Ravnskjaer, K., Kester, H., Liu, Y., Zhang, X., Lee, D., Yates, J. R. 3rd., & Montminy, M. (2007). Cooperative interactions between CBP and TORC2 confer selectivity to CREB target gene expression. *EMBO J*, 26, 2880-2889.
94. Wiernsperger, N. F., & Bailey, C. J.(1999). The antihyperglycaemic effect of metformin: therapeutic and cellular mechanisms. *Drugs*, 58, 31-39.
95. Zhou, X. Y., Shibusawa, N., Naik, K., Porras, D., Temple, K., Ou, H., Kaihara, K., Roe, M. W., Brady, M. J., & Wondisford, F. E. (2004). Insulin regulation of

- hepatic gluconeogenesis through phosphorylation of CREB-binding protein. *Nat Med*, 10, 633-637.
96. Lee, J. M., Seo, W. Y., Song, K. H., Chanda, D., Kim, Y. D., Kim, D. K., Lee, M. W., Ryu, D., Kim, Y. H., Noh, J. R., Lee, C. H., Chiang, J. Y., Koo, S. H., & Choi, H. S. (2010). AMPK-dependent repression of hepatic gluconeogenesis via disruption of CREB.CRTC2 complex by orphan nuclear receptor small heterodimer partner. *J Biol Chem*, 285, 32182-32191.
97. Korzus, E., Rosenfeld, M. G., & Mayford, M. (2004). CBP histone acetyltransferase activity is a critical component in memory consolidation. *Neurons*, 42, 961-972.
98. Tanaka, Y., Naruse, I., Hongo, T., Xu, M., Nakahata, T., Maekawa, T., & Ishii, S. (2000). Extensive brain hemorrhage and embryonic lethality in a mouse null mutant of CREB-binding protein. *Mech Dev*, 95(1-2), 133-145.
99. Nucifora Jr., F. C, Sasaki, M, Peters, M. F., Huang, H., Cooper, J. K., Yamada, M., *et al.* (2001). Interference by huntingtin and atrophin-1 with cbp-mediated transcription leading to cellular toxicity. *Science*, 291, 2423-2428.
100. Caccamo, A., Maldonado, M. A., Bokov, A. F., Majumder, S., & Oddo, S. (2010). CBP gene transfer increases BDNF levels and ameliorates learning and memory deficits in a mouse model of Alzheimer's disease. *Proc Natl Acad Sci USA*, 107, 22687-22692.
101. Gang, E. J., Hsieh, Y., Pham, J., Zhao, Y., Nguyen, C., Huantes, S., Park, E., Naing, K., Klemm, L., Swaminathan, S., Conway, E. M., *et al.* (2014). Small

- molecule inhibition of CBP/catenin interactions eliminates drug resistance clones in acute lymphoblastic leukemia. *Oncogene*, 33(17), 2169-2178.
102. Lenz, H. J., & Kahn, M. (2014). Safely targeting cancer stem cells via selective catenin coactivator antagonism. *Cancer Sci*, 105, 1087-1092.
 103. Henderson, W. R., Chi, E. Y., & Ye, X. (2010). Inhibition of Wnt/beta-catenin/CREB binding protein (CBP) signaling reverses pulmonary fibrosis. *Proc Natl Acad Sci USA*, 107, 14309-14314.
 104. Hao, S., He, W., & Li Y. (2011). Targeted inhibition of β -catenin/CBP signaling ameliorates renal interstitial fibrosis. *J Am Soc Nephro*, 22, 1642-1653.
 105. Sasaki, T., Hwang, H., Nguyen, C., Kloner, R. A., & Kahn, M. (2013). The small molecule Wnt signaling modulator ICG-001 improves contractile function in chronically infarcted rat myocardium. *PLoS ONE*, 8, e75010.
 106. Best, J. L., Amezcua, C. A., Mayr, B., Flechner, L., Murawsky, C. M., Emerson, B., *et al.* (2004). Identification of small-molecule antagonists that inhibit an activator: coactivator interaction. *Proc Natl Acad Sci USA*, 101(51), 17622–17627.
 107. Lee, J. W., Park, H. S., Park, S., Ryu, S., Meng, W., Jurgensmeier, J. M., Kurie, J. M., Kong, W. K., Boyer, J. L., Herbst, R. S., & Koo, J. S. (2015). A novel small molecule inhibitor targeting CREB-CBP complex possesses anti-cancer effects along with cell cycle regulation, autophagy suppression and endoplasmic reticulum stress. *PLoS ONE*, 10(4), e0122628.
 108. Ait-Si-Ali, S., Ramirez, S., Barre, F. X., Dkhissi, F., Magnaghi-Jaulin, L., Girault, J. A., Robin, P., Knibiehler, M., Pritchard, L. L., Ducommun, B., Trouche, D., &

- Harel-Bellan, A. (1998). Histone acetyltransferase activity of CBP is controlled by cell cycle-dependent kinases and oncoprotein E1A. *Nature (London)*, 396, 184-186.
109. Hamamori, Y., Sartorelli, V., Ogryzko, V., Puri, P. L., Wu, H. Y., Wang, J. Y., Nakatani, Y., & Kedes, L. (1999). Regulation of histone acetyltransferases p300 and PCAF by the bHLH protein twist and adenoviral oncoprotein E1A. *Cell*, 96, 405-413.
110. Soutoglou, E., Viollet, B., Vaxillaire, M., Yaniv, M., Pontoglio, M., & Talianidis, I. (2001). Transcription factor-dependent regulation of CBP and P/CAF histone acetyltransferase activity. *EMBO J*, 20, 1984-1992.
111. Miyake, S., Sellers, W. R., Safran, M., Li, X., Zhao, W., Grossman, S. R., Gan, J., DeCaprio, J. A., Adams, P. D., & Kaelin Jr., W. G. (2000). Cells degrade a novel inhibitor of differentiation with E1A-like properties upon exiting the cell cycle. *Mol Cell Biol*, 20, 8889-8902.
112. Impey, S., Fong, Y. W., Cardinaux, J. R., Fass, D. M., Obrietan, K., Wayman, G. A., Storm, D., Soderling, T. R., & Goodman, R. H. (2002). Phosphorylation of CBP mediates transcriptional activation by neural activity and CaM kinase IV. *Neuron*, 34, 235-244.
113. Ait-Si-Ali, S., Carlisi, D., Ramirez, S., Upegui-Gonzalez, L. C., Duquet, A., Robin, P., Rudkin, B., Harel-Bellan, A., & Trouche, D. (1999). Phosphorylation by p44 MAP Kinase/ERK1 stimulates CBP histone acetyl transferase activity in vitro. *Biochem Biophys Res Commun*, 262, 157-162.

114. Huang, W., Ju, T., Hung, M., & Chen, C. (2007). Phosphorylation of CBP by IKK α promotes cell growth by switching the binding preference of CBP from p53 to NF- κ B. *Molecular Cell*, 26, 75-87.
115. Zeng, L., Zhang, Q., Gerona-Navarro, G., Moshkina, N., & Zhou, M. M. (2008). Structural basis of site-specific histone recognition by the bromodomains of human coactivators PCAF and CBP/p300. *Structure*, 16(4), 643-652.
116. Mujtaba, S., *et al.* (2004). Structural mechanism of the bromodomain of the coactivator CBP in p53 transcriptional activation. *Mol Cell*, 13(2), 251-263.
117. Das, C., Roy, S., Namjoshi, S., Malarkey, C., Jones, D. N., Kutateladze, T., Churchill, M. E., & Tyler, J. (2014). Binding of the histone chaperone ASF1 to the CBP bromodomain promotes histone acetylation. *PNAS*, E1072-E1081.
118. Shi, D., Pop, M. S., Kulikov, R., Love, I. M., Kung, A. L., & Grossman, S. R. (2009). CBP and p300 are cytoplasmic E4 polyubiquitin ligases for p53. *Proc Natl Acad Sci USA*, 106(38), 16275-16280.
119. Kuo, H. Y. (2005). SUMO modification negatively modulates the transcriptional activity of CREB-binding protein via the recruitment of Daxx. *PNAS*, 102(47), 16973-16978.
120. Chevillard-Briet, M., Trouche, D., & Vandiel, L. (2002). Control of CBP co-activating activity by arginine methylation. *EMBO*, 21(20), 5457-5466.
121. Grossman, S. R., Deato, M. E., Brignone, C., Chan, H. M., Kung, A. L., Tagami, H., Nakatani, Y., & Livingston, D. M. (2003). Polyubiquitination of p53 by a ubiquitin activity of p300. *Science*, 300(5617), 342-344.

122. St-Germain, J. R., Chen, J., & Li, Q. (2008). Involvement of PML nuclear bodies in CBP degradation through the ubiquitin-proteasome pathway. *Epigenetics*, 3(6), 342-349.
123. Mahajan, R., Delphin, C., Guan, T., Gerace, L., & Melchior, F. (1997). A small ubiquitin-related polypeptide involved in targeting RanGAP1 to nuclear pore complex protein RanBP2. *Cell*, 88, 97-107.
124. Kerscher, O. (2007). SUMO junction - what's your function? New insights through SUMO-interacting motifs. *EMBO Rep*, 8, 550-555.
125. Lapenta, V., Chiurazzi, P., van der Spek, P., Pizzuti, A., Hanaoka, F., & Brahe, C. (1997). SMT3A, a human homologue of the *S. cerevisiae* SMT3 gene, maps to chromosome 21qter and defines a novel gene family. *Genomics*, 40, 362-366.
126. Li, S. J., & Hochstrasser, M. (1999). A new protease required for cell-cycle progression in yeast. *Nature*, 398, 246-251.
127. Shih, H.M., Chang, C. C., Kuo, H. Y., & Lin, D. Y. (2007). Daxx mediates SUMO-dependent transcriptional control and sub-nuclear compartmentalization. *Biochem Society transactions*, 35, 1397-1400.
128. Ryan, C. M., Kindle, K. B., Collins, H. M., & Heery, D. M. (2010). SUMOylation regulates the nuclear mobility of CREB binding protein and its association with nuclear bodies in live cells. *Biochemical and Biophysical Research Communications*, 391, 1136-1141.
129. Jones, P. A., & Baylin, S. B. (2002). "The fundamental role of epigenetic events in cancer". *Nature Reviews Genetics*, 3, 415-428.

130. Xu, W., Chen, H., Du, K., Asahara, H., Tini, M., Emerson, B. M., Montminy, M., & Evans, R. M. (2001). A transcriptional switch mediated by cofactor methylation. *Science*, 294, 2507-2511.
131. Lambert, P. F, Kashanchi, F., Radonovich, M. F., Shiekhattar, R., & Brady, J. N. (1998). Phosphorylation of p53 serine 15 increases interaction with CBP. *J Biol Chem*, 273, 33048-33053.
132. Jenkins, L. M., Yamaguchi, H., Hayashi, R., Cherry, S., Tropea, J. E., Miller, M., Wlodawer, A., Appella, E., & Mazur, S. J. (2009). Two distinct motifs within the p53 transactivation domain bind to the Taz2 domain of p300 and are differentially affected by phosphorylation. *Biochemistry*, 48(6), 1244-1255.
133. Matsuzaki, H., Daitoku H., Hatta, M., Aoyama, H., Yoshimochi, K., Fukamizu, A. (2005). Acetylation of Foxo1 alters its DNA-binding ability and sensitivity to phosphorylation. *PNAS*,102,11278-11283.
134. Hochstrasser, M. (1995). Ubiquitin, proteasome, and regulation of intracellular protein degradation. *Science Direct*, 7(2), 215-223.
135. Isaksson, A., Musti, A., & Bohmann, D. (1996). Ubiquitin in signal transduction and cell transformation. *Biochimica et Biophysica Acta (BBA)- Reviews on cancer*, 1228(1), F21-F29.
136. Deng, L., Wang, C., Spencer, L., Braun, A., You, J., Slaughter, C., & Chen, Z. (2000). Activation of the I κ B kinase complex by TRAF6 requires a dimeric ubiquitin-conjugating enzyme complex and a unique polyubiquitin chain. *Cell*, 103, 351-361.

137. Plosky, B., Vidal, A., Henestrosa, A., McLenigan, M., McDonald, J., Mead, S., & Woodgate, R. (2006). Controlling the subcellular localization of DNA polymerases ι and η via interactions with ubiquitin. *EMBO Journal*, 25, 2847-2855.
138. Hoege, C., Pfander, B., Moldovan, G. L., Pyrowolakis, G., & Jentsch, S. (2002). RAD6-dependent DNA repair is linked to modification of PCNA by ubiquitin and SUMO. *Nature*, 419, 135-141.
139. Randow, F., & Lehner P. J. (2009). Viral avoidance and exploitation of the ubiquitin system. *Nature Cell Biology*, 11, 527-534.
140. Huibregtse, J. M., Scheffner, M., Howley, P. M. (1994). E6-AP directs the HPV E6-dependent inactivation of p53 and is representative of a family of structurally and functionally related proteins. *Cold Spring Harbor Symp Quant Biol*, 59, 237-245.
141. Huang, L., Kinnucan, E., Wang, G., Beaudenon, S., Howley, P., Huibregtse, J. M., & Pavletich, N. P. (1999). Structure of an E6AP-UbcH7 complex: insights into ubiquitination by the E2-E3 enzyme cascade. *Science*, 286, 1321-1326.
142. Lorick, K. L., Jensen, J. P., Fang, S., Ong, A. M., Hatakeyama, S., & Weissman, A. M. (1999). RING fingers mediate ubiquitin-conjugating enzyme (E2)-dependent ubiquitination. *Proc. Natl. Acad. Sci. USA*, 96, 11364-11369.
143. Haupt, Y., Maya, R., Kazaz, A., & Oren, M. (1997). MDM2 promotes rapid degradation of p53. *Nature*, 387, 296-299.

144. Picksley, S. M., & Lane, D. P. (1993). The p53-MDM2 autoregulatory feedback loop: a paradigm for the regulation of growth control by p53? *BioEssays*, 15, 689-690.
145. Koeg, M., Hoppe, T., Schlenker, S., Ulrich, H., Mayer, T., & Jentsch, S. (1999). A novel ubiquitination factor, E4, is involved in multiubiquitin chain assembly. *Cell*, 96(5), 635- 644.
146. Hoppe, T. (2005). Multiubiquitylation by E4 enzymes: 'one size' doesn't fit all. *Trends Biochem Sci*, 30, 183-187.
147. Hoege, C., Pfander, B., Moldovan, G., Pyrowolakis, G., Jentsch, S. (2002). RAD-6 dependent DNA repair is linked to modification of PCNA by ubiquitin and SUMO. *Nature*, 419, 13-141.
148. Pickart, C. M., & Fushman, D. (2004). Polyubiquitin chains: Polymeric protein signals. *Curr Opin Chem Biol*, 8, 610-616.
149. Kim, I., & Rao, H. (2006). What's Ub chain linkage got to do with it? *Science Signaling*, 330, DOI:10.1126/stke.3302006pe18.
150. Murray-Zmijewski, F., Slee, E. A., & Lu, X. (2008). A complex barcode underlies the heterogenous response of p53 to stress. *Nat Rev*, 9, 702-712.
151. Vogelstein, B., & Kinzler, K. W. (1992). p53 function and dysfunction. *Cell*, 70, 523-526.
152. Honda, R., Tanaka, H., & Yasuda, H. (1997). Oncoprotein MDM2 is a ubiquitin ligase E3 for tumor suppressor p53. *FEBS lett*, 420, 25-27.

153. Grossman, S. R., Perez, M., Kung, A. L., Joseph, M., Mansur, C., Xiao, Z. X., Kumar, S., Howley, P. M., & Livingston, D.M. (1998). P300/MDM2 complexes participate in MDM2-mediated p53 degradation. *Mol Cell*, 2, 405-415.
154. Thut, C. J., Goodrich, J. A., & Tjian, R. (1997). Repression of p53-mediated transcription by MDM2: a dual mechanism. *Genes Dev*, 11, 1974-1986.
155. Shieh, S. Y., Ikeda, M., Taya, Y., & Prives, C. (1997). DNA damage-induced phosphorylation of p53 alleviates inhibition by MDM2. *Cell*, 91, 325-334.
156. Ito, A., Lai, C., Zhao, X., Saito, S., Hamilton, M., Appella, E., & Yao, T. (2001). P300/CBP-mediated p53 acetylation is commonly induced by p53-activating agents and inhibited by MDM2. *EMBO Journal*, 20(6), 1331-1340.
157. Grossman, S. R. (2001). p300/CBP/p53 interaction and regulation of the p53 response. *Eur J Biochem*, 268, 2773–2778.
158. Pearson, M., Carbone, R., Sebastiani, C., Cioce, M., Fagioli, M., Saito, S., Higashimoto, Y., Appella, E., Minucci, S., & Andolfi, P. (2000). PML regulates p53 acetylation and premature senescence induced by oncogenic Ras. *Nature*, 406, 207-210.
159. Le Cam L., *et al.* (2006). E4F1 is an atypical ubiquitin ligase that modulates p53 effector functions independently of degradation. *Cell*, 127, 775-788.
160. Mattera, R., Tsai, Y. C., Weissman, A. M., & Bonifacino, J. S. (2006). The Rab5 guanine nucleotide exchange factor Rabex-5 binds ubiquitin (Ub) and functions as a Ub ligase through an atypical Ub-interacting motif and a zinc finger domain. *J Biol Chem*, 281, 6874-6883.

161. Abraham, R., T. (2001). Cell cycle checkpoint signaling through the ATM and ATR kinases. *Genes & Development*, 15, 2177-2196.
162. Stokes, M. P., Rush, J., Macneil, J., Ren, J. M., Sprott, K., Nardone, J., Yang, V., Beausoleil, S. A., Gygi, S. P., Livingstone, M., Zhang, H., Polakiewicz, R. D., & Comb, M. J. (2007). Profiling of UV-induced ATM/ATR signaling pathways. *Proc Natl Acad Sci USA*, 104(50), 19855-19860.
163. Smith, J., Tho, I.M., Xu, N., Gillespie, D.A.(2010). The ATM-Chk2 and ATR-Chk2 pathways in DNA damage signaling and cancer. *Adv Cancer Res.* 108, 73-112.
164. Bode, A. M., & Dong, Z. (2004). Post-translational modification of p53 in tumorigenesis. *Nat Rev Cancer*, 4, 793–805.
165. Brooks, C. L., & Gu, W. (2003). Ubiquitination, phosphorylation, and acetylation: The molecular basis for p53 regulation. *Curr Opin Cell Biol*, 15, 164–171.
166. Li, M., Brooks, C. L., Wu-Baer, F., Chen, D., Baer, R., & Gu, W. (2003). Mono- versus polyubiquitination: Differential control of p53 fate by Mdm2. *Science*, 302, 1972–1975. doi: 10.1126/science.1091362.
167. Brooks, C. L., Li, M., & Gu, W. (2004) Monoubiquitination: The signal for p53 nuclear export? *Cell Cycle*, 3, 436–438.
168. Maki, C.G., Howley, P.M., 1997. Ubiquitination of p53 and p21 is differentially affected by ionizing and UV radiation. *Molecular and Cellular Biology*, 355-363.

169. Panier, S., Durosher, D. (2009). Regulatory ubiquitylation in response to DNA double-strand breaks. *DNA repair* 8(4):436-43.
170. Das, C., Lucia, M, Hansen, K, Tyler, J. (2009). CBP/p300- mediated acetylation of histone H3 on lysine 56. *Nature* 459(7243):113-17.
171. Hamaguchi, M., Meth, J. L., Von Klitzing, C., Wei, W., Esposito, D., Rodgers, L., Walsh, T., Welcsh, P., King, M. C., & Wigler, M. H. (2002). DBC2, a candidate for tumor suppressor gene involved in breast cancer. *Proc Natl Acad Sci USA*, 99, 13647-13652.
172. Kim, J. E., Chen, J., & Lou, Z. (2009). p30 DBC is a potential regulator of tumorigenesis. *Cell Cycle*, 8, 2932–2935.
173. Fu, J., Jiang, J., Li, J., Wang, S., Shi, G., Feng, Q., White, E., Qin, J., & Wong, J. (2009). Deleted in breast cancer 1, a novel androgen receptor (AR) coactivator that promotes AR DNA-binding activity. *J Biol Chem*, 284, 6832–6840.
174. Chini, C. C., Escande, C., Nin, V., & Chini, E. N. (2013). DBC1 (Deleted in Breast Cancer 1) modulates the stability and function of the nuclear receptor Rev-erba. *Biochem J*, 451, 453–461.
175. Trauemicht , A. M., Kim, S. J., Kim, N. H., & Boyer, T. G. (2008). Modulation of estrogen receptor α protein level and survival function by DBC1. *Mol Endocrinol*, 21, 1526–1536.
176. Zhao, W., Kruse, J. P., Tang, Y., Jung, S. Y., Qin, J., & Gu, W. (2008). Negative

- regulation of the deacetylase SIRT1 by DBC1. *Nature*, 451, 587–590.
177. Chini, C. C., Escande, C., Nin, V., & Chini, E. N. (2010). HDAC3 is negatively regulated by the nuclear protein DBC1. *J Biol Chem*, 285, 40830–40837.
178. Li, Z., Chen, L., Kabra, N., Wang, C., Fang, J., & Chen, J. (2009). Inhibition of SUV39H1Methyltransferase activity by DBC1. *J Biol Chem* 284, 10361–10366.
179. Park, J. H., Lee, S. W., Yang, S. W., Yoo, H. M., Park, J. M., Seong, M. W., Ka, S. H., Oh, K. H., Jeon, Y. J., & Chung, C. H. (2014). Modification of DBC1 by SUMO2/3 is crucial for p53-mediated apoptosis in response to DNA damage. *Nature Communications*, DOI: 10.1038.
180. Bo, Q., Minter-Dykhouse, K., Wang, L., Lou, Z. (2015). DBC1 functions as a tumor suppressor by regulating p53 stability. *Cell Reports* 10,1324-34.
181. Sundararajan, R., Chen, G., Mukherjee, C., White, E.(2005). Caspase-dependent processing activates the proapoptotic activity of deleted in breast cancer-1 during tumor necrosis factor-alpha-mediated death signaling. *Oncogene* 24, 4908-4920.
182. Gao, J., Aksoy, B., Dogrusoz, U., Dresdner, G., Gross B. *et al.* (2013). Integrative analysis of complex cancer genomics and clinical profiles using the cBioPortal. *Sci. Signal* 6 (269), p11: doi: 10.1126.
183. Cerami, E., Gao,J., Dorusoz, U, Gross, B., Sumer, S *et al.* (2012). The cBio cancer genomics portal: An open platform for exploring multidimensional cancer genomic data. *Cancer Discov* 2(5), 401-404.

184. Jensen, K., Sheils, C., Freemont, P. (2001). PML protein isoforms and the RBCC/TRIM motif. *Oncogene* 20, 7223-7233.